AALBORG UNIVERSITY
DENMARK

Probabilistic Models and Computational Methods for Chloride Ingress in Concrete

Engelund, S.

Publication date:
1997

Document Version
Publisher's PDF, also known as Version of record

Link to publication from Aalborg University

Citation for published version (APA):
Engelund, S. (1997). *Probabilistic Models and Computational Methods for Chloride Ingress in Concrete.* Dept. of Building Technology and Structural Engineering, Aalborg University. Structural Reliability Theory Vol. R9707 No. 144

STRUCTURAL RELIABILITY THEORY
PAPER NO. 144

Ph.D.-Thesis defended publicly at Aalborg University January 14, 1997

S. ENGELUND
PROBABILISTIC MODELS AND COMPUTATIONAL METHODS FOR CHLORIDE INGRESS IN CONCRETE

STRUCTURAL RELIABILITY THEORY
PAPER NO. 144

Ph.D.-Thesis defended publicly at Aalborg University January 14, 1997

S. ENGELUND
PROBABILISTIC MODELS AND COMPUTATIONAL METHODS FOR
CHLORIDE INGRESS IN CONCRETE

Acknowledgements

Aalborg, December 1996   Svend Engelund

4

Contents

Chapter 1

Introduction

Within the last decades it has been recognized that reinforced concrete structures are subject to a number of destructive mechanisms which might affect the structure in such a way that it is not able to fulfill its purpose efficiently. The present report focuses on chloride ingress and chloride-initiated corrosion of the reinforcement, because experience has shown that in Denmark this is one of the most common destructive mechanisms.

In order to ensure that a given reinforced concrete structure is able to fulfill its purpose extensive measurements are performed and on the basis of these measurements it is determined whether repair and maintenance are necessary. A decision maker is faced with the question of how to perform the measurements such that most information is obtained at the lowest cost and which repair and maintenance strategy to apply if this turns out to be necessary. The measurements and repairs are costly, and careful planning is mandatory. The planning can be performed on the basis of classical decision theory (see e.g. Raiffa and Schlaifer [4]). However, in order to use decision theory, it is necessary to formulate a probabilistic model of the considered problem.

1.1 Probabilistic Models

A probabilistic model must be based on a physical model of the problem which encompasses the most important features. However, in recent years there has been some discussion about the models for chloride ingress in concrete, see e.g. Poulsen [7] and Johansen [5]. With a view to this it might seem a bit premature to formulate a probabilistic model. However, for a large number of existing structures the decisions about experimental plans and repair strategies are already overdue. It is, therefore, necessary to formulate a model based on our present knowledge of the problem. Further, it is important that the reader bears in mind that the purpose of a probabilistic model is not to produce a perfect model of reality, but rather to develop a model which can be used in order to make optimal decisions using the available data.

The deterioration of concrete depends on a number of environmental factors, such as the concentration of chloride on the surface of the structure, and the characteristics of the concrete, e.g. the ability of the concrete to transport chloride. It is evident that the environmental factors will show some variation from one structure to another. Also

the characteristics of the concrete will vary from structure to structure because they depend on the concrete composition as well as a number of factors concerned with the construction process such as the transporting, handling and compacting of the concrete. Further, it has been shown that for a given structure both the environmental factors and the characteristics of the concrete exhibit a substantial random variation in space, see e.g. Stoltzner and Sørensen [9].
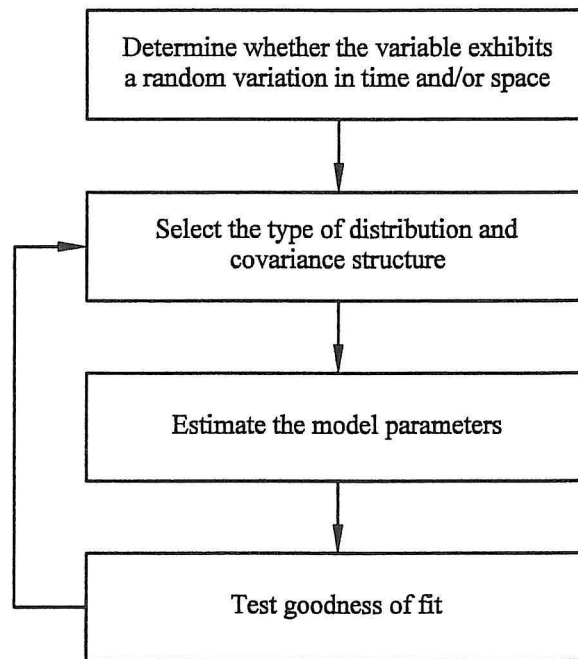
Figure 1.1: *Formulation of a probabilistic model.*

The first step in the formulation of a probabilistic model is to determine if a variable should be modelled as a deterministic parameter, a stochastic variable or a stochastic field (a variable exhibiting a random spatial variation). This decision can be based on considerations as given above and on the available measurements.

The second step consists of selecting the probability distributions for the stochastic variables and the covariance structure for the stochastic fields. In many cases this is the most difficult task since only a very limited number of prior observations is available. It will often be possible to fit these observations to any probability distribution. The selection of the probability distribution will often have to be based solely on the prior knowledge about the variable.

Having selected the probability distributions and the covariance structure the unknown parameters in the model can be estimated by some parameter estimation method. Further, if the number of observations is sufficiently high a test for fit can be performed. Of course if the test shows that a better fit is obtained by another distribution type, the model must be changed accordingly. Especially if the purpose of the model is to determine the probability of some extreme event it is important to ensure a good fit to the observations in the tails of the distributions. Even though some reasoning based on a physical model

of a given problem suggests a given distribution type, this distribution should not be selected if it does not provide a good fit in the tail of the distribution.

In figure 1.1 the steps in the formulation of the probabilistic model are shown schematically

The idea of using probabilistic models to describe the deterioration of concrete is a relatively new one. However, the problem of chloride ingress in concrete has attracted some attention in recent years, see e.g. Hoffman [2], Pedersen [6], Ting [10] and Thoft-Christensen [11]. Unfortunately, the models presented by these authors do not take into account the spatial variation of the characteristics of the concrete and the environmental factors.

Hergenröder [1] presents a detailed probabilistic model of carbonation in concrete beams which takes the random spatial variation of the alkalinity interface into account. The model parameters are determined on the basis of measurements of the alkalinity interface in a number of test specimens. On the basis of the model it is possible to estimate the probability that the alkalinity interface has reached the reinforcement.

Probabilistic models of destructive mechanisms are sure to attract much attention in the future. In fact, a number of research programmes has been initiated to investigate destructive mechanisms, see e.g. Vesikari [12], and to define probabilistic models for the destructive mechanisms, see Rostam and Faber [8].

1.2   Scope of Thesis

The main objectives of the thesis are the following

- Formulate a probabilistic model for chloride ingress and initiation of corrosion.
- Investigate numerical methods for determining the chloride concentration in a given structure.
- Estimate the parameters in the probabilistic model on the basis of measurements.
- Determine the probability that corrosion is initiated in a given structure on the basis of the probabilistic model and the estimated parameters.
- Determine the optimal repair and maintenance strategy for a given structure.
- Determine optimal experimental plans for performing measurements.

It is the aim of the thesis to use traditional reliability methods and decision analysis to solve the above-mentioned problems. These methods are widely known among researchers and are now beginning to find recognition among practising engineers. Using these methods, therefore, ensure that the methodologies developed here can be applied by practising engineers familiar with reliability analysis.

1.3   Reader's Guide

The structure of the thesis follows from the main objectives stated above.

The purpose of *chapter 2* is to provide the reader with little knowledge about chloride-initiated corrosion with some basic concepts which will be used through the later work.

Further, the methods used at present for estimating the lifetime of concrete structures subject to chloride ingress are reviewed.

In *chapter 3* a probabilistic model for chloride ingress in concrete and initiation of corrosion of the reinforcement is formulated. Further, various methods for solving the governing equations for the chloride flow are investigated in order to determine the most efficient and accurate ones.

Chapter 4 presents the basic tools for estimating the parameters in the probabilistic model formulated in chapter 3 and it provides some probabilistic methods which are used in order to determine the time to initiation of corrosion and which can be used in conjunction with experimental planning.

In *chapter 5* a number of examples is used to illustrate how the probabilistic model presented in chapter 3 together with the computational methods also presented in chapter 3 can be used in conjunction with the probabilistic methods presented in chapter 4 to estimate the time to initiation of corrosion in a given structure.

Chapter 6 presents the basic concepts for determining optimal repair and maintenance strategies and in an illustrative example it is demonstrated how optimal plans can be determined for a bridge in a marine environment.

Chapter 7 is devoted to optimal planning of measurements. The basic principles are presented and the effect of performing additional measurements is investigated using the same example as in chapter 6.

A summary of the thesis and the main conclusions which can be reached on the basis of the work are presented in *chapter 8*.

In *appendix A* short descriptions of the programme modules used in the work are given. A list of the notations used in the report is given in *appendix B*. A summary in Danish is given in *appendix C*.

The report is meant to be of interest for both engineers working within the field of maintenance and repair of concrete structures as well as engineers working with reliability theory. It must, however, be noted that some prior knowledge of probabilistic methods and stochastic fields will be an advantage when reading the report.

1.4   References

[1] Hergenröder, M., Zur Statistischen Instandhaltungsplanung für bestehende Betonbauwerke bei Karbonatisierung des Betons und möglicher Korrosion der Bewehrung, Berichte aus dem Konstruktiven Ingenieurbau 4/92, Technische Universität München, 1992.

[2] Hoffman, P. C., Weyers, R. E., Probabilistic Analysis of Reinforced Concrete Bridge Decks, in: Frangopol, D. M., Grigoriu, M. D., (eds.), Probabilistic Mechanics and Structural Reliability, ASCE, New York, 1996, pp. 290-293.

[3] Kroon, I. B., Decision Theory Applied to Structural Engineering Problems, Ph.D.-Thesis, Structural Reliability Theory, Paper No. 132, Dept. of Building Technology and Structural Engineering, Aalborg University, Denmark, 1994.

[4] Raiffa, H., Schlaifer, R., Applied Statistical Decision Theory, Harverd University Press, Cambridge, Mass., 1961.

[5] Johansen, V., The Modelling of Microstructure and its Potential for Studying Transport Properties and Durability, Rilem Workshop, Saint-Remy-les-Chevreuse, July, 1994.

[6] Pedersen, C., Thoft-Christensen, P., Reliability Analysis of Prestressed Concrete Beams with Corroded Tendons, Structural Reliability Theory, Paper No. 109, Dept. of Building Technology and Structural Engineering, Aalborg University, Denmark, 1993.

[7] Poulsen, E., Chloride Profiles, Determination, Interpretation and Practice, Corrosion of Reinforcement, Proceedings of the Nordic Seminar in Lund, Editor: Kyösti Tuutti, Lund, Sweden, 1995.

[8] Rostam, S., Faber, M. H., Probabilistic Performance Based Durability Design of Concrete Structures (Duracrete), in: Nordic Concrete Research, Proceedings Nordic Concrete Research Meeting, 1996, pp. 316-317.

[9] Stoltzner, E., Sørensen, B., Chloridundersøgelser på Farøbroerne, Dansk Beton, 11, 1 pp. 16-18, in Danish.

[10] Ting, S.-C., The Effects of Corrosion on the Reliability of Concrete Bridge Girders, Ph.D.-Thesis, University of Michigan, USA, 1989.

[11] Thoft-Christensen, P., Advanced Bridge Management Systems, Structural Engineering Review, 7, 1995, pp. 151-163.

[12] Vesikari, E., Service Life Design of Concrete Bridges, in: Nordic Concrete Research, Proceedings Nordic Concrete Research Meeting, 1996, pp. 310-311.

Chapter 2

Chloride-Initiated Corrosion in Reinforced Concrete Structures

One of the dominant factors when determining the lifetime of a concrete structure with respect to chloride-initiated corrosion is the rate at which chloride can be transferred from the surroundings into the concrete. The rate of transport depends on the porestructure of the concrete, the existence of cracks and the ability of the concrete to bind chloride. Therefore, a probabilistic model of chloride ingress in concrete structures must be based on an understanding of the concrete microstructure and the principles and reactions involved in its formation.

2.1 The Nature of Concrete

Concrete can be defined as an anorganic material consisting of cement, water and aggregates. By the mixing of water and cement chemical reactions known as hydration take place which bind the different materials together. Thus, concrete is a composite material of aggregate particles bound together by hydrated cement. In the following the hydration process, the pore structure and permeability of the concrete are described.

2.1.1 The Hydration Process

Ordinary Portland cement mainly consists of the four minerals shown in table 2.1. During the hydration process the calcium silicates C_3S and C_2S react with water giving calcium silicate hydrates (like $3CaO \cdot 2SiO_2 \cdot 3H_2O$) and calcium hydroxide ($Ca(OH)_2$). The C_3A and C_4AF react with water and the added lime to give calcium aluminate hydrates (like $4CaO \cdot 2Al_3 \cdot nH_2O$). The lime is added in order to slow the reaction between C_3A and water. Without lime the setting time would be very short (Herholdt et al. [11]). Due to the large amount of calcium hydroxide the water contained in the concrete becomes strongly alkaline (pH 12-14).

Apart from the four minerals shown in table 2.1 the cement may further contain mineral additives such as natural Puzzolan, fly ash or microsilica. All the mentioned additions (in general denoted puzzolans) do not react with water but with calcium hydroxide under the

15

Name	Composition	Abbreviation	Contents
Tricalcium silicate	$3CaO \cdot SiO_2$	C_3S	58 %
Dicalcium silicate	$2CaO \cdot SiO_2$	C_2S	24 %
Tricalcium aluminate	$3CaO \cdot Al_2O_3$	C_3A	4 %
Tetracalcium aluminate ferrite	$4CaO \cdot Al_2O_3 \cdot Fe_2O_3$	C_4AF	8 %

Table 2.1: *The most important clinker minerals.*

production of calcium silicate hydrates. Since this reaction consumes calcium hydroxide the pH of the water contained in the concrete decreases.

The hydration process starts immediately when water and cement come in contact. In the beginning the cement remains fluid and heat is developed (Herholdt et al. [11]). After a few days the concrete has hardened. The hydration process, however, continues infinitely as a result of which important properties such as strength and permeability change continuously (Schießl [28]). It takes months or even years until a stable condition is reached. The reaction rate depends on the type of cement. If the cement contains e.g. a puzzolan the strength and permeability continue to change over a long period of time. If there is no deterioration of the structure these properties improve with time. The *degree of hydration* is defined as the relation between the amount of hydrated cement and the amount of cement in the concrete.

2.1.2   Porosity and Permeability

During the hydration process the volume of the cement paste remains approximately constant. However, the solid products of hydration occupy a volume which is less than the sum of the volumes of the original cement and water. Therefore, there is a residual space within the paste which takes the form of so-called *capillary pores* with a diameter of about 1 μm.

The setting of solid particles in the concrete causes excess water to rise and form further capillary pores and channels or capillaries which connect the capillary pores. Some of the water is trapped below reinforcement and aggregate particles forming *macro pores* with a size of about 0.1 mm. Yet another part of the water fills the void between the cement particles. The hydration of the cement decreases the size of these voids but will never be able to eliminate them completely. These so-called *gel pores* are very small, about 2 nm. In conclusion, there is a whole range of pore sizes throughout the hardened cement paste. The amount of pores of a given size can be described by the pore size distribution.

It is evident that the porosity depends on the w/c-ratio and the degree of hydration. As the w/c-ratio decreases the amount of excess water decreases which leads to fewer capillaries and capillary pores. Also, the size of the gel pores decreases with the degree of hydration. Further, the porosity depends on the curing of the concrete. Insufficient curing leads to a larger amount of pores because the curing leads to a higher degree of hydration. The porosity of the cement paste is also influenced by the reaction between pozzolans and calcium hydroxide. This reaction leads to filling of the pores.

Of particular interest to the durability of concrete structures is the permeability of the
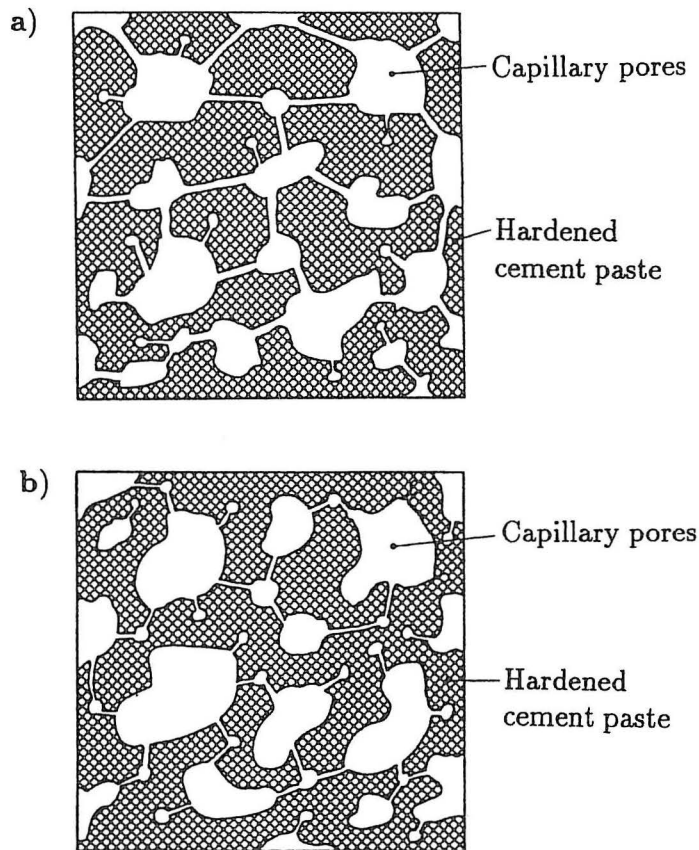
Figure 2.1: a: *High permeability,* b: *Low permeability, from Neville* [18].

hardened cement paste. The permeability depends on the amount of capillary pores and the connectivity of the pores. If the w/c-ratio is low there is no or very little excess water which can lead to formation of capillaries. The pore system is then discontinuous and consists of clusters without mutual interconnection. Only the outermost clusters will be connected to the concrete surface and will be subject to chloride penetration. See also figure 2.1. Johansen [14] states that if the w/c-ratio is less than 0.7 the pore system consists of clusters of pores that are not interconnected. Neville and Brooks [18] concludes that the pore system becomes discontinuous at w/c-ratios below 0.6. However, it can be argued that the permeability of the concrete also depends on the existence of microcracks, developed by differential volume changes between cement paste and coarse aggregate caused by differences in stress-strain behavior and by thermal movements. These microcracks may connect otherwise isolated clusters of capillary pores and thereby ensure that the entire pore structure in the concrete becomes connected. The amount of cracks formed depends on the concrete composition and a number of factors associated with the construction process such as casting and vibration. It is, therefore, very difficult to predict the amount of cracks that will be present in a given structure. This also implies that it is very difficult to predict if the system of pores and microcracks is connected and at what rate a given agent is conveyed into the structure.

2.2   Chloride-Initiated Corrosion

The reinforcement in concrete structures is protected from corrosion by a chemical as well as a physical barrier. Due to the strong alkalinity of the pore solution a microscopic oxide layer is formed on the reinforcement steel which prevents corrosion. The reinforcement is further protected by the cover layer. In order to initiate corrosion harmful agents must penetrate the cover layer and dissolve the protective oxide layer. This process is called the initiation phase. The initiation phase is followed by a propagation phase where the reinforcement corrodes. The lifetime of a structure, T_L, therefore, is modelled as the sum of two parts

$$T_L = T_1 + T_2 \qquad (2.1)$$

where T_1 is the initiation period and T_2 is the propagation period. The deterioration process is shown schematically in figure 2.2.
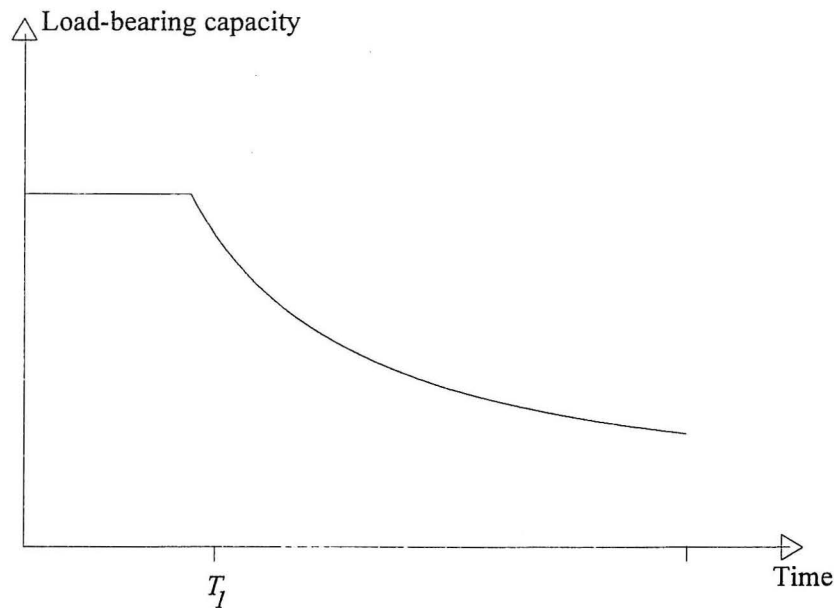
Figure 2.2: *General deterioration model.*

Corrosion can be initiated by chloride ions cl^- which penetrate to the reinforcement. When the concentration of chloride ions around the reinforcement exceeds a threshold value the protective layer dissolves and corrosion begins. There is a number of consequences of the corrosion of the reinforcement. First, the corrosion products occupy a larger volume than the original steel. The concrete, therefore, begins to crack and spall, making it easier for water and oxygen to penetrate towards the steel which leads to an increasing rate of corrosion (see section 2.2.7). Second, the reduction of the cross-sectional area of the reinforcement leads to a decreased load-bearing capacity. Finally, the corrosion makes the reinforcement brittle, implying that the structure might fail without warning.

2.2.1   Sources of Chloride

Chloride may have been added to the fresh concrete in order to accelerate the hydration process or it may originate from the aggregates or the water. In order to prevent corrosion of the reinforcement there are, however, codified values for the amount of chloride which may be present in the fresh concrete.

Chloride may also originate from a number of external sources. Concrete structures in a marine environment receive chloride directly from the sea water and the surface concentration is generally largest in the tidal and splash zone. However, a significant contribution to the surface concentration originates from air-borne chloride.

Swimming pools, pipe-lines and other containers with salt-water are also subject to chloride-ingress. For bridges placed close to roadways. The major source of chloride is de-icing salts. De-icing salts can lead to chloride-initiated corrosion in roadway bridges where mainly the piers have a large surface concentration. For piers placed close to a roadway the surface concentration is largest at terrain on the sides facing the roadway. The surface concentration depends on the distance to the roadway, the traffic intensity and the amount of de-icing salts spread on the roadway.

2.2.2   Transport Ways for Penetration of Chloride

The transport ways for chloride can according to Johansen [14] be classified as

1. The capillary pore system.
2. Cracks.
3. The hydration products.

Chloride can be transported from the surface of a given structure into the interior through the part of the capillary pores and microcracks that are directly connected with the surface. Further, the chloride may be transported through the hydration products. However, the rate of transport through the hydration products is so small that this transport way can be disregarded.

Apart from microcracks there may be larger cracks in the concrete structure. These cracks are important because chloride can penetrate through these cracks much faster than through the system of capillary pores and microcracks. This, of course, leads to a lower initiation time.

It is normal to distinguish between three types of cracks

- Small cracks, cracks of small depth compared to the thickness of the cover layer.
- Medium cracks, cracks of depth which is not small compared to the thickness of the cover layer. The cracks, however, do not penetrate all the way to the reinforcement.
- Large cracks, cracks which penetrate all the way to the reinforcement.

Various researchers conclude that if the crack width is smaller than 0.1-1.0 mm, the effect of the crack can be neglected (e.g. Tuutti [33]). CEB [7] suggests that the critical crack

width is 0.2 mm. Okada and Miyagawa [26] conclude on the basis of a series of experiments that the critical crack width is 0.1-0.2 mm.

The presence of medium sized cracks will lead to a decrease of the initiation time. If a 2- or 3-dimensional model of the concrete structure is used when determining the initiation time, the cracks can be taken into account, see e.g. Schießl [29].

When the crack penetrates all the way to the reinforcement, the initiation time is negligible. Tuutti [33] states that when the crack runs parallel to the reinforcement, corrosion will propagate fast. However, if the crack runs at right angles to the reinforcement only a very small area of the reinforcement is exposed. For these cracks Tuutti [33] concludes that the rate of corrosion must be low. The reason is that the crack is sometimes healed by unhydrated cement or that some substance required for corrosion is missing.

2.2.3   Bound and Free Chloride

Concrete contains both "free" chloride, chloride that is dissolved in the pore water, and "bound" chloride, chloride that is bound. Only the free chloride can cause corrosion. Unfortunately, it is difficult to obtain samples of the pore water on the basis of which the concentration of free chloride can be measured. Usually, the total (both bound and free) chloride concentration is measured.

The chloride can be bound physically, adsorbed at the hydration products, or they can be bound chemically. The different minerals in the cement all have the ability to bind chloride. Most important is the reaction of chloride with tricalciumaluminat (C_3A) which forms the so-called Friedel Salt, see e.g. Müller [17]. It follows that more chloride is bound as the C_3A content is higher and when the cement content of the mix is higher. It was, therefore, earlier thought that chloride-initiated corrosion was less likely to occur if a cement with a high C_3A content was used in the mix. However, the bound chloride may later be released and lead to a higher concentration of free chloride. It is e.g. a well-known fact that bound chloride is released when the concrete is carbonated. In addition the carbonation leads to a lowering of the pH of the pore solution, implying that the protective layer on the reinforcement is dissolved and that corrosion is more easily initiated.

2.2.4   Ingress of Chloride

When the concentration of chloride in the surroundings is higher than the concentration in the concrete, chloride will be transferred into the concrete by diffusion taking place in the non-streaming water in the totally or partially water-filled system of pores and micro-cracks. The rate of transport depends on the permeability of the concrete and the temperature and humidity in the pores. As the temperature increases also the rate of transport increases, see Sørensen [31]. Diffusion only takes place if the relative humidity in the pores is higher than 75-80 %, see e.g. Poulsen [22]. If the relative humidity is lower there is no longer a connected system of pore solution.

Chloride can also be conveyed into concrete by the flow of chloride-containing water. The flow of water can be caused by capillary suction of dry concrete or by permeation (a flow caused by differences in pressure). Especially, alternate cycles of wetting and drying are

believed to lead to a build-up of chloride, see e.g. Neville [18], and Poulsen [22]. A dry concrete which is wetted with salt water on the surface will absorb the water by capillary suction. When the concrete surface dries out the flow of water will be reversed. However, only pure water evaporates from the surface. The chloride is left behind. Obviously, at the depth where the concrete never dries out no chloride is transported by this mechanism. Apart from the permeability of the concrete this depth, according to Bakker [2], depends on the lengths of the periods of wetting and drying.

On the basis of models of the heat and moisture transport in concrete developed by Bažant and Thonguthai [5] and Bažant and Najjar [4] Saetta et al [27], formulated a model which takes the various transport mechanisms into account as well as their dependence on temperature and humidity. The build-up of the chloride concentration over a period of years is determined on the basis of a FEM-model where the timesteps are measured in hours. Evidently, this methodology is very time-consuming in terms of CPU-time. Further, in order to implement the model to determine the chloride concentration in a given structure a complete set of boundary conditions must exist. That is a set of meteorological data describing the humidity and temperature of the air. Finally, the functions describing the dependence of the transport mechanisms on the humidity and temperature are nothing but crude approximations. This complicated model, therefore, mainly has academic interest and can only be used in order to quantify the importance of the many parameters in the model.

It is evident that any prediction of the chloride concentration must be based on a simplified model. It is usually assumed that a given volume of concrete can be regarded as a semi-infinite isotropic medium with a transport coefficient, D which is constant in both time and space, and surface concentration, c_s which is also assumed to be constant in both time and space. The chloride concentration as a function of the distance from the surface, x, and time, t, can then be described by the solution to the 1-dimensional linear diffusion problem

$$c\left(x,t\right) = c_0 + \left(c_s - c_0\right)\left(1 - \text{erf}\left[\frac{x}{\sqrt{4tD}}\right]\right) \qquad (2.2)$$

where erf (.) denotes the error function of (.) and where c_0 is the initial chloride concentration. The model cannot be used to determine the variation of the chloride concentration over a short period of time since the different transport mechanisms are not taken into account. However, the model can be used to determine the build-up of the chloride concentration over a period of years. The advantage of this model apart from its relative simplicity, is the fact that measurements from existing structures can be brought to fit the expression, eq. (2.2).

Various researchers have modified eq. (2.2). E.g. Østergård [34] has used a model where the variation of the transport coefficient with the distance from the surface is taken into account. Poulsen [23] has suggested a model where the variation of the transport coefficient as a function of time is taken into account. Also, on the basis of experimental data, Mangat and Malloy [15] suggest that the transport coefficient depends on time. These models lead to a better fit to the observed chloride concentration in existing structures. However, a larger number of model parameters has to be estimated on the basis of a limited data material.

The model, eq. (2.2), is based on the assumption that the pore system in the concrete is connected. On the basis of *percolation theory* it can in theory be determined if a connected system of pores exists, see e.g. Johansen [14] and Bentz and Garboczi [6]. In a simple model the pores in the concrete are regarded as sites that are connected with a probability p. It is evident that if p is small only few sites are connected and the model predicts that the concrete only contains small isolated clusters of pores and that no transport of chloride takes place. As p increases, the size of the clusters increases until at some value of p a connected net of pores through the entire structure is formed. Unfortunately, it is unclear how the probability, p, can be determined on the basis of observations from a given structure. In fact, the percolation theory does not yet seem to be able to predict if the pore system in a given structure is connected. The safest approach, therefore, is to assume that chlorides are able to penetrate all the way to the reinforcement and to use eq. (2.2) to predict the chloride concentration in a given position at a given time.

2.2.5   Threshold Value for Corrosion

As earlier mentioned, corrosion is initiated when the chloride concentration around the reinforcement exceeds a critical threshold, c_{cr}. A large number of experiments has been carried out to determine the critical threshold concentration of chloride at which the passive oxide layer on the reinforcement is dissolved. One of the earliest results is due to Hausmann [9] who suggested that corrosion is initiated when the ratio between the concentrations of hydroxyl and free chloride ions exceeds 0.61. This value has been verified by Tuutti [33]. These findings, however, have been obtained on the basis of experiments in a simulated pore solution, which does not properly represent the transport mechanisms in concrete and the ability of the concrete to bind chloride ions. Pettersson [21] performed a series of laboratory experiments in order to quantify the influence of a number of factors. Pettersson [21] concluded that the critical threshold value increases with decreasing w/c-ratio and that micro silica reduces the critical threshold approximately by a factor two.

In order to determine c_{cr} Henriksen and Stoltzner [10] have investigated a number of concrete bridges which were all situated close to roadways. In table 2.2 the number of cases is shown where a given chloride concentration around the reinforcement was observed, together with the number of cases where corrosion was found to have been initiated at the given chloride concentration. The chloride concentration is given in % relative to the dry weight of concrete.

	Chlorideconcentration at reinforcement, c (%)						
	$\leq 0.04\%$	$= 0.05\%$	$= 0.06\%$	$= 0.07\%$	$= 0.08\%$	$= 0.09\%$	$c \geq 0.10\%$
Tests	21	8	2	3	3	0	11
Corrosion	0	3	2	1	2	0	10

Table 2.2: *Critical threshold for initiation of corrosion (Henriksen and Stoltzner [10]).*

Henriksen and Stoltzner [10] conclude that the lower limit for initiation of corrosion is 0.05 % chloride relative to the dry weight of concrete. The measurements also show that in some cases corrosion has not been initiated even though the concentration is higher

than 0.1 % relative to the dry weight of concrete. The large variability of the results can be explained by the fact that the total chloride concentration is measured and the binding capacity of the concrete is not taken into account and the fact that the critical threshold depends on the humidity of the concrete, see CEB [7]. The findings of Henriksen and Stoltzner [10] are supported by CEB [7], who concludes that the critical total chloride content depends on various parameters and that there is no single generally valid value.

2.2.6 Simplified Corrosion Model

An electrochemical corrosion element consists of a cathode and an anode that are connected both electrically and electrolytically. The reinforcement bar in the concrete acts as an electrical conductor and the pore water as electrolyte. The reinforcement is dissolved by the anodic process which takes place in the presence of chloride ions. The anodic process is normally written as

$$Fe \longrightarrow Fe^{2+} + 2e^- \qquad (2.3)$$

The liberated electrons move through the steel towards the cathodic area. If water and oxygen are present the surplus electrons will combine with these in the cathodic process

$$4e^- + O_2 + H_2O \longrightarrow 4OH^- \qquad (2.4)$$
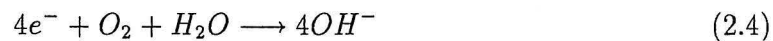
The hydroxyl ions are transferred towards the anode where they neutralize the Fe^{2+} dissolved in the pore water

$$Fe^{2+} + 2OH^- \longrightarrow Fe\,(OH)_2 \qquad (2.5)$$
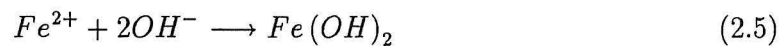
The Ferrous hydroxide $(Fe\,(OH)_2)$ reacts with oxygen and water

$$4Fe\,(OH)_2 + O_2 + 2H_2O \longrightarrow 4Fe\,(OH)_3 \qquad (2.6)$$
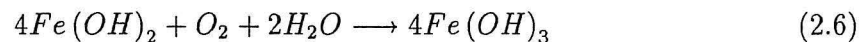
This is a simplified model of the electrochemical reactions. It should also be noted that depending on the amount of oxygen present, different types of rust are formed. It is evident that corrosion can only take place when both oxygen and water is present. Corrosion will not occur in dry concrete, because there is no water present, or in watersaturated concrete, where no oxygen is available. For structures in a normal outdoor climate in Denmark sufficient amounts of water and oxygen will always be present. In figure 2.3 the corrosion process is shown schematically.

When the chloride concentration at some place along the reinforcement exceeds the threshold value a very small anode and a large cathode will develop (see figure 2.3). The production of hydroxyl ions at the cathodic areas raises the pH and thus reduces the risk of attack in these areas. If the passive oxide layer on the majority of the steel surface can be maintained, the corrosion will only occur in the direction towards the interior of the reinforcement, the so-called *pitting corrosion*. This is the most dangerous form of corrosion since the cross-section of the reinforcement decreases rapidly and because it is difficult to detect.
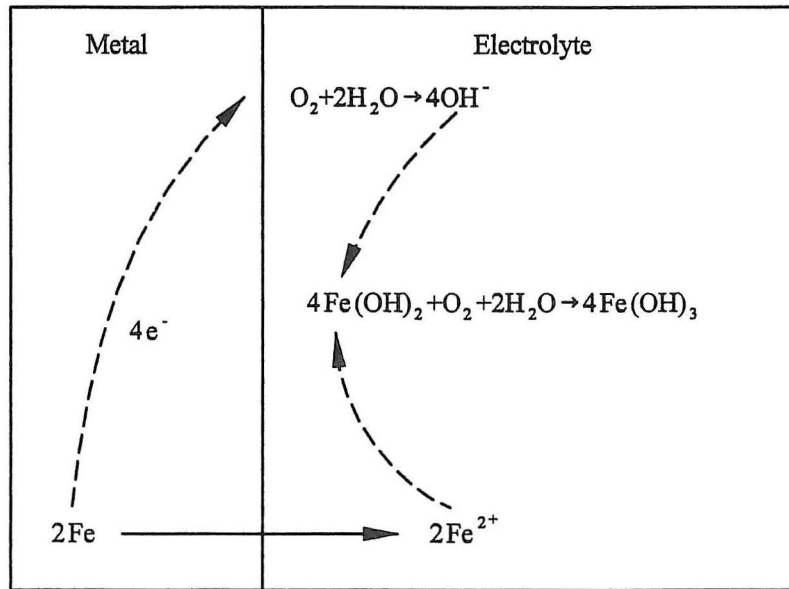
Figure 2.3: *The corrosion process.*

2.2.7 The Rate of Corrosion

For the corrosion process to propagate, oxygen and moisture must be available and the chloride concentration around the anode must be maintained at a level higher than the critical threshold value, Tredaway [32]. Bažant [3] states that the limiting factor of the corrosion process is the amount of oxygen available. If the available amount of oxygen and the corrosion process are known the rate of corrosion can be determined. The penetration of oxygen through the concrete, however, is also a complicated process for which no exact models exist. Further, the chemical composition of the corrosion products also depends on the availability of oxygen and of the moisture of the concrete, see e.g Herholdt et al. [11].

The corrosion rate, in conclusion, depends on a large number of factors which are impossible or very difficult to predict with any accuracy. Any model used to predict the corrosion rate in reinforced concrete structures, therefore, must be some empirical model based on measurements from existing models. However, such measurements shows a very large scatter and, therefore, can only lead to very imprecise estimates of the corrosion rate in a given structure, see e.g. Melchers [16], which again lead to very imprecise estimates of the lifetime of the structure.

2.3 Inspection Methods

The estimation of the lifetime of a given concrete structure can be based on information gained from inspections and measurements performed on the given structure. The most common types of inspections/measurement made on structures subject to chloride ingress are

- Visual inspection.
- Half-cell measurements.
- Dust samples.
- Chloride profiles.
- Measurement of the cover thickness.

Visual Inspection

The most simple method is the visual inspection by which the surface of the structure is examined, e.g. by the use of a hammer, in order to determine signs of corrosion such as discoloring, cracking, spalling and cavities. As earlier mentioned these signs only occur some time after corrosion has been initiated. Hence, the visual inspection only reveals if corrosion has propagated for some time.

Half-Cell Measurements

When a reinforcement bar corrodes the electro-chemical process taking place can be detected by a so-called half-cell measurement. The method consists of measuring the difference in potential between a half-cell placed on the surface on the concrete structure and the reinforcement. Within recent years this method has become a popular tool for detection of corrosion. New developments have led to an automation of the method such that a map of potentials for a given structure can be obtained with relative ease, see Nilsen-Dharmaratne [19]. However, the method is very uncertain. Usually the results are interpreted in the following way

- If the potential is less than -350 mV there is a 90 % probability that corrosion has been initiated.
- If the potential is larger than -200 mV there is a 90 % probability that corrosion has not been initiated.

Due to the uncertainty related to the half-cell measurements it is common to remove the cover if the half-cell measurement indicates that corrosion has been initiated in order to perform a visual inspection of the reinforcement bars.

Dust Samples

The chloride concentration in a given structure is often determined on the basis of dust samples of the concrete. The samples can be obtained with a power drill using e.g. a 18 mm drill. In order to obtain a sample large enough for analysis more than one drilling must be made. The distance between the bore holes should be 50 mm, see Poulsen et al. [24]. Hence, the results of the dust samples cannot be interpreted as the chloride concentration at a given point in the structure but must be regarded as an average over a given volume. If the distance between the bore holes is too large the measurements cannot be used to estimate the transport coefficient and surface concentration at a given position. If the bore holes are placed relatively close the results can be used in the same manner as the chloride profiles (see below). However, the samples are usually only used in order to determine whether a more detailed analysis should be performed or not.

The Chloride Profile

The description of chloride penetration is often based on the so-called chloride profile where the measured chloride concentrations are shown as a function of the distance from the chloride exposed surface. The chloride concentration is usually given relative to the mass of concrete or the mass of binder. In figure 2.4 a typical example of a chloride profile is shown. The chloride concentration in figure 2.4 is given in % relative to the dry weight of concrete.
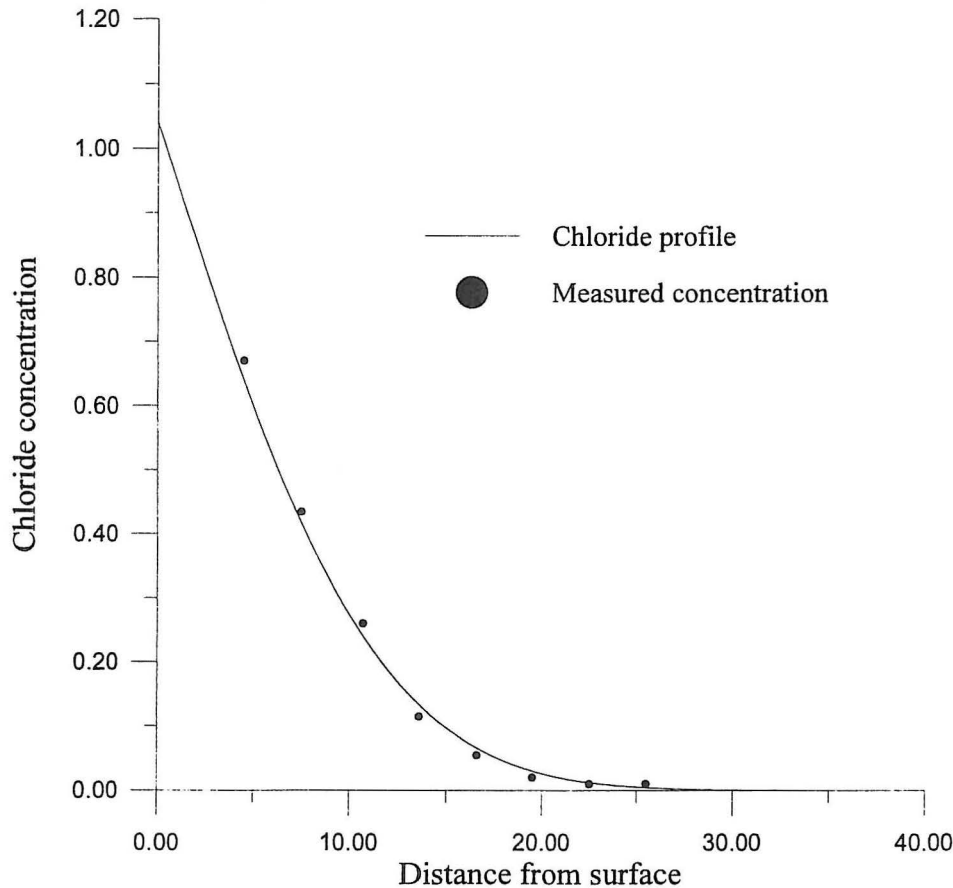
Figure 2.4: *Measured Chloride Profile*

The chloride profiles are determined by drilling out a concrete core, cutting the core into thin slices and measuring the chloride content in the slices. The thickness of these slices might be as small as 0.5-1.0 mm, see Poulsen [22]. According to DS 423.28 [8] the diameter of the core must be at least three times the maximum size of the aggregates in the concrete.

The chloride is contained in the hardened cement paste, the pores and microcracks. The aggregates contain no chloride. This variation between the paste and the aggregates cannot be taken into account. The chloride concentration, therefore, is defined as the mean value (the local average) over a given region. The volume of this region must be large enough to ensure that all such regions have about the same relation between the

amount of cement paste and aggregate.

Measurement of the Cover Thickness

It is evident that in order to estimate when corrosion of the reinforcement is initiated it is necessary to know the thickness of the cover. The cover thickness can be measured by using an electromagnet. When the electromagnet is placed on the surface of a concrete structure with reinforcement bars in steel, the magnetic field around the magnet is changed. The change depends on the distance to the reinforcement bars. This principle is used in modern measurement devices. According to Poulsen [24] the method is very accurate.

2.4 Lifetime Estimation

The estimation of the time to initiation of corrosion in a given structure is traditionally based on chloride profiles obtained from the given structure (see section 2.3) and the simple model for chloride ingress, based on Fick's law, eq. (2.2). Under the assumption that the initial chloride content is negligible, $c_0 = 0$ the transport coefficient, D, and the surface concentration, c_s, can be estimated. If the critical threshold for initiation of corrosion, c_{cr}, and the thickness of the cover, δ, are known, the time to initiation of corrosion can be determined by simple extrapolation, see e.g. Stoltzner and Sørensen [30]. As earlier mentioned the model based on Fick's law, eq. (2.2) has been modified such that the variation of the transport coefficient with time or space can be taken into account. These methods can in a similar manner be used in order to estimate the model parameters and the time to initiation of corrosion, see e.g. Poulsen [23] and Østergård [34].

Traditionally a purely deterministic analysis is carried out where the variability of the parameters is not taken into account. It is, however, in this type of analysis possible to include the statistical uncertainty related to the estimated parameters and the measurement uncertainty. Especially for models with a large number of parameters it is important to take the statistical uncertainty into account. As the number of parameters increases the uncertainty related to the estimated parameters increases. Therefore, it is likely, even though a better fit to the observations has been obtained, that the estimate of the time to initiation of corrosion will be very uncertain. The advantage of the traditional method is the fact that it is based on measurements from the considered structure. This makes it likely that the deterministic analysis yields a good estimate of the mean of the time to initiation of corrosion. It is, however, important to bear in mind that the result of the analysis is an estimate of the time to initiation of corrosion at the point where the measurement was performed. The spatial variation of the model parameters has not been accounted for.

Pedersen and Thoft-Christensen [20] suggest to determine the probability that corrosion has been initiated at a given time, T, by reliability analysis. On the basis of eq. (2.2) the initiation probability, P_I, can be determined by

$$P_I(T) = 1 - P(c(\delta, t) < c_{cr} \quad \forall\, t \in [0, T]) \tag{2.7}$$

where $c(\delta, t)$ denotes the chloride concentration around the reinforcement at the time t and where it has been used that the chloride concentration is a monotonic increasing function of time. The method is based on the same model of chloride ingress as the traditional analysis. The surface concentration, the transport coefficient and the critical threshold for initiation of corrosion are modelled as stochastic variables. However, no information from measurements performed on a given structure is included in the analysis. However, as earlier mentioned, D depends on a number of factors: time, w/c-ratio, cement content, the presence of additional constituents such as micro-silica or fly-ash and factors connected with the construction process as e.g. casting and vibration. This implies that D is very difficult to predict. Any probabilistic model of D which is not based on measurements from a given structure, therefore, has to indicate that the coefficient of variation of D is large. This again implies that the estimate of the initiation time also has a large coefficient of variation. This has also been demonstrated by Hoffman and Weyers [12] who perform a similar analysis using data from more than 300 different bridges. In an example they show that the probability that corrosion has been initiated after 10 years is about 0.02 and that the probability after 50 years is 0.8. This demonstrates the large variation of the estimated lifetime. Another setback of this simple method is that the size of the considered structure is not taken into account. Clearly, the probability that corrosion has been initiated increases with increasing size of the structure because for a large structure the transport coefficient and surface concentration are more likely to be high at some point.

On the basis of this type of analysis it can be concluded that in order to reduce the variability of the estimate of the time to initiation of corrosion it is necessary to take into account information about the state of the structure whose lifetime is to be estimated.

Karlsson and Poulsen [13] also use probabilistic methods. However, they determine the required cover thickness in order to reach a given probability that corrosion is initiated within a given time period. The model is based on the model for chloride transport suggested by Poulsen [23] where the transport coefficient is modelled as a function of time. Also in this analysis the size of the structure is not taken into account.

2.5   Repair and Maintenance Methods

Given an estimate of the lifetime of a structure the engineer has to choose among a number of different repair and maintenance strategies. These strategies are associated with different costs and can be applied at different stages of the deterioration process. The most commonly used methods are

- Surface coating.
- Cathodic protection.
- Removal of Chloride-contaminated concrete.

It must be emphazised that the above-mentioned methods are not actual repair and maintenance strategies. Actual strategies will often consist of a combination of the different methods.

Surface Coating
The purpose of applying a surface coating is to prevent or at least reduce the chloride flow. It is usual to distinguish between two types of surface coating: paints and membranes. The major difference between paints and membranes is that membranes are tighter. For a more detailed description see e.g. Poulsen [24]. The major disadvantage of the method is that the surface coating must be applied at a relative early stage because it must be ensured that the chloride which is already contained in the concrete does not redistribute itself in such a way that the chloride concentration around the reinforcement exceeds the critical level. The method is, however, not expensive.

Cathodic Protection
There is a large number of systems for applying cathodic protection to concrete structures, see e.g. Andersen and Strunge [1] and Rostam and Buhr [25]. The methods, however, are all based on the same principle. By the use of an external anode a current is applied to the reinforcement. The steel thus is rendered a cathode and does, therefore, not corrode. The current can be provided by a sacrificial anode of a more reactive metal or it can be provided by applying a current. Cathodic protection can be used to prevent corrosion from being initiated and to stop corrosion which is already in progress. The method can be applied at a later stage of deterioration than the surface coating. It is, however, more expensive.

Removal of Chloride-Contaminated Concrete
An orthodox way of dealing with the problem of chloride ingress is simply to remove and replace the chloride-contaminated concrete and the corroded reinforcement. This type of extensive repair is usually carried out when the concrete surface shows distinct signs of corrosion and no preventive measures can be carried out. The major advantage of this method is that it allows for the repair to be postponed to a very late stage of the deterioration process and that it is fairly easy to detect the visible signs which suggest that the repair must be carried out. However, the method is much more expensive than the two methods presented above.

2.6 References

[1] Andersen, O. V., Strunge, H., En metode til aktiv korrosionsbeskyttelse af armering i beton, Dansk Beton, 2, 5, pp. 8-17, in Danish.

[2] Bakker, R. F. M., Initiation Period, Corrosion of Steel in Concrete, Ed.: Schießl, P., Chapman and Hall, New York, USA.

[3] Bažant, Z. P., Physical Model for Steel Corrosion in Concrete Sea Structures, Journal of the Structural Division, 105, pp. 1137-153.

[4] Bažant, Z. P., Najjar, L. J., Drying of Concrete as a Nonlinear Diffusion Problem, Cement and Concrete Research, 1, pp. 461-473.

[5] Bažant, Z. P., Thonguthai, W., Pore Pressure and Drying of Concrete at High Temperature, Jounral of Engineering Mechanics, ASCE, 104, 5, pp. 1059-1080.

[6] Bentz, D. P., Garboczi, E. J., Percolation of Phases in a Three-Dimensional Cement Paste Microstructural Model, Cement and Concrete Research, 21, pp. 325-344.

[7] Comité Euro-International du Beton, Durable Concrete Structures, Thomas Telford, London, England.

[8] DS423.28, Betonprøvning, Hærdnet Beton, Chloridindhold, Dansk Standard, Hellerup, Denmark, 1984. In Danish.

[9] Hausmann, D. A., Steel Corrosion of Concrete, Materials Protection, 1967, pp. 19-23.

[10] Henriksen, C. F., Stoltzner, E., Kloridbetinget Korrosion, Dansk Beton, 3, 1992. In Danish.

[11] Herholdt, A. D.et al., Betonbogen, Aalborg Portland, Cementfabrikkernes Tekniske Oplysningskontor, 1985, in Danish.

[12] Hoffman, P. C., Weyers, R. E., Probabilistic Analysis of Reinforced Concrete Bridge Decks, in: Frangopol, D.M., Grigoriu, M. D., (Eds.), Probabilistic Mechanics and Structural Reliability, ASCE, New York, 1996, pp. 290-293.

[13] Karlsson, M., Poulsen, E., Design of Rebar Concrete Covers in Marine Concrete Structures, Probabilistic Approach, International RILEM Workshop, Chloride Penetration into Concrete, Saint-Rémy-Les-Chevreuse, 1995.

[14] Johansen, V., The Modelling of Microstructure and its Potential for Studying Transport Properties and Durability, Rilem Workshop, Saint-Remy-les-Chevreuse, July, 1994.

[15] Mangat, P. S., Molloy, B. T., Prediction of Long Term Chloride Concentration in Concrete, Materials and Structures, 1994, 27, pp. 338-346.

[16] Melchers, R. E., Probabilistic Modelling of Seawater Corrosion of Steel Structures, Applications of Statistics and Probability, Eds.: Lemaire, Favre and Mebarki, ICASP7-conference, Paris, 1995.

[17] Müller, H. H., Bestimmung des Korrosionsaktiven Chlorids in Abhängigkeit von Zementart und W/C-Wert, Internal Report, Technical University of Munich, Germany.

[18] Neville, A. M., Brooks, J. J., Concrete Technology, Longman Scientific and Technical, Harlow, England, 1987.

[19] Nielsen-Dharmaratne, Potential and Resistance Mapping, 1990, Dansk Beton, 2, 1990, p. 11.

[20] Pedersen, C., Thoft-Christensen, P., Reliability Analysis of Prestressed Concrete Beams with Corroded Tendons, Structural Reliability Theory Paper No. 109, Aalborg University, 1993.

[21] Pettersson, K., Corrosion Threshold Value and Corrosion Rate in Reinforced Concrete, CBI Report 2.92, Cement- och betoninstitutet, Stockholm, Sweden.

[22] Poulsen, E., Chloride Profiles, Determination, Interpretation and Practice, Corrosion of Reinforcement, Proceedings of the Nordic Seminar in Lund, Editor: Kyösti Tuutti, Lund, Sweden, 1995.

[23] Poulsen, E., Design of Rebar Concrete Covers in Marine Concrete Structures, Deterministic Approach, International RILEM Workshop, Chloride Penetration into Concrete, Saint-Rémy-Les-Chevreuse, 1995.

[24] Poulsen, E., Böttzau, J., Hansen, P., Malinger og membraner til betons overfladebeskyttelse, 1993, Dansk Teknologisk Institut, R60-93, In Danish.

[25] Rostam, S., Buhr, B., Katodisk beskyttelse af brosøjler, Dansk Beton, 2, 5, pp. 24-28, in Danish.

[26] Okada, K., Miyagawa, T., Chloride Corrosion of Reinforcing Steel in Cracked Concrete, ACI Special Publication SP65, Performance of Concrete in Marine Environment, 1980, Detroit, Michigan, pp. 237-254.

[27] Saetta, A. V., Scotta, R. V., Vitaliani, R. V., Analysis of Chloride Diffusion into Partially Saturated Concrete.

[28] Schießl, P., Corrosion of Steel in Concrete, Report of the Technical Comittee 60-CSC RILEM, Chapman and Hall, London,England, 1988.

[29] Schießl, P., Diffusionsmodell zur rechnerischen Erfassung der Chloridionendiffusion in Beton, IBS, Technische Universität München, 1983, in German.

[30] Stoltzner, E., Sørensen, B., Chloridundersøgelser på Farøbroerne, Dansk Beton, 11, 1, pp. 16-18, in Danish.

[31] Sørensen, B., Kloridtransport i Beton, Beton-Teknik, 3, 17, 1990, in Danish.

[32] Tredaway, K., Corrosion Period, Corrosion of Steel in Concrete, Ed.: Schießl, P., Chapman and Hall, New York, USA.

[33] Tuutti, K., Corrosion of Steel in Concrete, CBI Forskning 4.82, Cement- och betoninstitutet, Stockholm, Sweden.

[34] Østergård, A. S., Analyse af Chloridprofiler i Beton, Masters Thesis, Technical Univeristy of Denmark, IMM-DTU, 1995, in Danish.

Chapter 3

Probabilistic Model and the Stochastic Finite Element Method

On the basis of the discussion of the nature of concrete and chloride-initiated corrosion in chapter 2 it is now possible to formulate a probabilistic model of chloride ingress in concrete structures. When formulating a probabilistic model for reliability analysis it is normal to distinguish between the following types of uncertainty

- Inherent physical uncertainty.
- Statistical uncertainty.
- Model uncertainty.
- Human Error.

Physical quantities such as loads, material properties and dimensions have an inherent uncertainty which can be described in terms of stochastic variables, processes or fields. The parameters in the stochastic model of the inherent uncertainty can be determined on the basis of measurements and experiments. However, since only a limited number of measurements or experiments will be available the estimated parameters are subject to some uncertainty, the so-called statistical uncertainty.

The analysis of structural elements and systems is based on mathematical models which only in very few cases are able to predict the response of the considered element or system. It is, in general, necessary to take the accuracy of the model into account when performing a reliability analysis. The uncertainty related to the model can, of course, be reduced by using a more refined model.

The most common cause of failure of civil engineering structures is human errors made during either the design or construction of the given structure. These errors, however, are not taken into account when performing a reliability analysis. These errors must be taken care of by quality assurance, see e.g. Engelund and Rackwitz [7].

3.1 Probabilistic Model of Chloride Ingress

In chapter 2 it was established that chloride is transferred from the surroundings into the concrete through the system of capillary pores and microcracks and that the transport

is a complex phenomenon involving various mechanisms such as diffusion of chloride and transport of chlorides by the flow of water. However, measurements from existing un-cracked structures (cracks smaller than 0.1 mm, see e.g Tuutti (1982)) with not too low w/c-ratios support the assumption that the chloride concentration can be considered as the solution to a suitable diffusion problem which in a general form can be stated as

$$\begin{aligned}
\frac{\partial c(\mathbf{x},t)}{\partial t} &= \nabla^T \left(\mathbf{D}\left(\mathbf{x},t\right) \nabla c\left(\mathbf{x},t\right) \right) & \\
c\left(\mathbf{x},t\right) &= c_s\left(t\right) & \mathbf{x} \in \{S_g\}
\end{aligned} \right\} \qquad (3.1)$$

where $\mathbf{x}$ denotes a point in a Cartesian coordinate system, $\nabla^T = \begin{bmatrix} \partial/\partial x_1 & \partial/\partial x_2 & \partial/\partial x_3 \end{bmatrix}$ is the gradient operator, $\mathbf{D}$ is the constitutive matrix and $\{S_g\}$ is the part of the surface with known chloride concentration,

It is important to notice that it is not assumed that chloride ingress is caused by diffusion only. The diffusion equation has been selected because the solution can be brought to fit measurements from existing structures and because the parameters in the model can be given a physical interpretation. Any other model which can be brought to fit the measured chloride concentrations can in principle be implemented. However, it is difficult to gain any physical understanding of the problem if the parameters in the model have no physical meaning.

As stated earlier the pore system of concretes with low w/c-ratios may not be connected. It can, therefore, be argued that the chloride can only penetrate to a certain depth. It is evident that this problem cannot be described by the suggested model, eq. (3.1), see also section 2.2.4.

3.1.1   Constitutive Model

Since concrete is a composite material consisting of aggregates bound together by hydrated cement paste, it is evident that the resistance of the concrete to chloride ingress, is a non-differentiable function of the position, $\mathbf{x}$. In reality, however, the chloride concentration at a given point $\mathbf{x}$ is the local average of the chloride concentration over a given volume. In a similar manner the elements in the constitutive matrix must be interpreted as a local average over a given volume of the concrete structure. This averaging implies that the constitutive matrix becomes a differentiable function of $\mathbf{x}$, see e.g. Ostra-Starzewski [16].

The random distribution of aggregates, capillary pores and microcracks within concrete structures leads to an inherent random spatial fluctuation of the constitutive matrix. Since this variability is associated with the microstructure of the concrete the correlation length of the field describing these fluctuations must be assumed to be very small. Further, it has been proved that the constitutive matrix exhibits a random spatial variation with a much larger correlation length of about 200-500 mm. Hergenröder [10] states that this variability can be caused by the spatial variation of the compression of the fresh concrete and Stoltzner and Sørensen [22] report that the variability can be caused by fluctuations of the w/c-ratio within the structure. The porosity of the outer layers of a concrete structure is usually different from the porosity of the rest of the structure. Hence, the mean value of the constitutive matrix is not constant within the material. We consider the following general model of the constitutive matrix

$$\{\mathbf{D}(\mathbf{x})\} = \mathbf{D}_0(\mathbf{x}) + \{\mathbf{D}_1(\mathbf{x})\} + \{\mathbf{D}_2(\mathbf{x})\} \tag{3.2}$$

where $\mathbf{D}_0(\mathbf{x})$ is a deterministic function of $\mathbf{x}$, $\{\mathbf{D}_1(\mathbf{x})\}$ is a zero mean matrix where the elements are modelled as random fields with a low scale of fluctuation and $\{\mathbf{D}_2(\mathbf{x})\}$ is a zero mean matrix where the elements are modelled as random fields with a larger scale of fluctuation.

On the basis of a large number of measurement series Hergenröder [10] suggested a similar model for the alkalinity interface in carbonated concrete. For carbonation to take place CO_2 must be conveyed from the surroundings, where the concentration is constant, into the concrete. Therefore, the spatial variation of the alkalinity interface also expresses the spatial variation of the permeability of the concrete.

The matrices $\{\mathbf{D}_1(\mathbf{x})\}$ and $\{\mathbf{D}_2(\mathbf{x})\}$ in the general 3-dimensional case consists of nine elements which all can be modelled as stochastic fields. However, only a very limited number of measurements from a given structure is available, making it difficult to estimate more than a few parameters with sufficient accuracy. Further, it will be difficult to ensure that the constitutive matrix is always positive definite. It will always be necessary to apply a simplified model taking into account that the model uncertainty increases as the constitutive model is simplified. The model, in fact, must depend on the available data.

A substantial simplification is achieved by assuming that the material is isotropic, i.e. $\{\mathbf{D}(\mathbf{x})\} = \{D(\mathbf{x})\}\mathbf{I}$ where $\{D(\mathbf{x})\} = D_0(\mathbf{x}) + \{D_1(\mathbf{x})\} + \{D_2(\mathbf{x})\}$ denotes the transport coefficient and $\mathbf{I}$ is the identity matrix. The mean value is $D_0(\mathbf{x})$ and $\{D_1(\mathbf{x})\}$ and $\{D_2(\mathbf{x})\}$ are stochastic fields with different correlation lengths. Alternatively, it could be assumed that the relations between the elements in the constitutive matrix are constant within the material such that $\{\mathbf{D}(\mathbf{x})\} = \{D(\mathbf{x})\}\mathbf{d}$, where $\mathbf{d}$ is a deterministic positive definite matrix.

The most simple models of $\{D_1(\mathbf{x})\}$ and $\{D_2(\mathbf{x})\}$ are obtained by assuming that they are independent and homogeneous Gaussian fields. It is then only necessary to estimate the parameters in the auto-covariance functions $\kappa_{D_1 D_1}$ and $\kappa_{D_2 D_2}$. It has then implicitly been assumed that the variability of the fields is small enough, compared to the mean value, $D_0(\mathbf{x})$, to ensure that the probability of obtaining negative values of the transport coefficient is negligible. If the probability of obtaining negative values is not negligible the transport coefficient can, alternatively, be assumed to follow a log-normal distribution.

In the above model the transport coefficient has been assumed to be constant with the time t. However, some investigators argue that the transport coefficient is a function of time, see e.g. Poulsen [18]. This variation can also be included in the presented model, e.g. simply by letting the parameters in the model be time-dependent. The estimation of the parameters then of course is more complicated and requires a larger amount of data.

3.2 Surface Concentration

When the surface of a structure is subject to a spray of salt-containing water it results in the build-up of a surface concentration of chloride. The most common examples of this phenomenon are piers in a marine environment and bridge piers placed by a roadway. The surface concentration depends on the amount of spray of salt-containing water. E.g. for

piers in a marine environment the surface concentration depends on whether the surface faces up-stream or down-stream and on the distance to the mean water level. It is evident that the spray of salt-containing water is not performed in some regular manner and that the surface concentration, therefore, will exhibit a random spatial fluctuation. The surface concentration is modelled by

$$\{c_s(\mathbf{x})\} = c_{s_0}(\mathbf{x}) + \{c_{s_1}(\mathbf{x})\} \qquad \mathbf{x} \in \{S_g\} \tag{3.3}$$

where $c_{s_0}(\mathbf{x})$ denotes the mean value function and $\{c_{s_1}(\mathbf{x})\}$ represents the random spatial fluctuation.

A substantial simplification can be obtained if only a relatively small area on a given structure is investigated, e.g. the area where the mean value, $c_{s_0}(\mathbf{x})$, attains its maximum value. Within this area $\{c_s(\mathbf{x})\}$ may be assumed to be a homogeneous Gaussian field with unknown mean and auto-covariance. Again it is assumed that the variability of the field is so small compared to the mean value that the probability of obtaining negative values of $\{c_s(\mathbf{x})\}$ is negligible. Again, a log-normal distribution can be assumed if the probability of obtaining negative values is not negligible.

Also the surface concentration might be a function of time and as for the transport coefficient this variation can be taken into account if the data suggests so.

3.3   Cover Thickness

The cover is defined as the distance from a point on the surface of a structure to the reinforcement. According to the Danish design criteria the cover thickness, δ, must have a given minimum value, d_0. However, it must not be larger than $d_0 + \Delta$, where Δ denotes the tolerance. During the construction phase it is checked that the cover lies within the given limits. If the control were perfect, δ could be modelled as a stochastic variable uniformly distributed in the interval $[d_0; d_0 + \Delta]$. However, the control is not perfect and the cover exhibits a substantial variation. The following model is suggested

$$\{\delta(\mathbf{x})\} = \delta_0 + \{\delta_1(\mathbf{x})\} \qquad \mathbf{x} \in \{S_g\} \tag{3.4}$$

where δ_0 is the mean cover and $\{\delta_1(\mathbf{x})\}$ is a stochastic field describing the spatial variation of the cover. The mean cover can be modelled as a normal distribution with mean $d_0 + \Delta/2$ and a given standard deviation. Detailed investigations of the spatial variation of the cover in a given structure are not known to the author. But the spatial variation can e.g. be assumed to follow a simple deterministic function of the sine-type with unknown amplitude. The amplitude can also be assumed to be normally distributed with a given mean and standard deviation which can be determined on the basis of measurements. The frequency of the fluctuation depends on the distance between the spacers and the thickness of the reinforcement.

Very little data is available on the basis of which such models can be formulated. Such models depend on the considered structure as well as the knowledge and beliefs of the model builder. It is evident that the result of any analysis performed on this basis also

depends on the beliefs of the model builder and that different model builders might reach different conclusions.

3.4 Finite Element Formulations

According to the model introduced in section 3.1 the chloride concentration in a given structure can be determined on the basis of the diffusion equation. Furthermore, the transport coefficient is believed to exhibit a random spatial variation which must be taken into account. This problem can be treated within the framework of the Stochastic Finite Element Method. However, different formulations of the finite element method exist and a number of ways by which the spatial variation of the transport coefficient can be taken into account has been suggested by various researchers. In the following sections a number of these methods are presented and it is investigated if the different finite element methods lead to results that are substantially different.

The finite element method is a numerical method by which a set of partial differential equations which hold over a given region with known boundary conditions can be solved. The method is based on a discretization of the entire region into smaller parts, so-called finite elements. It is assumed that the response within each element can be approximated by simple shape functions which depend on the values in the nodes of the element. The problem has now been reduced to determining a finite number of unknowns, the nodal values. For each finite element a number of equations is obtained. By assembling the equations for all elements in a suitable manner an approximate solution to the differential equations can be found, see e.g Bathe [1], Zienkiewicz and Taylor [26] or Ottosen and Petersson [17].

The diffusion problem, eq. (3.1) can, alternatively, be given by the conservation equation, eq. (3.6), and the constitutive equation, eq. (3.5)

$$\mathbf{q} = -\mathbf{D}\nabla c \tag{3.5}$$
$$\nabla^T \mathbf{q} = \dot{c} \tag{3.6}$$

and a set of boundary conditions

$$\left. \begin{array}{rclcl} \mathbf{q}^T \mathbf{n} &=& q_n & \text{on } \{S_q\} \\ c &=& c_s & \text{on } \{S_g\} \end{array} \right\} \tag{3.7}$$

where $\mathbf{q}$ is the flow vector, c the concentration, $\mathbf{D}$ is the constitutive matrix and $\dot{c}$ is the derivative of the concentration with respect to time. In most cases it is assumed that the material is isotropic which implies that $\mathbf{D} = D\mathbf{I}$ where $\mathbf{I}$ denotes the identity matrix and D the transport coefficient. Further, $\mathbf{n}$ is an unit vector normal to the surface and pointed outwards, and $\{S_q\}$ and $\{S_g\}$ are the parts of the surface with known flux and concentration, respectively. The surface concentration c_s and surface flux q_n are known quantities.

3.5   The Finite Element Method

The partial differential equations can be solved by the Finite Element Method. A number of different finite element formulations of the diffusion problem exists. Four different finite element formulations of the diffusion problem are investigated

- Standard Formulation.
- Mixed Formulation.
- Hybrid Formulation.
- Flux-based Formulation.

The finite element method is based on a discretization of the region over which the differential equations 3.6 and 3.5 hold into finte elements. For each of these elements an approximation of the variation of c and q is then carried out.

By the standard formulation the chloride concentration within each element is allowed to vary according to given shape functions and the stiffness matrix is found as a weighted integral of D where the weights are the derivatives of the shape functions. The stiffness matrix is in fact a weighted integral of the conductivity. The standard formulation ensures that the concentration, c, is continuous over the element boundaries. The flux vector q, however, will not be continuous. In most cases this problem is of little importance and the standard formulation is the most widely used method due to its relative simplicity and large efficiency.

By the mixed formulation both the concentration and the flow vector are approximated by the use of shape functions. The advantage of the mixed method over the standard method is that it ensures inter-element continuity of q, and, therefore, gives a better representation of the flux. This is, however, achieved at the expense of having a larger number of variables, which implies that the number of equations increase, and that the solution of the FEM-equations becomes more expensive in terms of CPU-time. It should also be noted that, if the diffusion coefficient is constant within the elements and the shape functions only allows q and c to vary in the same way as by the standard formulation, then the mixed formulation and the standard formulation will lead to the same result (see Ziankiewicz and Taylor [26]).

The hybrid method is based on the mixed method. The flux is defined as a local variable within the interior of each element and the concentrations are defined as global variables on the boundary of the elements. The flux vector can now be eliminated from the problem. The inverse of the stiffness matrix is now a weighted integral of the inverse of the transport coefficient, D, i.e. the inverse of the stiffness matrix becomes a weighted integral of the resistance of the material. Like the standard formulation the hybrid formulation does not ensure inter-element continuity of the flux vector q. Further, in order to determine the element stiffness matrices it is necessary to compute the inverse of $n \times n$-matrix, where n denotes the number of nodes in the element. For models with a large number of elements with a large number of nodes this might imply a significant reduction of the efficiency of the mixed method in comparison with the standard formulation.

The flux-based method is not like the other three methods based on shape functions which describe the variation of c and q within the elements, but on the assumption that

the variation of c along the element boundaries is inversely proportional to the transport coefficient. The fact that c does not have to vary according to given shape functions should imply that larger elements can be used and that the method becomes more efficient. In order to determine the element stiffness matrix it is, however, necessary to solve an integral of the inverse of the transport coefficient over the area of the element and a line integral of D^{-1} along each side of the element. The computational effort required to determine the element stiffness matrices thereby increases.

In the following sections the four formulations of the finite element method are presented in more detail.

3.5.1 Standard Formulation

The conservation equation, eq. (3.6), is multiplied by a weight, w, and integrated over the volume, V, of the considered element

$$\int_V w\nabla^T \mathbf{q}dV + \int_V w\dot{c}dV = 0 \qquad (3.8)$$

Using partial integration on the first term of the integral, eq. (3.8) gives

$$-\int_V (\nabla w)^T \mathbf{q}dV + \int_V w\dot{c}dV = -\int_S wq_n dS \qquad (3.9)$$

where $q_n = \mathbf{q}^T\mathbf{n}$. This is the so-called weak form of the conservation equation. Using the constitutive equation, eq.(3.5), eq. (3.9) can be rewritten as

$$\int_V (\nabla w)^T \mathbf{D}\nabla c dV + \int_V w\dot{c}dV = -\int_S wq_n dS \qquad (3.10)$$

Now the FEM approximation $c = \mathbf{N}_c\bar{\mathbf{c}}^e$ is introduced, where $\mathbf{N}_c$ are the shape functions for c and $\bar{\mathbf{c}}^e$ are the nodal concentrations in a given element. According to the Galerkin method the weight, $w = \mathbf{N}_c\mathbf{a} = \mathbf{a}^T\mathbf{N}_c^T$ is chosen, where $\mathbf{a}$ is an arbitrary vector.

$$\mathbf{a}^T\int_V (\nabla \mathbf{N}_c)^T \mathbf{D}\nabla\mathbf{N}_c dV\bar{\mathbf{c}}^e + \mathbf{a}^T\int_V \mathbf{N}_c^T\mathbf{N}_c dV\dot{\bar{\mathbf{c}}}^e = -\mathbf{a}^T\int_S \mathbf{N}_c^T q_n dS \qquad (3.11)$$

Using the fact that this equation must hold for arbitrary $\mathbf{a}$ it is now found that

$$\mathbf{K}^e\bar{\mathbf{c}}^e + \mathbf{E}^e\dot{\bar{\mathbf{c}}}^e = \mathbf{R}^e \qquad (3.12)$$

where

$$\mathbf{K}^e = \int_V \mathbf{B}_c^T\mathbf{D}\mathbf{B}_c dV, \qquad \mathbf{E}^e = \int_V \mathbf{N}_c\mathbf{N}_c^T dV, \qquad \mathbf{R}^e = -\int_S \mathbf{N}_c^T q_n dS \qquad (3.13)$$

where $\mathbf{B}_c = \nabla\mathbf{N}_c$.

By assembling the global stiffness matrix, $\mathbf{K}$, the global mass matrix, $\mathbf{E}$, and the global load vector, $\mathbf{R}$, in a suitable manner a set of global equations is obtained

$$\mathbf{K}\bar{\mathbf{c}} + \mathbf{E}\dot{\bar{\mathbf{c}}} = \mathbf{R} \qquad (3.14)$$

where $\overline{c}$ is the vector of global nodal concentrations. The finite element equation, eq. (3.14), can be solved by a backward difference scheme.

3.5.2 Mixed Formulation

By the so-called mixed formulation both the chloride concentration, c, and the chloride flow vector, $\mathbf{q}$, are approximated by the use of appropriate shape functions.

$$c = \mathbf{N}_c \overline{\mathbf{c}}^e \tag{3.15}$$

$$\mathbf{q} = \mathbf{N}_q \overline{\mathbf{q}}^e \tag{3.16}$$

where $\mathbf{N}_q$ are the shapefunctions for the chloride flow vector and $\overline{\mathbf{q}}^e$ contains the nodal flow vectors. Eq. (3.5) is multiplied by $\mathbf{D}^{-1}$ and a weight function w and integrated over the volume of the finite element, V

$$\int_V w \mathbf{D}^{-1} \mathbf{q} \, dV + \int_V w \nabla c = 0 \tag{3.17}$$

Now the approximations for c and $\mathbf{q}$ given by eqs. (3.15) and (3.16) are introduced and the weight $w = \mathbf{a}^T \mathbf{N}_q^T$ is selected, where $\mathbf{a}$ is an arbitrary vector

$$\mathbf{a}^T \int_V \mathbf{N}_q^T \mathbf{D}^{-1} \mathbf{N}_q \, dV \overline{\mathbf{q}}^e + \mathbf{a}^T \int_V \mathbf{N}_q^T \nabla \mathbf{N}_c \, dV \overline{\mathbf{c}}^e = 0 \tag{3.18}$$

Eq. (3.18) must hold for an arbitrary vector $\mathbf{a}$, whereby

$$\mathbf{A}^e \overline{\mathbf{q}}^e + \mathbf{G}^e \overline{\mathbf{c}}^e = 0 \tag{3.19}$$

where

$$\mathbf{A}^e = \int_V \mathbf{N}_q^T \mathbf{D}^{-1} \mathbf{N_q} \, dV, \qquad \mathbf{G}^e = \int_V \mathbf{N}_q^T \nabla \mathbf{N}_c \, dV \tag{3.20}$$

By introducing the approximations for $\mathbf{q}$ and c given by eqs. (3.16) and (3.15) in the weak form of the conservation equation, eq. (3.9), and choosing the weight $w = \mathbf{N}_c \mathbf{a}$ the following is obtained

$$\mathbf{a}^T \int_V \nabla \mathbf{N}_c^T \mathbf{N}_q \, dV \overline{\mathbf{q}}^e - \mathbf{a}^T \int_V \mathbf{N}_c^T \mathbf{N}_c \, dV \dot{\overline{\mathbf{c}}}^e = \mathbf{a}^T \int_S \mathbf{N}_c^T q_n \, dS \tag{3.21}$$

This equation holds for an arbitrary vector $\mathbf{a}$ which implies that

$$\mathbf{G}^{eT} \overline{\mathbf{q}}^e - \mathbf{E}^e \dot{\overline{\mathbf{c}}}^e = -\mathbf{R}^e \tag{3.22}$$

where

$$\mathbf{E}^e = \int_V \mathbf{N}_c^T \mathbf{N}_c \, dV, \qquad \mathbf{R}^e = -\int_S \mathbf{N}_c^T q_n \, dS \tag{3.23}$$

For each element the equations (3.19) and (3.22) are obtained which can be written as

$$\begin{bmatrix} \mathbf{A}^e & \mathbf{G}^e & \mathbf{0} \\ \mathbf{G}^{eT} & \mathbf{0} & \mathbf{E}^e \end{bmatrix} \begin{bmatrix} \overline{\mathbf{q}}^e \\ \overline{\mathbf{c}}^e \\ \dot{\overline{\mathbf{c}}}^e \end{bmatrix} = \begin{bmatrix} \mathbf{0} \\ -\mathbf{R}^e \end{bmatrix} \tag{3.24}$$

where $\mathbf{0}$ denotes the a zero matrix. These equations can be assembled in a suitable manner to a global set of equations.

3.5.3 Hybrid Method

By defining $\overline{\mathbf{q}}^e$ as a local variable describing the flux within a given element, $\overline{\mathbf{q}}^e$ can be isolated in eq. (3.19) and inserted into eq. (3.22). The following equation in the variables $\overline{\mathbf{c}}^e$ defined on the element interfaces is obtained

$$\left(\mathbf{G}^{eT} \mathbf{A}^{e-1} \mathbf{G}^e \right) \overline{\mathbf{c}}^e + \mathbf{E}^e \dot{\overline{\mathbf{c}}}^e = \mathbf{R}^e \Leftrightarrow$$
$$\mathbf{S}^e \overline{\mathbf{c}}^e + \mathbf{E}^e \dot{\overline{\mathbf{c}}}^e = \mathbf{R}^e \tag{3.25}$$

This representation is only valid in case the rank of the matrix $\left(\mathbf{G}^{eT} \mathbf{A}^{e-1} \mathbf{G}^e \right)$ is equal to the number of unknowns in $\mathbf{c}^e$, n_c. The rank of $\left(\mathbf{G}^{eT} \mathbf{A}^{e-1} \mathbf{G}^e \right)$, however cannot be larger than the rank of $\mathbf{A}^{e-1}$ which is equal to the number of unknowns in the vector $\overline{\mathbf{q}}^e$, n_q. Therefore, a necessary condition for eq. (3.25) to be valid is that $n_q \geq n_c$.

As by the standard formulation it is now possible to gather the equations for all elements in a suitable manner and to solve these for $\overline{\mathbf{c}}$ by a backward difference method.

3.5.4 Flux-Based Formulation

In order to obtain a flux-based formulation of the diffusion problem the functional Π describing the total energy is considered

$$\Pi = -\frac{1}{2} \int_V (\nabla c)^T \mathbf{D} \nabla c \, dV + \int_S \mathbf{q} \mathbf{n} c \, ds \tag{3.26}$$

Under the assumption that the material is isotropic and by using the constitutive equation, eq. (3.5), the functional can be written

$$\Pi = -\frac{1}{2} \int_V \frac{1}{D} \mathbf{q}^T \mathbf{q} \, dV + \int_S \mathbf{q} \mathbf{n} c \, ds \tag{3.27}$$

Using the fact that a solution to the diffusion problem can be found by determining the function c for which Π is stationary, the variation of Π is found

$$\delta \Pi = \delta \mathbf{q} \left(-\mathbf{q} \int_V \frac{1}{D} dV + \int_S \mathbf{n} c \, ds \right) = 0 \quad \Rightarrow \tag{3.28}$$

$$\mathbf{q} = \frac{1}{\int_V \frac{1}{D} dV} \int_S \mathbf{n} c \, dS \tag{3.29}$$
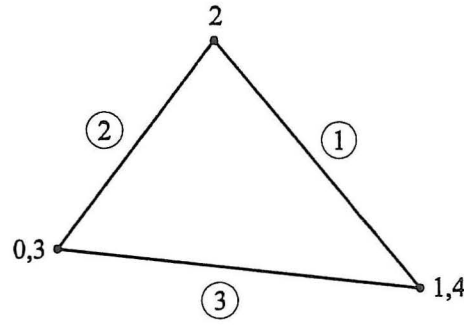
Figure 3.1: *Flux-based triangle*

Now consider the three-node element shown in figure 3.1 where 1 and 4 denote the same node and 0 and 3 denote the same node. In eq. (3.29) it is necessary to solve the integral

$$\int_S \mathbf{n} c \, dS \tag{3.30}$$

Instead of performing a linear interpolation of c between the nodes it is assumed that along side j

$$\frac{dc}{ds} = \frac{a_j}{D} \tag{3.31}$$

where a_j is some constant. By integration of eq. (3.31) it is found that

$$c_{j+1} - c_j = \int_{S_j} \frac{dc}{ds} = a_j \int_{S_j} \frac{ds}{D} \tag{3.32}$$

The surface integral eq. (3.30) can now be written

$$
\begin{aligned}
\int_S \mathbf{n} c \, dS &= \sum_{j=1}^{3} \mathbf{n}_j \int_{S_j} 1 \cdot c \, ds \\
&= \sum_{j=1}^{3} \mathbf{n}_j \left([sc]_0^{l_j} - \int_{S_j} s \frac{dc}{ds} ds \right) \\
&= \sum_{j=1}^{3} \mathbf{n}_j l_j \left(c_{j+1} - (c_{j+1} - c_j) \frac{\int_{S_j} \frac{1}{D} s \, ds}{l_j \int_{S_j} \frac{1}{D} ds} \right)
\end{aligned}
\tag{3.33}
$$

where l_j denotes the length of side j. Now introduce γ_j which expresses the relative position of the centre of gravity of $\frac{1}{D}$ along side j

$$\frac{1}{2} + \frac{\gamma_j}{2} = \frac{\int_{S_j} \frac{1}{D} s \, ds}{l_j \int_{S_j} \frac{1}{D} ds} \tag{3.34}$$

It is seen that $-1 < \gamma_j < 1$ and that $\gamma_j = 0$ if D is constant along side j. Eq. (3.33) now can be written

$$\int_S \mathbf{n}c\,dS = \sum_{j=1}^{3} \mathbf{n}_j l_j \left(\frac{1}{2}(c_{j+1} + c_j) - \frac{\gamma_j}{2}(c_{j+1} - c_j) \right) \tag{3.35}$$

Using that $\sum_{j=1}^{3} \mathbf{n}l_j = 0$ and introducing $\mathbf{r}_j = \mathbf{n}_j l_j$ it is found that

$$
\begin{aligned}
\int_S \mathbf{n}c\,dS &= -\frac{1}{2}\sum_{j=1}^{3} \mathbf{r}_j \left(c_{j-1} + \gamma_j(c_{j+1} - c_j) \right) \\
&= -\frac{1}{2}\sum_{j=1}^{3} \mathbf{r}_j c_{j-1}^*
\end{aligned}
\tag{3.36}
$$

where

$$\mathbf{c}^{e*} = \begin{bmatrix} c_0^* \\ c_1^* \\ c_2^* \end{bmatrix} = \begin{bmatrix} 1 & -\gamma_1 & \gamma_1 \\ \gamma_2 & 1 & -\gamma_2 \\ -\gamma_3 & \gamma_3 & 1 \end{bmatrix} \begin{bmatrix} c_0 \\ c_1 \\ c_2 \end{bmatrix} = \mathbf{H}^e \mathbf{c}^e \tag{3.37}$$

Using eq. (3.27) the total energy now can be written

$$\Pi = \frac{1}{2}\mathbf{c}^{e*T}\mathbf{K}^{*e}\mathbf{c}^{*e} = \frac{1}{2}\mathbf{c}^{eT}\mathbf{H}^{eT}\mathbf{K}^{e*}\mathbf{H}^e\mathbf{c}^e \tag{3.38}$$

where $\mathbf{K}^{e*}$ is given by

$$\mathbf{K}^{e*} = \frac{1}{4\int_V \frac{1}{D}dV} \begin{bmatrix} \mathbf{r}_1^T\mathbf{r}_1 & \mathbf{r}_1^T\mathbf{r}_2 & \mathbf{r}_1^T\mathbf{r}_3 \\ \mathbf{r}_1^T\mathbf{r}_2 & \mathbf{r}_2^T\mathbf{r}_2 & \mathbf{r}_2^T\mathbf{r}_3 \\ \mathbf{r}_1^T\mathbf{r}_3 & \mathbf{r}_2^T\mathbf{r}_3 & \mathbf{r}_3^T\mathbf{r}_3 \end{bmatrix} \tag{3.39}$$

The local stiffness matrix is evidently given by $\mathbf{H}^{eT}\mathbf{K}^{e*}\mathbf{H}^e$. The load vector and the mass-matrix can be determined in the usual manner, and the equations can be assembled to a global set of equations.

3.6 Stochastic Finite Element Method

The stochastic finite element method is simply a method which, within the framework of the traditional finite element method, takes into account the random spatial variation of the material properties. The purpose of a stochastic finite element analysis is to determine the statistics of the response or to determine the probability of some extreme event which depends on the response.

A number of methods has been proposed by which the statistics of the response of a given system can be determined or by which an outcome of the response can be determined on the basis of an outcome of the material properties. The most widely used methods are

- Monte Carlo simulation.
- Neumann expansion.
- Pertubation method.
- Weighted integrals.

3.6.1 Monte Carlo Simulation

The most simple method is Monte Carlo simulation where the FEM-equations are determined and solved for each simulation of the randomly varying properties. Outcomes of the stochastic field(s) can e.g. be obtained by the spectral representation method first suggested by Borgmann [2] and generalized by Shinozuka and Jan [19] and others. However, it is in fact only necessary to determine the values of the field(s) at the Gauss-points used for the numerical integration necessary to determine the stiffness, mass and load matrices. If the mean value vector and the covariance matrix for these variables are known, outcomes of the variables can be generated.

As earlier stated, Monte Carlo simulation is inefficient if a large number of evaluations of the response is required in order to determine the statistics of the response or the probability of some event.

3.6.2 Neumann Expansion

The efficiency of the simulation can be improved by using the Neumann Expansion method. Consider a problem where the FEM-equations are given by

$$\mathbf{K}\overline{\mathbf{c}} = \mathbf{R} \tag{3.40}$$

and where the stiffness matrix can be expressed as a sum of two matrices

$$\mathbf{K} = \mathbf{K}_0 + \mathbf{K}_1 \tag{3.41}$$

where $\mathbf{K}_0$ and $\mathbf{K}_1$ express the mean of the stiffness matrix and the deviations from the mean, respectively. The solution to the problem given in eq. (3.40) is

$$\overline{\mathbf{c}} = (\mathbf{K}_0 + \mathbf{K}_1)^{-1}\mathbf{R} \tag{3.42}$$

The term $\mathbf{K}^{-1} = (\mathbf{K}_0 + \mathbf{K}_1)^{-1}$ can be expanded in a geometric series by

$$(\mathbf{K}_0 + \mathbf{K}_1)^{-1} = \sum_{i=1}^{\infty} \left(-\mathbf{K}_0^{-1}\mathbf{K}_1\right)^i \mathbf{K}_0^{-1} \tag{3.43}$$

The solution to the FEM-problem, eq. (3.42) now can be written as

$$\overline{\mathbf{c}} = \sum_{i=0}^{\infty} \left(\mathbf{K}_0^{-1}\mathbf{K}_1\right)^i \mathbf{K}_0^{-1}\mathbf{R} = \sum_{i=0}^{\infty} \left(\mathbf{K}_0^{-1}\mathbf{K}_1\right)^i \overline{\mathbf{c}}_0 = \overline{\mathbf{c}}_0 - \overline{\mathbf{c}}_1 + \overline{\mathbf{c}}_2 - \overline{\mathbf{c}}_3 \ldots \tag{3.44}$$

This problem can be solved by a recursive formula

$$\mathbf{K}_0\overline{\mathbf{c}}_i = \mathbf{K}_1\overline{\mathbf{c}}_{i-1} \tag{3.45}$$

The Neumann Expansion method is very efficient in comparison with the traditional Monte Carlo method because it is only necessary to determine the inverse of the first part of the stiffness matrix representing the mean values. The response of the system can then

be determined by using the recursive formula, eq. (3.45). Usually, the series given in eq. (3.44) is truncated after a few terms. The number of terms necessary to achieve a good approximation of the response depends on the coefficient of variation of the randomly varying property. As the coefficient of variation increases a larger number of terms has to be included in the series. The method, therefore, is most efficient if the coefficient of variation of the randomly varying property is low.

Usually, the Neumann expansion method is used in order to solve static problems. However, it can in principle also be used to solve time-variant problems. The solution of time-variant problems can as earlier mentioned be performed by the backward difference method where $\bar{c}(n\Delta t)$ is determined on the basis of $\bar{c}((n-1)\Delta t)$, where n is the number of time steps and Δt denotes the length of the time steps. By each time step the error made by truncating the series given in eq. (3.44) accumulates. Hence, the Neumann expansion method can only be used if the number of time steps is small.

3.6.3   Pertubation Method

The most widely used stochastic finite element method is probably the pertubation method which according to Shinozuka and Yamazaki [20] has been developed by several researchers. The spatially varying properties are represented by a n-dimensional vector of stochastic variables, $\mathbf{Z}$. The method is based on a Taylor series expansion of the stiffness matrix, the load vector and the response vector around the mean values of the elements of the stochastic vector, $\mathbf{Z}$. Assuming all the variables in the vector $\mathbf{Z}$ has zero mean and that the outcome of each element in $\mathbf{Z}$, z_i, is small, the stiffness matrix can be written

$$\mathbf{K} = \mathbf{K}_0 + \sum_{i=1}^{n} \mathbf{K}_i^I z_i + \frac{1}{2} \sum_{i=1}^{n} \sum_{j=1}^{n} \mathbf{K}_{ij}^{II} z_i z_j + \ldots \qquad (3.46)$$

where n denotes the number of variables, where $\mathbf{K}_0$ is determined on the basis of the mean values of $\mathbf{Z}$, and where $\mathbf{K}_i^I$ and $\mathbf{K}_{ij}^{II}$ are given by

$$\mathbf{K}_i^I = \left. \frac{\partial \mathbf{K}}{\partial z_i} \right|_{\mathbf{z}=\mathbf{0}} \qquad\qquad \mathbf{K}_{ij}^{II} = \left. \frac{\partial^2 \mathbf{K}}{\partial z_i \partial z_j} \right|_{\mathbf{z}=\mathbf{0}} \qquad (3.47)$$

In a similar manner the load vector can be Taylor expansioned

$$\mathbf{R} = \mathbf{R}_0 + \sum_{i=1}^{n} \mathbf{R}_i^I z_i + \frac{1}{2} \sum_{i=1}^{n} \sum_{j=1}^{n} \mathbf{R}_{ij}^{II} z_i z_j + \ldots \qquad (3.48)$$

where $\mathbf{R}_0$ is determined on the basis of the mean value vector of $\mathbf{Z}$ and where $\mathbf{R}_i^I$ and $\mathbf{R}_{ij}^{II}$ are given by

$$\mathbf{R}_i^I = \left. \frac{\partial \mathbf{R}}{\partial z_i} \right|_{\mathbf{z}=\mathbf{0}} \qquad\qquad \mathbf{R}_{ij}^{II} = \left. \frac{\partial^2 \mathbf{R}}{\partial z_i \partial z_j} \right|_{\mathbf{z}=\mathbf{0}} \qquad (3.49)$$

Finally, the response vector can be written

$$\overline{c} = \overline{c}_0 + \sum_{i=1}^{n} \overline{c}_i^I z_i + \frac{1}{2} \sum_{i=1}^{n} \sum_{j=1}^{n} \overline{c}_{ij}^{II} z_i z_j + \dots \qquad (3.50)$$

where $\overline{c}_0$, $\overline{c}_i^I$ and $\overline{c}_{ij}^{II}$ can be determined by

$$\overline{c}_0 = \mathbf{K}_0^{-1} \mathbf{R}_0 \qquad (3.51)$$

$$\overline{c}_i^I = \mathbf{K}_0^{-1} \left(\mathbf{R}_i^I - \mathbf{K}_i^I \overline{c}_0 \right) \qquad (3.52)$$

$$\overline{c}_{ij}^{II} = \mathbf{K}_0^{-1} \left(\mathbf{R}_{ij}^{II} - \mathbf{K}_i^I \overline{c}_j^I - \mathbf{K}_j^I \overline{c}_i^I - \mathbf{K}_{ij}^{II} \overline{c}_0 \right) \qquad (3.53)$$

The series is usually truncated after the first or second order term. On this basis it is possible to determine analytical expressions for the mean values and covariances of the response. The evaluation of higher order moments is very difficult and the method, therefore, is restricted to Gaussian stochastic fields. Further, the method is not accurate for fields with a large coefficient of variation (Brenner [3]). If the coefficients of variation are large, the assumption that the outcomes of the variables, z_i, are small is not valid.

Like the Neumann expansion method the pertubation method is usually used for time-invariant problems. If the method is used to solve time-variant problems the error made by truncating the Taylor series after the first or second term will accumulate. Hence, like the Neumann expansion method the pertubation method can only be used for time-variant problems if the number of time-steps is small.

3.6.4   Weighted Integrals

Unlike the pertubation method, the weighted integral method does not involve a discretization of the stochastic field and an exact expression for the stochastic stiffness matrix in terms of the spatially varying material properties is obtained.

The weighted integral method is based on the fact that the stiffness matrix can be expressed in terms of weighted integrals of the randomly varying material properties. Since the weighted integrals are stochastic variables, whose parameters can be determined on the basis of the probabilistic description of the stochastic field, the problem now can be treated within the framework of FORM/SORM-analysis, see section 4.2.1.

The basic idea originates from a series of articles by Shinozuka [21], Bucher and Shinozuka [4] and Karada et al. [12], where simple frame structures with randomly varying Young's modulus were treated purely analytically. The method has been extended to include FEM-analysis in a number of articles by Deodatis [5], Deodatis and Shinozuka [6] and Takada [23], [24].

The method can most easily be illustrated by an example. Consider the simple 2-node linear element shown in figure 3.2. Using the hybrid formulation the stiffness matrix for this element will be determined. The weighted integral method can be formulated for different types of elements and for different finite element formulations in a similar manner.

The matrix A^e is determined by, see eq. (3.20)
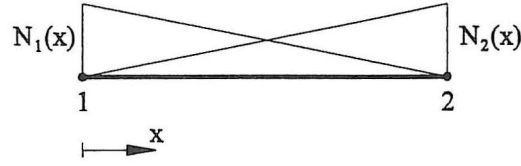
Figure 3.2: *2-node one-dimensional element*

$$\mathbf{A}^e = \int_V \mathbf{N}_q^T \mathbf{D}^{-1} \mathbf{N}_q \, dV \tag{3.54}$$

Assume that the material is isotropic such that $\mathbf{D} = D\mathbf{I}$, where $\mathbf{I}$ denotes the identity matrix.

$$\mathbf{A}^e = \int_V \frac{1}{D} \mathbf{N}_q^T \mathbf{N}_q \, dV \tag{3.55}$$

Both the transport coefficient, D, and the shape functions are functions of the position, x. Let the transport coefficient be given by

$$\frac{1}{D(x)} = \frac{1}{D_0} (1 + f(x)) \tag{3.56}$$

where D_0 is the constant mean value and $f(x)$ denotes a homogenous stochastic field with mean value function $\mu_f(x) = 0$ and auto-covariance function $\kappa_{ff}(x_1, x_2)$.

The chloride flow, q is approximated by a linear function in the interval between the two nodes.

$$q = \begin{bmatrix} N_1 & N_2 \end{bmatrix} \begin{bmatrix} q_1 \\ q_2 \end{bmatrix} \tag{3.57}$$

where

$$\left. \begin{matrix} N_1 & = & \left(1 - \frac{x-a_i}{b_i-a_i}\right) & = & 1 - \xi \\ N_2 & = & \left(\frac{x-a_i}{b_i-a_i}\right) & = & \xi \end{matrix} \right\} \tag{3.58}$$

In eq. (3.58) the local coordinate system $\xi = (x - a_i) / (b_i - a_i)$ has been introduced. It is now possible to determine the local matrix $\mathbf{A}_i^e$ as

$$\begin{aligned}
\mathbf{A}_i^e &= \int_{a_i}^{b_i} \frac{1}{D_0} (1 + f(x)) (x) \mathbf{N}_q^T(x) \mathbf{N}_q(x) \, dx \\
&= (b_i - a_i) \int_0^1 \frac{1}{D_0} (1 + f(\xi)) \mathbf{N}_q^T(\xi) \mathbf{N}_q(\xi) \, d\xi \\
&= \frac{(b_i - a_i)}{D_0} \int_0^1 \mathbf{N}_q^T(\xi) \mathbf{N}_q(\xi) \, d\xi + \frac{(b_i - a_i)}{D_0} \int_0^1 f(\xi) \mathbf{N}_q^T(\xi) \mathbf{N}_q(\xi) \, d\xi
\end{aligned}$$

$$
\begin{aligned}
&= \mathbf{A}_{0_i}^e + \frac{(b_i - a_i)}{D_0} \int_0^1 f(\xi) \begin{bmatrix} 1 - \xi \\ \xi \end{bmatrix} \begin{bmatrix} 1 - \xi & \xi \end{bmatrix} d\xi \\
&= \frac{(b_i - a_i)}{D_0} \begin{bmatrix} \int_0^1 f(\xi)(1-\xi)^2 d\xi & \int_0^1 f(\xi)(1-\xi)\xi d\xi \\ \int_0^1 f(\xi)(1-\xi)\xi d\xi & \int_0^1 f(\xi)\xi^2 d\xi \end{bmatrix} \\
&= \mathbf{A}_{0_i}^e + \mathbf{W}_{0_i}^e + \mathbf{W}_{1_i}^e + \mathbf{W}_{2_i}^e
\end{aligned} \tag{3.59}
$$

where

$$
\left.
\begin{aligned}
\mathbf{A}_{0_i}^e &= \tfrac{1}{6} \frac{(b_i - a_i)}{D_0} \begin{bmatrix} 2 & 1 \\ 1 & 2 \end{bmatrix} \\[2mm]
\mathbf{W}_{0_i} &= \frac{(b_i - a_i)}{D_0} \int_0^1 f(\xi)\, d\xi \begin{bmatrix} 1 & 0 \\ 0 & 0 \end{bmatrix} = \frac{(b_i - a_i)}{D_0} W_{0_i} \begin{bmatrix} 1 & 0 \\ 0 & 0 \end{bmatrix} \\[2mm]
\mathbf{W}_{1_i} &= \frac{(b_i - a_i)}{D_0} \int_0^1 f(\xi)\,\xi d\xi \begin{bmatrix} -2 & 1 \\ 1 & 0 \end{bmatrix} = \frac{(b_i - a_i)}{D_0} W_{1_i} \begin{bmatrix} -2 & 1 \\ 1 & 0 \end{bmatrix} \\[2mm]
\mathbf{W}_{2_i} &= \frac{(b_i - a_i)}{D_0} \int_0^1 f(\xi)\,\xi^2 d\xi \begin{bmatrix} 1 & -1 \\ -1 & 1 \end{bmatrix} = \frac{(b_i - a_i)}{D_0} W_{2_i} \begin{bmatrix} 1 & -1 \\ 1 & -1 \end{bmatrix}
\end{aligned}
\right\} \tag{3.60}
$$

The mean values and covariances of the weighted integrals, W_{L_i} can be evaluated

$$
E[W_{L_i}] = (b_i - a_i) \int_0^1 \xi^L \mu_f(\xi)\, d\xi \tag{3.61}
$$

$$
COV[W_{L_i} W_{M_j}] = (b_i - a_i)(b_j - a_j) \int_0^1 \int_0^1 \xi_1^L \xi_2^M \kappa_{ff}(\xi_1, \xi_2)\, d\xi_1 d\xi_2 \tag{3.62}
$$

If the load and mass matrices involve stochastic integrals these can be evaluated in a similar manner. The weighted integral method can also be used for other types of elements than the simple one-dimensional 2-node element treated here. However, the dimension of the integrals for the mean value and covariance matrix increases with the number of dimensions of the element. Therefore, it may be difficult to evaluate the covariance matrix with sufficient accuracy for larger dimensions.

3.7   Discretization of Stochastic Fields

A number of stochastic finite element methods are based on a discretization of the stochastic fields. One of these methods is the pertubation method presented in section 3.6.3 where the fields have be be represented by a vector of stochastic variables. A discretization of a stochastic field can be obtained by a number of different methods. The most simple and most widely used methods are the *midpoint method* and the *local average method*. In contrast to the weighted integral method it is only possible to determine an approximation to the stochastic stiffness matrix on the basis of these discretization methods. Further, when using the midpoint or the local average method all the previously presented finite

element methods yield identical results because the transport coefficient is assumed to be constant within each element.

On the basis of a discretization of the stochastic fields where the fields are represented by a vector of stochastic variables the probability of some extreme event can be determined by traditional FORM/SORM-analysis, see section 4.2.1. This type of analysis is very efficient. However, the FORM/SORM analysis cannot be used in order to determine the statistics of the response. Further, it may require a large number of variables to represent the stochastic fields. In that case the computational effort involved in the FORM/SORM analysis may also bee large.

3.7.1 Midpoint Method

By the midpoint method the stochastic field, $D(\mathbf{x})$, is discretized and the value of the field within each element is assumed to be constant, the constant being equal to the value of the field at the midpoint of the element, $\mathbf{x}_i^*$

$$D_i = D\left(\mathbf{x}_i^*\right) \tag{3.63}$$

The mean value, μ_{D_i} and the covariances, $C_{D_i D_j}$ of the discrete stochastic variables are determined on the basis of the mean value function and auto-covariance function of $D(\mathbf{x})$, respectively

$$\mu_{D_i} = \mu_D\left(\mathbf{x}_i^*\right) \tag{3.64}$$

$$C_{D_i D_j} = \kappa_{DD}\left(\mathbf{x}_i^*, \mathbf{x}_j^*\right) \tag{3.65}$$

where $\mu_D(\mathbf{x})$ and $\kappa_{DD}(\mathbf{x}_1, \mathbf{x}_2)$ denote the mean value function and auto-covariance function of $D(\mathbf{x})$, respectively.

The mesh used to discretize the stochastic fields need not be the same as the FEM mesh. The FEM mesh is chosen such that the response can be represented with sufficient accuracy. The stochastic mesh must be chosen such that the variability of the stochastic field can be represented. However, the stochastic mesh must be coarser than or equal to the FEM mesh. Der Kiureghian and Ke [13] suggest to use a stochastic mesh such that the size of the elements is one fourth to one half of the correlation length of the stochastic field. The upper limit is to ensure that the variation of the field can be represented. The lower limit is introduced in order to avoid large correlation coefficients between the stochastic variables which may cause numerical instability in the probability transformation used in conjunction with the FORM/SORM-analysis which will be introduced in section 4.2.1.

It is important to notice that the midpoint tends to overrepresent the variability of the field, $D(\mathbf{x})$, see e.g [3].

3.7.2 Local Average Method

By the local average method the value of the field within each element is also assumed to be constant, the constant value in this case being the local average of the field over the volume of the element. That is

$$D_i = \frac{1}{V_i} \int_{V_i} D\left(\mathbf{x}\right) dV \qquad (3.66)$$

where V_i denotes the volume of stochastic element i. Vanmarcke [25] has derived expressions for the mean and covariances of the discrete stochastic variables, D_i. However, these expressions are only valid for rectangular or cubic elements. For elements which are not rectangular the mean and covariances are difficult to evaluate. Further, the method can only be used for Gaussian fields. For non-Gaussian fields the distribution function of D_i will be unknown. The considerations about the size of the stochastic elements which were made for the midpoint method are also valid for this method. However, one additional problem exists. Experience has shown that due to numerical problems it is difficult to ensure that the covariance matrix of the variables D_i is positive definite which causes problems in the probability transformation, see section 4.2.1.

The local average method tends to underrepresent the variability of the field, see e.g. Brenner [3]. The midpoint method and the local average method, therefore, are often applied to the same problem in order to bracket the solution.

3.8 Example: Comparison of FEM-Formulations

In section 3.4 four different formulations of the FE-method were presented. It is not obvious whether these formulations lead to results that are substantially different or which formulation best describes the problem of diffusion in random media. In order to compare the methods an example is investigated. The mixed method is not included in the analysis because it is known to be less efficient than the other methods because it involves a much larger number of variables.

Figure 3.3 shows two FEM-meshes of a reinforced concrete structure subject to a constant chloride concentration, $c_s = 1.0$, on three sides. On the fourth side and around the reinforcement the chloride flow, q_n, is zero. The meshes are chosen such that the fine mesh is a subdivision of each element in the coarse mesh into four elements. The material is assumed to be isotropic and the logarithm of the transport coefficient is modelled as a Gaussian stochastic field with mean μ_D, standard deviation σ_D and auto-correlation coefficient function

$$\rho_{DD}\left(d\right) = \exp\left(-d^2 / \left(al^2\right)\right) \qquad (3.67)$$

where d denotes the distance between two points in the structure, l is a characteristic length defined in figure 3.3 and a is the scale of fluctuation.

The statistics of the concentration in the nodes are obtained by simulating the values of the transport coefficient at the Gauss-points used for the numerical integration of the local stiffness matrices. It is important to use a high order of Gauss-integration in order to ensure that the variability of D within the elements can be represented. If the variability of D cannot be represented with sufficient accuracy by the chosen integration scheme no fair comparison of the different FEM-formulations can be performed. The computations have been performed within the framework of the MATLAB toolbox FEMLAB, see Hededal
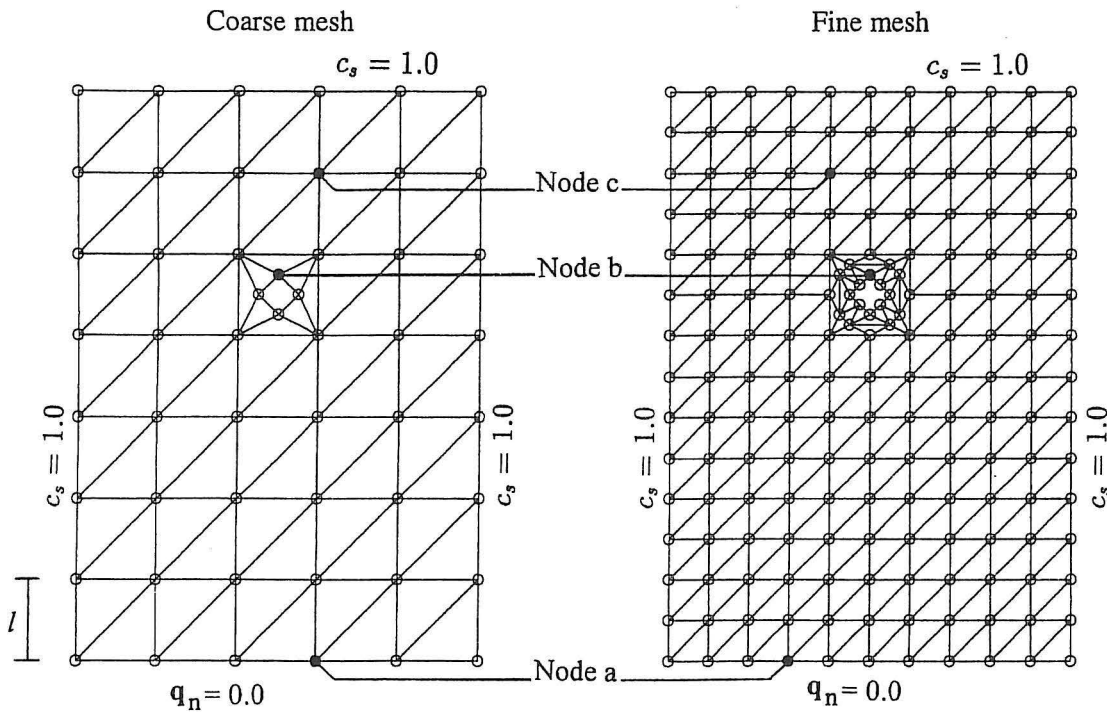
Figure 3.3: *Finite element meshes*

and Krenk [9]. For a brief description of the toolbox and the modules programmed for this example see appendix A.

In table 3.1 the mean values, μ, and standard deviations, σ, of the concentrations at the time $t = 5l^2$ are shown for the nodes a, b and c shown in figure 3.3. The statistics are determined on the basis of 1000 simulations of D. The parameters of D have been chosen as $\mu_D = 1.0$, $\sigma_D = 0.4$ and $a = 1.5$.

It is seen that for the fine FEM-mesh there is virtually no difference between the results obtained on the basis on the three different FEM-formulations. However, for the coarse mesh the flux-based method tends to yield mean values of the nodal concentrations that are slightly smaller than the mean values found by the other two methods. The reason for this difference is that the stiffness matrix by the flux-based method is proportional to the inverse of the mean value of the resistance, D^{-1}, of the element. The conductivity of the flux-based element, therefore, in general is smaller. This effect becomes more pronounced as the variation of D within the elements increases, i.e. as the FEM-mesh becomes coarser. It is also interesting to notice that for node b there is a substantial difference between the mean values of the concentrations obtained by the two different meshes.

In table 3.2 the results of the simulations are shown for $\mu_D = 1.0$, $\sigma_D = 1.0$ and $a = 1.5$. Only the standard deviation of D has been changed. This increase of the standard deviation of D implies that the variation of D within the elements increases. This also implies that the difference between the results obtained by the flux-based method and the other two methods increases. The example also shows that the results obtained on

		node a		node b		node c	
Mesh	Method	μ	σ	μ	σ	μ	σ
Coarse	Standard	0.23295	0.053373	0.35760	0.053593	0.77630	0.046782
	Hybrid	0.23089	0.052387	0.36059	0.054345	0.77608	0.046621
	Flux-based	0.21753	0.056021	0.34573	0.051684	0.77429	0.046938
Fine	Standard	0.23947	0.050214	0.43756	0.059657	0.78061	0.047434
	Hybrid	0.23779	0.052030	0.43963	0.058578	0.78186	0.048125
	Flux-based	0.23322	0.049805	0.43131	0.059601	0.77736	0.047963

Table 3.1: *Results for $\mu_D = 1.0$, $\sigma_D = 0.4$ and $a = 1.5$.*

		node a		node b		node c	
Mesh	Method	μ	σ	μ	σ	μ	σ
Coarse	Standard	0.19529	0.10766	0.30629	0.11394	0.74820	0.11192
	Hybrid	0.19568	0.10814	0.31886	0.11677	0.75168	0.11084
	Flux-based	0.13118	0.097747	0.25427	0.10572	0.72044	0.12053
Fine	Standard	0.19043	0.097313	0.37252	0.12564	0.72670	0.12060
	Hybrid	0.18808	0.099950	0.37639	0.12282	0.73051	0.12183
	Flux-based	0.16881	0.092959	0.34846	0.12381	0.70982	0.12552

Table 3.2: *Results for $\mu_D = 1.0$, $\sigma_D = 1.0$ and $a = 1.5$.*

the basis of the standard and hybrid methods by the coarse mesh are much closer to the more "exact" result obtained by the finer mesh. It must, therefore, be concluded that the hybrid and standard methods yield the most accurate results. Further, the standard method is the most efficient and the most simple to implement. In conclusion, the problem is best solved by the standard formulation of the FE-method.

3.9   Summary and Conclusions

A probabilistic model has been formulated on the basis of which the lifetime of concrete structures subject to chloride-initiated corrosion can be estimated. The build-up of chloride is described by the diffusion equation. The transport coefficient, the surface concentration and the critical threshold for initiation of corrosion are modelled as stochastic fields. Also the cover thickness is modelled in such a way that the spatial variation is taken into account.

A number of stochastic finite element methods has been presented. Some methods such as the pertubation method can be used in order to determine the statistics of the response of a given system. Other methods such as the midpoint method, the local average method and the weighted integral method can be used in order to determine an outcome of the response for a given outcome of the randomly varying properties.

In the analyses performed later in this report FORM/SORM-analysis is implemented. It is, therefore, necessary to determine the outcome of the response for a given outcome of the stochastic field, see section 4.2.1. Hence, the midpoint method, the local average method and the weighted integral method are the best suited. It must, however, be taken into account that the number of stochastic variables used by the weighted integral method can be substantially larger than the number of variables used by the midpoint and local average methods.

A number of formulations of the finite element method has been compared on the basis of an example. It can be concluded that the problem is best and most efficiently solved by using the standard finite element formulation.

3.10   References

[1] Bathe, K.-J., Finite Element Procedures in Engineering Analysis, Prentice-Hall, Englewood-Cliffs, New Jersey, 1982.

[2] Borgman, L. E., Ocean Wave Simulation for Engineering Analysis, Journ. Watrwy. and Harb. Div., ASCE, 95, 1969, pp. 557-583.

[3] Brenner, C. E., Stochastic Finite Element Methods (Literature Review), Internal Working Report No. 35-91, Institute of Engineering Mechanics, University of Innsbruck, Austria, 1991.

[4] Bucher, C. G., Shinozuka, M., Structural Response Variability II, Journ. Eng. Mech., 114, 12, 1988, pp. 2035-2054.

[5] Deodatis, G., Weighted Integral Method I: Stochastic Stifness Matrix, Journ. Eng. Mech, 117, 8, 1991, pp. 1851-1864.

[6] Deodatis, G., Shinozuka, M., Weighted Integral Method II: Response Variability and Reliability, Journ. Eng. Mech., 117, 8, 1991, pp. 1865-1877.

[7] Engelund, S., Rackwitz, R., Quality Assurance in Structural Design, Structural Saftey and Reliability, Shinozuka & Yao (eds.), Balkema, Rotterdam, 1994.

[8] Engelund, S., Sørensen, J. D., Krenk, S., Estimation of the Time to Initiation of Corrosion in Uncracked Concrete Structures, ICASP7, 1995

[9] Hededal, O., Krenk, S., FEMLAB, MATLAB Toolbox for the Finite Element Method, Version 1.0, Aalborg Univeristy, 1995.

[10] Hergenröder, M., Zur statistischen Instandhaltungsplanung für bestehende Bauwerke bei Karbonatisierung des Betons und möglicher Korrosion der Bewehrung, Berichte aus dem Konstruktiven Ingenieurbau, TU München, 4/92, 1992. In German.

[11] Henriksen, C. F., Stoltzner, E., Kloridbetinget Korrosion, Dansk Beton, 3, 1992. In Danish.

[12] Kadara, A., Bucher, C. G., Shinozuka, M., Structural Response Variability III, Journ. Eng. Mech. 115, 8, pp. 1726-1747.

[13] Kiureghian, A. D., Ke. J.-B., The Stochastic Finite Element Method in Structural Reliability, Prob. Eng. Mech., 3, 2, 1988, pp. 83-91.

[14] Liu, P.-L., Kiureghian, A. D., Finite-Element Reliability Methods for Geometrically Nonlinear Stochastic Structures, Report No. UCB/SEMM-89/05, Structural Engineering, Mechanics and Materials, Department of Civil Engineering, University of California, Berkeley, 1989.

[15] Madsen, H. O., Krenk, S., Lind, N. C., Structural Safety, Prentice Hall, New Jersey, 1986.

[16] Ostra-Starzewski, M., Micromechanics as a Basis of Stochastic Finite Elements and Differences: An Overview, ASME Appl. Mech. Rev., vol 46, 2, 1993.

[17] Ottosen, N., Peterson, H., Introduction to the Finite Element Method, Prentice-Hall, Engelwood-Cliffs, New Jersey, 1992.

[18] Poulsen, E., Description of Exposure to Chloride of Marine Concrete Structures, Proposal for a Standard, Proceedings of the International RILEM workshop, Chloride Penetration into Concrete, Saint-Rémy-Les-Chevreuse, 1995.

[19] Shinozuka, M., Jan, C.-M., Digital Simulation of Random Processes, Journ. of Sound and Vibration, 26, 1973, pp. 417-428.

[20] Shinozuka, M., Yamazaki, F., Stochastic Finite Element Analysis: an Introduction, in: Ariaratnam, S. T., Schuëller, G. I., Elishakoff, I. (eds.), Stochastic Structural Dynamics, Elsevier Applied Science Publishers Ldt., 1988, pp. 241-291.

[21] Shinozuka, M., Structural Response Variability, Journ. Eng. Mech., 113, 1987, pp. 825-842.

[22] Stoltzner, E., Sørensen, B., Chloridundersøgelser på Farøbroerne, Dansk Beton, 11, 1, 1994, pp. 16-18. In Danish.

[23] Takada, T., Weighted Integral Method in Stochastic Finite Element Analysis, Prob. Eng. Mech., 5, 1990, pp. 146-156.

[24] Takada, T., Weighted Integral Method in Multi-Dimensional Stochastic Finite Element Analysis, Prob. Eng. Mech., 5, 1990, pp. 158-166.

[25] Vanmarcke, E., Random Fields, Analysis and Synthesis, The MIT Press, Cambridge, Massachusetts, 1988.

[26] Zienkiewicz, O. C., Taylor, R. L., The Finite Element Method, McGraw-Hill, London, 1988.

Chapter 4

Probabilistic Methods

On the basis of the probabilistic model of chloride-initiated corrosion presented in section 3.1 it is possible to determine the probability that corrosion has been initiated in a given structure at a given time T. However, in order to use the model, the model parameters must be estimated on the basis of measurements obtained from the structure to be investigated. A number of different methods for parameter estimation and reliability analysis exist. In this chapter the merits and disadvantages of the various methods are discussed and some of the methods are presented in more detail.

4.1 Parameter Estimation

Estimates of the parameters of a given probability distribution can be obtained by a number of methods such as the method of moments, least squares estimation, maximum likelihood and Bayesian estimation. The goodness of the estimates can be evaluated according to a number of criteria such as unbiasedness and minimum variance. For a detailed discussion of parameter estimation, see e.g. Mann et al. [16].

In the present problem the parameters in the probabilistic model describing the surface concentration and the transport coefficient need to be estimated. However, no measurements of these quantities are available. The available data consists of a number of chloride profiles on the basis of which the parameters can be estimated. The best methods in this case are the maximum likelihood method and Bayesian estimation. These methods are presented below.

4.1.1 Maximum Likelihood Estimation

For a given set of generally correlated experimental outcomes, $\hat{z}_i$, $i = 1, 2 \ldots n$, where n denotes the number of experiments, the parameters, $\mathbf{p}$, can be estimated by maximizing the likelihood of obtaining the given outcomes. The likelihood function is given by

$$l(\hat{\mathbf{z}}|\mathbf{p}) = f_{\mathbf{Z}|\mathbf{p}}(\hat{\mathbf{z}}|\mathbf{p}) \tag{4.1}$$

where $f_{\mathbf{Z}|\mathbf{p}}(\hat{\mathbf{z}}|\mathbf{p})$ is the density function of the measured concentration for a given set of parameters $\mathbf{p}$. If the outcomes are independent the likelihood is

$$l\left(\hat{\mathbf{z}}|\mathbf{p}\right) = \prod_{i=1}^{n} f_{Z_i|\mathbf{p}}\left(\hat{z}_i|\mathbf{p}\right) \tag{4.2}$$

where $f_{Z_i|\mathbf{p}}\left(z_i|\mathbf{p}\right)$ is the density function of the ith measurement given the parameters $\mathbf{p}$. For the given set of outcomes the likelihood function, obviously, is a function of the unknown parameters, $\mathbf{p}$. The maximum likelihood estimates are obtained by maximizing the likelihood function. The maximum likelihood estimates of the parameters can be regarded as the parameters for which the likelihood of obtaining the given experimental outcomes is largest. The parameters estimated by maximum likelihood estimation are asymptotically unbiased and normally distributed with covariance matrix

$$\mathbf{C_{pp}} = -\boldsymbol{\Xi}^{-1} \tag{4.3}$$

where the elements of the matrix $\boldsymbol{\Xi}$ are given by

$$\Xi_{ij} = \frac{\partial^2}{\partial p_i \partial p_j} \ln l\left(\mathbf{p}\right) \tag{4.4}$$

The main advantage of the maximum likelihood estimation is that it provides an estimate of the statistical uncertainty which is particularly easy to handle, since the parameters are normally distributed. However, if the sample is small the parameters will not be normally distributed. Further, it is not possible to take into account prior information about the parameters.

4.1.2 Bayesian Analysis

Let the parameters $\mathbf{p}$ prior to the experiments have the *prior density function* $f_{\mathbf{p}}'\left(\mathbf{p}\right)$. This density represents the knowledge about the parameters available before the experiments are performed. It can be based on earlier experiments or it can express the subjective belief of the experimenter. The joint distribution of the parameters and the experimental outcomes, $\hat{\mathbf{z}}$, can then be written

$$f_{\mathbf{Zp}}\left(\hat{\mathbf{z}}, \mathbf{p}\right) = f_{\mathbf{Z}|\mathbf{p}}\left(\hat{\mathbf{z}}|\mathbf{p}\right) f_{\mathbf{p}}'\left(\mathbf{p}\right) = f_{\mathbf{p}|\mathbf{Z}}''\left(\mathbf{p}|\hat{\mathbf{z}}\right) f_{\mathbf{Z}}\left(\hat{\mathbf{z}}\right) \tag{4.5}$$

where $f_{\mathbf{p}|\mathbf{Z}}''\left(\mathbf{p}|\hat{\mathbf{z}}\right)$ is the so-called *posterior density function* of the parameters, $\mathbf{p}$, which can be written

$$f_{\mathbf{p}|\mathbf{Z}}''\left(\mathbf{p}|\hat{\mathbf{z}}\right) = \frac{f_{\mathbf{Z}|\mathbf{p}}\left(\hat{\mathbf{z}}|\mathbf{p}\right) f_{\mathbf{p}}'\left(\mathbf{p}\right)}{f_{\mathbf{Z}}\left(\hat{\mathbf{z}}\right)} \tag{4.6}$$

where

$$f_{\mathbf{Z}}\left(\hat{\mathbf{z}}\right) = \int_{\Omega_{\mathbf{p}}} f_{\mathbf{Z}|\mathbf{p}}\left(\hat{\mathbf{z}}|\mathbf{p}\right) f_{\mathbf{p}}'\left(\mathbf{p}\right) d\mathbf{p} \tag{4.7}$$

The integration is performed over the admissible range of $\mathbf{p}$, $\Omega_{\mathbf{p}}$. The distribution of the experimental outcomes for a given set of parameters, $f_{\mathbf{Z}|\mathbf{p}}\left(\hat{\mathbf{z}}|\mathbf{p}\right)$, is the likelihood function given by eq. (4.1) or eq. (4.2) if the outcomes are independent.

Socalled *sufficient statistics* play an important role in Bayesian statistic. Sufficient statistics are functions of the experimental outcomes which are said to contain all information from the outcomes, implying that only these functions are necessary in order to write down the likelihood function and the prior and posterior distributions. Whenever a set of sufficient statistics for a given parameter exists, also a *conjugate prior* exists (see e.g. Raiffa and Schlaifer [18]). The advantage of the conjugate prior is that the prior and posterior distributions belong to the same family. A normal prior e.g. yields a normal posterior. It is only necessary, on the basis of the experimental outcomes, to update the values of the sufficient statistics. This also makes the method computationally efficient.

An experimenter is often faced with a situation where the prior information about the parameters is negligible compared to the amount of information expected to be gained from the experiments. In that case a *non-informative prior* for the parameters can be chosen. In a number of special cases it is possible to determine priors which are truly non-informative, see e.g. Box and Tiao [4]. However, in many cases this is not possible. Further, there is some discussion whether some distributions are in fact non-informative, see Engelund and Rackwitz [7].

In conjunction with experimental planning the outcome of a future experiment must be predicted. The density function of the future experiment is given by the *predictive density*

$$f_{Z|Z}\left(z|\hat{z}\right) = \int_{\Omega_{\mathbf{p}}} f_{Z|\mathbf{p}}\left(z|\mathbf{p}\right) f''_{\mathbf{p}|Z}\left(\mathbf{p}|\hat{z}\right) d\mathbf{p} \tag{4.8}$$

In contrast to the maximum likelihood method, Bayesian analysis yields an accurate estimate of the statistical uncertainty even by small samples. Further, the method provides a framework which allows subjective information to be taken into account when formulating the prior distribution. However, if the posterior and predictive distributions cannot be determined analytically the numerical effort involved in solving the integrals, eq. (4.6) and eq. (4.8) can be excessive, especially if the number of parameters, $\mathbf{p}$, is large.

4.2 Reliability Methods

A number of reliability methods has been developed in order to solve problems of the type

$$P_f = \int_{\Omega_z} f_{\mathbf{Z}}\left(\mathbf{z}\right) d\mathbf{z} \tag{4.9}$$

where P_f denotes the probability of some extreme event (failure), $f_{\mathbf{Z}}\left(\mathbf{z}\right)$ is the joint density function of $\mathbf{Z}$ and Ω_z is the integration domain. The integration domain can be given in terms of a single failure function (or limit state function), as a union of intersections or can be given by equality constraints.

The probability integral, eq. (4.9), can only in a few cases be solved analytically. Further, simple numerical integration procedures such as Gauss-integration can only be applied if the dimension of the integral is not too large. Monte Carlo simulation is also in most cases inefficient because the probability of failure, P_f, is generally small. However, the efficiency of the simulation can be improved by a number of importance sampling schemes ensuring that most of the simulated outcomes of the stochastic variables fall in the area which

gives the largest contribution to the probability integral, see e.g. Engelund and Rackwitz [8]. The major advantage of the simulation methods is that they provide an estimate of the accuracy of the computed probability of failure. However, it is difficult to compute reliable derivatives of the probability of failure by simulation. In the following section the First Order Reliability Method (FORM) and the Second Order Reliability Method (SORM), which are widely acknowledged as the most efficient reliability methods, are presented (see also Thoft-Christensen and Baker [2] and Madsen et al. [14]).

4.2.1   First and Second Order Reliability Methods

First, consider the case where the domain, Ω_z, is given in terms of a single failure function, $\Omega_z = \{z : g(z) \leq 0\}$. FORM/SORM-analysis is based on the fact that if all variables are standard normally distributed the largest contribution to the probability integral, eq. (4.9), comes from the area around the point on the failure surface which lies nearest to the origin, see figure 4.1.
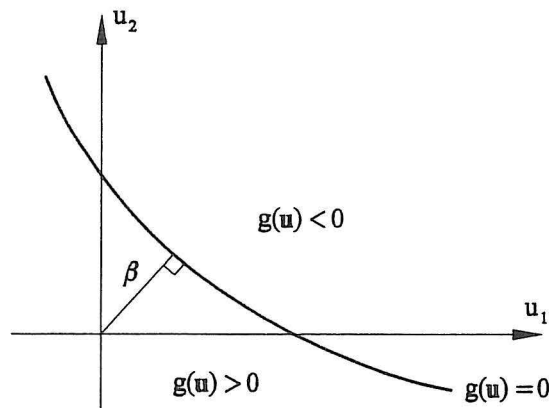
Figure 4.1: *Failure function in u-space.*

By the first and second order reliability methods all stochastic variables, $\mathbf{Z}$, are transformed into standardized independent normally distributed variables $\mathbf{U}$, $\mathbf{Z} = \mathbf{T}(\mathbf{U})$. Let the failure surface be given by $\partial\Omega_u = \{\mathbf{u} : g(\mathbf{T}(\mathbf{u})) = 0\}$. The reliability index, β, can now be determined on the basis of the minimum distance between origin in u-space and the failure surface, see fig. 4.1.

$$\beta = \begin{cases} \min_{\mathbf{u} \in \partial\Omega_u} \left(\mathbf{u}^T\mathbf{u}\right)^{\frac{1}{2}} & g(\mathbf{u} = 0) > 0 \\ -\min_{\mathbf{u} \in \partial\Omega_u} \left(\mathbf{u}^T\mathbf{u}\right)^{\frac{1}{2}} & g(\mathbf{u} = 0) \leq 0 \end{cases} \tag{4.10}$$

The optimization problem given in eq. (4.10) is normally solved by the so-called Rackwitz-Fiessler algorithm, see [17]. The solution point, $\mathbf{u}^*$, is called the beta-point, design point or the most likely failure point. The vector $\boldsymbol{\alpha} = \frac{\mathbf{u}^*}{\beta}$ is a unit vector normal to the failure surface.

By a FORM analysis the failure surface is approximated by its tangent at the design point. On the basis of the linearized failure surface the probability of failure can be determined as

$$P_f = \Phi(-\beta) \tag{4.11}$$

where Φ denotes the standard normal distribution function. The accuracy of this approximation depends of the non-linearity of the failure surface. The FORM-analysis, unfortunately, gives no information about the accuracy of the estimated probability of failure. The accuracy of the approximation can be improved by using a second order approximation to the failure surface at the design point. This is a so-called SORM-analysis. In this case it is necessary to determine the second order derivatives of the failure surface. This implies that the number of g-function calls for a SORM-analysis is proportional to n_v^2 where n_v denotes the number of variables. The number of g-function calls necessary to perform a FORM-analysis is proportional to n_v, see also Fujita and Rackwitz [9]. Taking into account that the evaluation of the failure function is usually the most time-consuming part of the analysis, the efficiency of SORM-analysis evidently decreases rapidly with increasing number of variables.

It has been argued that one of the disadvantages of FORM/SORM-analysis is the transformation from $u-$space to z-space for each evaluation of the failure function. However, in most cases the evaluation of the limit state function is much more time-consuming than the transformation. Further, the transformation provides an excellent scaling of the problem such that the design point is relatively easy to determine. Breitung [3] has developed a method which does not use the transformation to u-space. However, in order to locate the point in z-space which gives the largest contribution to the probability integral a general non-linear optimization algorithm such as NLPQL (see Schittkowski [20]) must be applied.

The major shortcoming of FORM/SORM-analysis is the fact that it based on the existence of only one important area which gives the largest contribution to the probability of failure. If the optimization problem, eq. (4.10), has more than one solution the method cannot be applied without some modifications.

4.2.2 Systems Reliability

There are two basic types of systems

- **Series systems**, where the entire system fails if a single element fails (weakest link system).
- **Parallel systems** which only fails if all elements fail. When a single element fails the load may be redistributed such that the system does not fail (redundant systems).

Series System
By a series system the failure region is $\Omega_z = \left\{ z : \cup_{i=1}^{n_f} g_i(z) \leq 0 \right\}$ where n_f denotes the number of failure modes. For each of the failure modes the reliability index, β_i, can be

determined according to the methodology outlined in section 4.2.1. Based on a linearization of the failure surfaces at the β-points the probability of failure can be determined by

$$P_f = 1 - \Phi_n\left(\boldsymbol{\beta}, \boldsymbol{\rho}\right) \tag{4.12}$$

where $\boldsymbol{\beta} = (\beta_1, \beta_2 \dots \beta_n)^T$ and the elements in the correlation coefficient matrix, $\boldsymbol{\rho}$, are determined by

$$\rho_{ij} = \boldsymbol{\alpha}_i^T \boldsymbol{\alpha}_j \tag{4.13}$$

where $\boldsymbol{\alpha}_i$ denotes the unit vector normal to failure surface i at the β-point. Since it is difficult to evaluate the general n-dimensional standard normal distribution a number of approximations for the probability of failure has been developed such as e.g. Ditlevsen bounds [5], the Hohenbichler approximation [12] and the approximation by Gollwitzer and Rackwitz [10].

Parallel System
The failure region is given by $\Omega_z = \left\{ \mathbf{z} : \cap_{i=1}^{n_f} g_i\left(\mathbf{z}\right) \leq 0 \right\}$. As for a series system, a reliability index, β_i, can be determined for each failure mode and the probability of failure can be determined by

$$P_f = \Phi_n\left(-\boldsymbol{\beta}, \boldsymbol{\rho}\right) \tag{4.14}$$

This approximation, however, is very poor if the failure surfaces are not linear. A better approximation is obtained if the so-called joint β-point is used, see e.g. Madsen et al. [14] or Enevoldsen [6].

Series System of Parallel Systems
Most systems can be represented by a so-called *minimal cut set* which is a series system of parallel systems. Each of the parallel systems can be analyzed in the way outlined above. Further, in order to determine the reliability of the series system it is necessary to determine the correlation between the parallel systems. This can be done approximately by replacing each parallel system by an equivalent element with a linear safety margin. The equivalent element is chosen such that it has the same probability of failure as the parallel system and the same sensitivity towards changes in the standardized variables, $\mathbf{u}$. For a detailed derivation of the results see Gollwitzer and Rackwitz [11]. Alternatively, Ditlevsen bounds for the system can be evaluated. These bounds are not based on the equivalent elements for the parallel systems. Further, if it is possible to evaluate the n-dimensional standard Normal distribution, these bounds are exact.

4.2.3 Equality Constraints

Let the failure region be given in terms of an equality constraint $g_e\left(\mathbf{u}\right)$ and n_f inequality constraints $g_i\left(\mathbf{u}\right)$ such that $\Omega_z = \left\{ \left\{ \mathbf{z} : g_e\left(\mathbf{u}\right) = 0 \right\} \cap \left\{ \mathbf{z} : \cap_{i=1}^{n_f} g_i\left(\mathbf{u}\right) \leq 0 \right\} \right\}$. All the failure

functions are linearized at the joint design point and the failure region is approximated by

$$\Omega_{\mathbf{z}} \approx \left\{ \left\{ \mathbf{z} : \boldsymbol{\alpha}_e^T \mathbf{u}^* - \boldsymbol{\alpha}_e^T \mathbf{u} = 0 \right\} \cap \left\{ \mathbf{z} : \cap_{i=1}^{n_f} \boldsymbol{\alpha}_i^T \mathbf{u}^* - \boldsymbol{\alpha}_i^T \mathbf{u}^* \leq 0 \right\} \right\} \qquad (4.15)$$

where $\mathbf{u}^*$ denotes the joint design point, $\boldsymbol{\alpha}_e$ is a unit vector which located at origin points towards the tangent of the equality constraint at the design point and which is normal to the tangent of the equality constraint at the design point. The vector, $\boldsymbol{\alpha}_i$, is defined in a similar manner. However, $\boldsymbol{\alpha}_i$ is normal to the tangent of the ith inequality constraint at the design point.

The likelihood of obtaining outcomes in the region given by $\Omega_{\mathbf{z}}$ can now be approximated by

$$
\begin{aligned}
l &= l\left(\left\{ \boldsymbol{\alpha}_e^T \mathbf{u}^* - \boldsymbol{\alpha}_e^T \mathbf{u} = 0 \right\} \cap_{i=1}^{n_f} \left\{ \boldsymbol{\alpha}_i^T \mathbf{u}^* - \boldsymbol{\alpha}_i^T \mathbf{u} \leq 0 \right\} \right) \\
&= l\left(\left\{ \beta_0 - y_0 = 0 \right\} \cap_{i=1}^{n_f} \left\{ \beta_i - y_i \leq 0 \right\} \right) \\
&= \frac{\partial}{\partial b} P\left(\left\{ b - y_0 \leq 0 \right\} \cap_{i=1}^{n_f} \left\{ \beta_i - y_i \leq 0 \right\} \right) \Big|_{b=\beta_0}
\end{aligned}
\qquad (4.16)
$$

where

$$
\begin{aligned}
\beta_0 &= \boldsymbol{\alpha}_e^T \mathbf{u}^* & & (4.17) \\
\beta_i &= \boldsymbol{\alpha}_i^T \mathbf{u}^*, & i = 1, 2, \ldots n_f & (4.18) \\
y_0 &= \boldsymbol{\alpha}_e^T \mathbf{u} & & (4.19) \\
y_i &= \boldsymbol{\alpha}_i^T \mathbf{u}, & i = 1, 2, \ldots n_f & (4.20)
\end{aligned}
$$

In order to evaluate eq. (4.16) it is convenient to reformulate the expression as

$$l = \frac{\partial}{\partial b} \left[\int_{-\infty}^{-b} P\left(\cap_{i=1}^{n_f} \left(y_i \leq -\beta_i | b = s \right) \right) \varphi(s) \, ds \right] \Big|_{b=\beta_0} \qquad (4.21)$$

Now perform a transformation of the variables y_i, $i = 1, 2, \ldots n_f$ such that these variables become independent of y_0. This transformation is given by

$$y_i = \rho_{0i} y_0 + \sqrt{1 - \rho_{0i}^2} \, \tilde{y}_i \qquad (4.22)$$

where $\rho_{0i} = \boldsymbol{\alpha}_e^T \boldsymbol{\alpha}$. Eq. (4.21) now can be written as

$$l = \varphi(\beta_0) P\left[\cap_{i=1}^{n_f} \tilde{y}_i \leq -\frac{\beta_i - \rho_{0i} \beta_0}{\sqrt{1 - \rho_{0i}^2}} \right] \qquad (4.23)$$

If the problem involves more than one equality constraint this scheme can be applied n_e times where n_e denotes the number of equality constraints.

4.2.4   Sensitivity Analysis

It is often of interest to determine the derivative of the reliability index, β, or the probability of failure, P_f, in order to quantify the relative importance of various parameters. Further, these derivatives are necessary when solving an optimization problem with reliability constraints. These derivatives can be computed numerically by the finite difference method. However, it is more efficient to use a semi-analytical expression. In fact, an important advantage of FORM-analysis is the relative ease by which these derivatives can be obtained. It can be shown that the derivative of the first order reliability index, β, with respect to a parameter p, which may be a parameter in a distribution function or in the limit state function, is

$$\frac{\partial \beta}{\partial p} = \frac{1}{|\nabla_{\mathbf{u}} g\left(\mathbf{u}^*, \mathbf{p}\right)|} \frac{\partial g\left(\mathbf{u}^*, \mathbf{p}\right)}{\partial p} \tag{4.24}$$

If a gradient-based algorithm is used in order to locate the β-point the gradient vector $\nabla_{\mathbf{u}} g\left(\mathbf{u}^*\right)$ is already available and it is only necessary to determine the derivative of the failure function with respect to the parameter p. The derivative of the first order estimate of the probability of failure with respect to p is

$$\frac{\partial P_f}{\partial p} = -\varphi\left(-\beta\right) \frac{\partial \beta}{\partial p} \tag{4.25}$$

where φ denotes the standard normal density function.

4.2.5   Conditional Sampling

As earlier mentioned FORM/SORM-analysis is based on the existence of only one important region. The problem of multiple design points can be overcome by using conditional sampling. By this method suggested by Ayub and Haldar [1] the stochastic variables, $\mathbf{Z}$ are partitioned into two sets $\mathbf{Z}_1$ and $\mathbf{Z}_2$. The probability of failure can now be evaluated by

$$P_f = \int_{\Omega_{\mathbf{Z}_1}} \int_{g(\mathbf{z}) \leq 0} f_{\mathbf{Z}_2 | \mathbf{Z}_1}\left(\mathbf{z}_2 | \mathbf{z}_1\right) f_{\mathbf{Z}_1}\left(\mathbf{z}_1\right) d\mathbf{z}_2 d\mathbf{z}_1 \tag{4.26}$$

where $\Omega_{\mathbf{Z}_1}$ denotes the admissible range of $\mathbf{Z}_1$. For a given outcome of $\mathbf{Z}_1$ the inner part of the integral can be evaluated by some analytical method such as FORM/SORM-analysis yielding a conditional probability of failure. The outer integral is solved by Monte Carlo simulation which can be performed using Importance Sampling. The method can also be used to solve problems where the failure region for the inner integral is given in terms of a system.

4.3   Reliability Updating

The reassessment of the reliability of existing structures can be based on two types of information. The first of these is information gained from samples of one or more stochastic

variables. On the basis of such information the parameters in the distribution functions can be estimated by the methods outlined in section 4.1. The second type of information is gained when the outcome of one or more of the elements of the stochastic vector $\mathbf{z}$ is known to belong to a given set $\Omega'_{\mathbf{z}}$. This set can be given in terms of a function $k(\mathbf{z})$ such that

$$\Omega'_{\mathbf{z}} = \{\mathbf{z} : k(\mathbf{z}) \leq 0\} \tag{4.27}$$

A typical example of such information is the information which can be gained from a proof loading where the load-bearing capacity is shown exceed a given value. The information can also be given in terms of an equality constraint $k(\mathbf{z}) = 0$ such that

$$\Omega'_{\mathbf{z}} = \{\mathbf{z} : k(\mathbf{z}) = 0\} \tag{4.28}$$

It will now be demonstrated how this type of information can be taken into account in a reliability analysis where the failure domain is given in terms of a single failure function. The method can be generalized to cases where the failure region is given by a union or an intersection and to cases where the new information is given in terms of several equality or inequality constraints, see e.g. Madsen [14].

Let the variable $M = g(\mathbf{z})$ where $g(\mathbf{z})$ is a failure function. Evidently the event $M \leq 0$ corresponds to failure. Further, let the variable $K = k(\mathbf{z})$. In case $\Omega'_{\mathbf{z}} = \{\mathbf{z} : h(\mathbf{z}) \leq 0\}$ the updated probability of failure can be determined by

$$P_f = P(M \leq 0 | K \leq 0) = \frac{P(M \leq 0 \cap K \leq 0)}{P(K \leq 0)} \tag{4.29}$$

If the new information is given by $\Omega'_{\mathbf{z}} = \{\mathbf{z} : k(\mathbf{z}) = 0\}$ the updated probability of failure now is

$$
\begin{aligned}
P_f &= P(M \leq 0 | K = 0) = \frac{P(M \leq 0 \cap K = 0)}{P(K = 0)} \\
&= \frac{\left. \frac{\partial P(M \leq 0 \cap K - \delta \leq 0)}{\partial \delta} \right|_{\delta=0}}{\left. \frac{\partial P(K - \delta \leq 0)}{\partial \delta} \right|_{\delta=0}}
\end{aligned} \tag{4.30}
$$

The partial derivative in eq. (4.30) can be regarded as the sensitivity of a parallel system. Madsen [15] has shown how a sensitivity analysis of a parallel system can be performed and how it relates to updating probabilities of failure. In theory several equality constraints can be taken into account by the method proposed by Madsen [15]. However, the solution of the problem then involves the calculation of higher order derivatives of the failure probability of a parallel system. These derivatives are very difficult to obtain. When more than one equality constraint must be taken into account the method proposed by Schall et al. [19] presented in section 4.2.3 is more efficient.

4.4   Solution of General Multidimensional Integrals

The FORM/SORM-analysis presented in section 4.2.1 can be used in order to solve more general integrals of the type

$$I = \int_{\Omega_{\mathbf{y}}} H(\mathbf{y}) \, d\mathbf{y} \qquad (4.31)$$

where $\Omega_{\mathbf{y}}$ is the integration domain and $H(\mathbf{y})$ is the integrand. In order to use FORM or SORM-analysis this integral is cast in the following form

$$I = \int_{\Omega_{\mathbf{y}}} \frac{H(\mathbf{y})}{f_{\mathbf{y}}(\mathbf{y})} f_{\mathbf{y}}(\mathbf{y}) \, d\mathbf{y} = \int_{\Omega_{\mathbf{y}}} h(\mathbf{y}) f_{\mathbf{y}}(\mathbf{y}) \, d\mathbf{y} \qquad (4.32)$$

where $f_{\mathbf{y}}(\mathbf{y})$ is an arbitrary probability density function, preferably chosen as the standard normal distribution, $\varphi_{\mathbf{y}}(\mathbf{y})$. If the integral involves another probability density function the variables can be transformed into standard normally distributed variables by the Rosenblatt-transformation. In the following only cases where the function $h(\mathbf{y})$ takes on values in the interval $[0; 1]$ will be considered. If the function is restricted this can always be obtained by a transformation. The problem can be formulated in the following way

$$I = \int_{\Omega_{\mathbf{u}}} h(\mathbf{u}) \, \varphi_{\mathbf{u}} d\mathbf{u} \qquad (4.33)$$

where $\mathbf{u}$ is a vector of independent standard normally distributed variables and $\Omega_{\mathbf{u}}$ is the integration domain in the u-space. This integral (eq. (4.33)), can be reformulated in the following way

$$
\begin{aligned}
I &= \int_{\Omega_{\mathbf{u}}} h(\mathbf{u}) \, \varphi_{\mathbf{u}} d\mathbf{u} & (4.34) \\[2mm]
&= \int_{\Omega_{\mathbf{u}}} \Phi\left[\Phi^{-1}[h(\mathbf{u})]\right] \varphi_{\mathbf{u}}(\mathbf{u}) \, d\mathbf{u} & (4.35) \\[2mm]
&= \int_{\Omega_{\mathbf{u}}} P\left(U_a \le \Phi^{-1}[h(\mathbf{u})|\mathbf{U} = \mathbf{u}]\right) \varphi_{\mathbf{u}}(\mathbf{u}) \, d\mathbf{u} & (4.36) \\[2mm]
&= \int_{\Omega_{\mathbf{u}} \cap \Omega_a} \varphi_1(u_a) \, \varphi_{\mathbf{u}}(\mathbf{u}) \, d\mathbf{u} du_a & (4.37)
\end{aligned}
$$

where U_a is an auxiliary standard normally distributed variable and the integration domain Ω_a is given by $\Omega_a = \{u_a - \Phi^{-1}[h(\mathbf{u})] = 0\}$. The integral has now been cast in a form which is suitable for for FORM/SORM-analysis. The advantage of the method over traditional numerical integration procedures such as Gauss-integration is that it requires less evaluations of the integrand and, therefore, is much more efficient. However, the method requires that only one important region which gives a large contribution to the integral exists. If this is not the case there will be multiple β-points and the method cannot be applied.

4.5 Nonlinear Optimization

By maximum likelihood estimation and later by experimental planning optimization problems it is necessary to solve optimiation problems which in the general form can be formulated as

$$\min \quad O(\mathbf{v}) \tag{4.38}$$

$$s.t. \quad f_i(\mathbf{v}) = 0, \quad i = 1, 2, \ldots n_e \tag{4.39}$$

$$f_i(\mathbf{v}) \geq 0, \quad i = n_e + 1, n_e + 2, \ldots n_q \tag{4.40}$$

$$v_{i,l} \leq v_i \leq v_{i,u} \quad i = 1, 2, \ldots, n_v \tag{4.41}$$

where $\mathbf{v}$ are the optimization variables, $O(\mathbf{v})$ is the object function and $f_i(\mathbf{v})$, $i = 1, 2, \ldots n_e$ and $f_i(\mathbf{v})$, $i = n_e + 1, n_e + 2, \ldots n_q$ are the equality and inequality constraints, respectively. The simple lower and upper bounds for the optimization variables are given by $v_{i,l}$ and $v_{i,u}$, respectively. The number of optimization variables is n_v.

If the object function and the constraints are differentiable functions of the optimization variables, $\mathbf{v}$, a gradient-based method can be implemented. By a general gradient-based nonlinear optimization program such as NLPQL (see Schittkowski [20]) a search direction is determined by minimizing a quadratic approximation to the Lagrange function on condition that the linearized constraints are fulfilled. A line search can now be performed where the augmented Lagrange function is used as the merit function.

In order to determine a quadratic approximation to the Lagrange function it is necessary to determine the first and second order derivatives of the object function. The first order derivatives can be determined either numerically or semi-analytically. Approximations of the second order derivatives are determined by the BFGS-method (see e.g Vanderplats [21]). By this method an approximation of the Hessian matrix is determined on the basis of information about the first order derivatives from several iterations. Experience has shown that after n_v iterations, where n_v denotes the number of variables, a good aproximation of the Hessian matrix is usually obtained.

4.6 References

[1] Ayub, B. M., Haldar, A., Practical Structural Reliability Techniques, Journ. of Struc. Eng., ASCE, 110, pp. 1707-1724, 1984.

[2] Thoft-Christensen, P., Baker, M., Structural Reliability Theory and Its Applications, Springer Verlag, Berlin, 1982.

[3] Breitung, K., Probability Approximations by Log Likelihood Maximization, Journ. Eng. Mech., 117, pp. 457-477, 1991.

[4] Box, G. E. P., Tiao, G. C., Bayesian Inference in Statistical Analysis, Addison-Wesley, Reading, MA, USA, 1972.

[5] Ditlevsen, O., Narrow Reliability Bounds for Structural Systems, Journ. Struc. Mech., 7, pp. 171-200, 1979.

[6] Enevoldsen, I., Reliability-Based Structural Optimization, Structural Reliability Theory Paper No. 87, Aalborg University, Denmark, 1991.

[7] Engelund, S., Rackwitz, R., On Predictive Distribution Functions for the Three Asymptotic Extreme Value Distributions, Structural Safety, 11, pp. 255-258, 1992.

[8] Engelund, S., Rackwitz, R., A Benchmark Study on Importance Sampling Techniques in Structural Reliability, Structural Safety, 12, pp. 255-276, 1993.

[9] Fujita, M., Rackwitz, R., Updating First- and Second-Order Reliability Estimates by Importance Sampling, Structural Eng./Earthquake Eng., 5, 1988, pp. 53-59, Japan Society of Civil Engineers (Proc. of JSCE No. 392/I-9).

[10] Gollwitzer, S., Rackwitz, R., An Efficient Numerical Solution to the Multinormal Integral, Probabilistic Engineering Mechanics, 1988, 3, 2, pp. 98-101.

[11] Gollwitzer, S., Rackwitz, R., Equivalent Components in First-Order System Reliability, Reliability Engineering, 1983, 5, pp. 99-115.

[12] Hohenbichler, M., An Asymptotic Formula for the Probability of Intersections, Berichte zur Zuverlässigkeitstheorie der Bauwerke, SFB 96, 69, Technical University of Munich, pp. 21-48, 1984.

[13] Lindley, D. V., Introduction to Probability and Statistics from a Bayesian Viewpoint, Vol 1+2, Cambridge University Press, Cambridge, 1976.

[14] Madsen, H. O., Krenk, S., Lind, N. C., Structural Safety, Prentice Hall, New Jersey, 1986.

[15] Madsen, H. O., Sensitivity Factors for Parallel Systems, in: G. Mohr (ed.), Miscellaneous Papers in Civil Engineering, Danish Engineering Academy, 1992.

[16] Mann, N. R., Schafer, R. E., Singpurwalla, N. D., Methods for Statistical Analysis of Reliability and Life Data, Wiley, New York, USA, 1974.

[17] Rackwitz, R, Fiessler, B., An Algorithm for Calculation of Structural Reliability under Combined Loading, Berichte zur Zuverlässigkeitstheorie, Technical University of Munich, 1977.

[18] Raiffa, H. and Schlaifer, R., Applied Statistical Decision Theory. Harvard University Press, Cambridge, Mass., 1961.

[19] Schall, G., Rackwitz, R., On the Integration of Multinormal Densities over Equalities, Berichte zur Zuverlässigkeitstheorie der Bauwerke, Technische Universität München, 83, 1988.

[20] Schittkowski, K., User's Guide for the Nonlinear Programming Code NLPQL, Institut für Informatik, Universität Stuttgart.

[21] Vanderplats, G. N., Numerical Optimization Techniques for Engineering Design: with Applications, McGraw-Hill, San Francisco, 1984.

Chapter 5

Estimation of the Time to Initiation of Corrosion

The statistical methods presented in the previous chapter (chapter 4) can be used to estimate the parameters in the probabilistic model presented in chapter 3 and to estimate the probability that corrosion has been initiated at a given time. In the following sections it will first be demonstrated how the analysis of a single chloride profile can be performed in order to determine the distribution of the time to initiation of corrosion at the point where the measurement was obtained. Further, it will be shown how the analysis of several profiles can be carried out and how the probability that corrosion has been initiated at an arbitrary point within a given region can be determined.

5.1 Probabilistic Analysis of a Single Chloride Profile

Estimation of the time to initiation of corrosion in a given structure subject to chloride ingress is based on chloride profiles obtained from the structure. In section 2.4 it was described how the time to initiation of corrosion is usually determined for a given chloride profile. However, by a traditional analysis not even the statistical uncertainty related to the estimated parameters is taken into account. In the following sections it will be shown how the analysis of a single chloride profile can be carried out when both the inherent uncertainty and the statistical uncertainty is taken into account.

Let the basis of the coordinate system describing the position, x, be given in the way shown in figure 5.1. The coordinates $(x_1; x_2)$ define a point on the surface of the structure and x_3 denotes the distance from the surface. The following analysis will be based on the same assumption as the traditional analysis, i.e. the concrete can be regarded as an isotropic material and the chloride transport can be described by a 1-dimensional diffusion equation given by

$$\left. \begin{array}{rcl} \frac{\partial c(x_3,t)}{\partial t} & = & \frac{\partial}{\partial x_3}\left(D\left(x_3\right)\frac{\partial}{\partial x_3}c\left(x_3,t\right)\right) \\ c\left(0,t\right) & = & c_s \end{array} \right\} \tag{5.1}$$

It is further assumed that the chloride concentration tends to zero as x_3 increases and that the initial chloride concentration (at t=0) is 0 % for all values of x_3 except on the

69
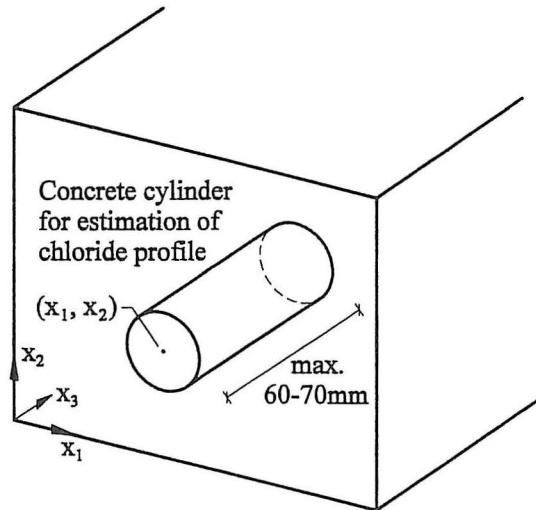
Figure 5.1: *Definition of coordinate system.*

surface, i.e. $x_3 = 0$.

5.1.1   Parameter Estimation

Based on a single chloride profile it is possible to estimate an outcome of the surface concentration at the point where the chloride profile was obtained, $\hat{c}_s = \hat{c}_s\left(x_{1i}; x_{2i}\right)$ where $\left(x_{1i}; x_{2i}\right)$ denotes the point on the surface of the structure where the ith chloride profile was obtained.

A chloride profile consists of a number of measurements of the chloride concentration as a function of the distance to the surface, x_3. The largest distance to the surface does usually not exceed 60 - 70 mm. At larger depths the chloride concentration is normally negligible. Further, as long as the chloride concentration around the reinforcement (at the depth 30 - 60 mm) is much lower than the surface concentration, the value of the transport coefficient at depths exceeding 100 mm will have no significant influence on the chloride concentration around the reinforcement. Since the correlation length of $\{D_2\left(\mathbf{x}\right)\}$ is about 200 - 500 mm it seems safe to assume that the variation of $\{D_2\left(\mathbf{x}\right)\}$ with the depth can be neglected. This implies that $\{D_2\left(\mathbf{x}\right)\} = \{D_2\left(x_1; x_2\right)\}$. Hence, for a given chloride profile obtained at the point $\left(x_{1i}; x_{2i}\right)$ the stochastic field $\{D_2\left(\mathbf{x}\right)\}$ can be approximated by a stochastic variable $D_2 = D_2\left(x_{1i}; x_{2i}\right)$. On the basis of a single chloride profile it is possible to determine an outcome of $D_0\left(\mathbf{x}\right) + \{D_2\left(x_1; x_2\right)\}$ given by $\hat{D}\left(x_{1i}; x_{2i}; x_3\right) = D_0\left(x_{1i}; x_{2i}; x_3\right) + \hat{D}_2\left(x_{1i}; x_{2i}\right)$. Assuming that $\{D_1\left(\mathbf{x}\right)\}$ can be modelled as a homogenous Gaussian field it is also possible to estimate the parameters in the autocovariance function of $\{D_1\left(\mathbf{x}\right)\}$. In conclusion, if $\{D_1\left(\mathbf{x}\right)\}$ is a homogenous Gaussian field the following parameters can be estimated on the basis of a single chloride profile

$$\mathbf{p} = \left(\hat{c}_s; \hat{D}, \sigma_{D_1}, a\right) \qquad (5.2)$$

where σ_{D_1} denotes the standard deviation of $\{D_1(\mathbf{x})\}$ and a denotes the scale of fluctuation of $\{D_1(\mathbf{x})\}$.

The parameters $\mathbf{p}$ are estimated by maximizing the likelihood, l, of the measurements $\left(\hat{c}(x_{3_1}, t_m), \hat{c}(x_{3_2}, t_m), \ldots, \hat{c}(x_{3_{n_m}}, t_m)\right)$ where x_{3_j} denotes the distance from the surface to the jth measurement of the chloride concentration, t_m is the time at which the measurements were obtained and n_m denotes the number of measurements in the given profile. The optimization problem is formulated as

$$\max_{\mathbf{p}} l(\mathbf{p}) = \max_{\mathbf{p}} l\left(\cap_{j=1}^{n_m} \{\hat{c}(x_{3_j}, t_m) = c(x_{3_j}, t_m) + \varepsilon_j\}|\mathbf{p}\right) \tag{5.3}$$

where $\varepsilon_j, j = 1, \ldots, n_m$ are assumed to be independent normally distributed stochastic variables describing the model and measurement uncertainty. The mean value of ε_i is zero and the standard deviation is s_ε.

The chloride concentration $c(x_3, t_m)$ is a function of the surface concentration at the point where the measurement was obtained and a function of the transport coefficient.

$$c(x_3, t_m) = c\left(x_3, t_m, \hat{c}_s(x_{1_i}; x_{2_i}), \hat{D}(x_{1_i}; x_{2_i}; x_3) + \{D_1(x_{1_i}; x_{2_i}; x_3)\}\right) \tag{5.4}$$

For a given discretization of $\{D_1(\mathbf{x})\}$ the variables describing $\{D_1(\mathbf{x})\}$ will be denoted by $\mathbf{Z}$. The density function of $\mathbf{Z}$ depends on the standard deviation and scale of fluctuation of $\{D_1(\mathbf{x})\}$, $\mathbf{Z} = \mathbf{Z}(\sigma_{D_1}, a)$. The density function of $\mathbf{Z}$ for a given set of parameters, $\mathbf{p}$, is denoted $f_{\mathbf{Z}|\mathbf{p}}(\mathbf{z}|\mathbf{p})$.

The likelihood, eq. (5.3), can be written

$$l(\mathbf{p}) = \int_{\Omega_\varepsilon} \int_{\Omega_z} f_{\mathbf{Z}|\mathbf{p}}(\mathbf{z}|\mathbf{p}) f_\varepsilon(\varepsilon) \, d\mathbf{z} d\varepsilon \tag{5.5}$$

where $\Omega_z = \left\{\mathbf{z} : \cap_{j=1}^{n_m}\left(\hat{c}(x_{3_j}, t_m) = c(x_{3_j}, t_m) + \varepsilon_j\right)\right\}$ and $\Omega_\varepsilon = R^{n_m}$. The likelihood, eq. (5.5), can be evaluated by a FORM/SORM analysis with equality constraints, see section 4.2.3.

5.1.2 Lifetime Estimation

The distribution function of the time to initiation of corrosion is $F_T(t) = P_I(t)$ where $P_I(t)$ is the probability that corrosion has been initiated at the time t. As earlier mentioned corrosion is initiated when the chloride concentration at some point along the reinforcement exceeds a critical threshold value, c_{cr}. The probability that corrosion is initiated at the point where the chloride profile was obtained is

$$P_I(t) = \int_{\Omega_\mathbf{p}} \int_{g \leq 0} f_{\mathbf{Z}|\mathbf{p}}(\mathbf{z}|\mathbf{p}) f_\mathbf{p}(\mathbf{p}) \, dy d\mathbf{z} d\mathbf{p} \tag{5.6}$$

where $\Omega_\mathbf{p}$ denotes the admissible range of $\mathbf{p}$, and g is a failure function given by $g = c_{cr} - c(\delta, t)$ where δ is the thickness of the cover and c_{cr} is a stochastic variable modelling the threshold value for initiation of corrosion at the point where the chloride profile was obtained. The vector $\mathbf{Y}$ contains the stochastic variables not included in $\mathbf{p}$ and $\mathbf{Z}$, i.e.

the critical threshold for initiation of corrosion and the thickness of the cover. Also this problem can be solved by FORM/SORM-analysis, see section 4.2.1.

5.2   Example: Probabilistic Analysis of a Single Chloride Profile

In table 5.1 a representative set of data, measured at $t = 10.0$ years is shown. The chloride concentration is given as % of the dry weight of concrete.

x_3 [mm]	c [%]
4.5	1.03
7.5	0.79
10.5	0.60
13.1	0.49
16.1	0.38
19.6	0.27
22.6	0.18
25.6	0.12
28.6	0.07
31.5	0.05
34.4	0.03
37.4	0.01

Table 5.1: *Measured chloride concentrations.*

The measurements have been obtained from a bridge pier of a highway bridge. The composition of the concrete is shown in table 5.2. It is important to notice that the w/c-ratio is 0.41 which should be sufficient to ensure that the system of capillary pores and microcracks is connected. An inspection of the pier has shown that no cracks larger than 0.01-0.1 mm exist. The concrete can, therefore, be regarded as uncracked.

Component	Content
Cement	340
Water	140
Fly ash	50
Sand	622
Fine gravel 2/8 mm	285
Coarse gravel 2/18 mm + 18/25 mm	920

Table 5.2: *Concrete composition (all units are kg/m^3).*

The cover thickness is assumed to be known for the given profile. In the present case the value $\delta = 50$ mm is used. The critical threshold, c_{cr} is modelled as a normally distributed

variable with mean 0.075 % and coefficient of variation 0.2. This model is based on the measurements from highway bridges shown in table 2.2.

As mentioned, the analysis will be based on a one-dimensional model of the chloride flow. In general it is, however, necessary to take into account the low-scale spatial variation of the transport coefficient. The simple analytical solution of the one-dimensional diffusion equation, therefore, cannot be applied. Instead, the calculation of the chloride concentrations is performed by using the standard formulation of the Finite Element Method described in section 3.5.1. The computations are performed using the program FEMAN described in Appendix A.2. The optimization problem, eq. (5.3), is solved by the use of the NLPQL-algorithm, see Schittkowski [3]. A brief description of the various program modules used in order to perform the computations necessary for this example is given in appendix A.

5.2.1 Least Squares Fit

Initially, a traditional analysis according to the methodology outlined in section 2.4 is performed. The model parameters, the transport coefficient, D, and the surface concentration, c_s, are estimated by least squares estimation where the parameters are determined by minimizing

$$s^2 = \sum_{j=1}^{n_m} \left(\hat{c} \left(x_{3_j}, t_m \right) - c \left(x_{3_j}, t_m \right) \right)^2 \tag{5.7}$$

It is found that $\hat{D} = 11.2$ mm²/year and that $\hat{c}_s = 1.31$ %. In table 5.3 the time to initiation of corrosion is shown for different values of the critical threshold value, c_{cr}. By this analysis the statistical uncertainty related to the estimated parameters and the uncertainty related to the critical threshold have not been taken into account. This implies that no uncertainty is related to the estimated time to initiation of corrosion.

c_{cr}	T
%	years
0.05	26.0
0.075	30.9
0.10	35.6

Table 5.3: *Time to initiation of corrosion determined by a traditional analysis.*

5.2.2 2-Parameter Model

The model used in order to obtain the least squares fit can be regarded as a simplification of the general model presented in section 3.1. The simple model is obtained by assuming that the low-scale random spatial fluctuation of the transport coefficient can be neglected and that the mean value of the transport coefficient does not depend on the position. The transport coefficient is, thereby, modelled by $D(\mathbf{x}) = \hat{D}$, where $\hat{D}$ is a constant.

Since the transport coefficient is modelled as a constant the chloride concentration at a given point can be determined analytically which implies that the parameters can be estimated with relative ease. Another advantage by the method is that the statistical uncertainty will be small, since there are only two parameters.

Parameter Estimation

The parameters in the simple model and their associated statistical uncertainty can now be estimated by the maximum likelihood method. Because the low-scale random fluctuation of the transport coefficient is neglected the problem does not involve the vector $\mathbf{Z}$ (which contains the stochastic variables describing the spatial variation of $\{D_1(\mathbf{x})\}$). The likelihood can, therefore, be evaluated by

$$l(\mathbf{p}) = \prod_{i=1}^{n_m} f_{\varepsilon_i}(\varepsilon_i) \tag{5.8}$$

where $\varepsilon_i = \hat{c}(x_3, t_m) - cc(x_3, t_m)$ and $f_{\varepsilon_i}(\varepsilon_i)$ is a normal distribution with zero mean and standard deviation s_ε.

In table 5.4 the estimated parameters are shown for different values of the standard deviation of the model and measurement uncertainty, s_ε. It is seen that the parameters are independent of s_ε. Further, the estimated parameters are in good accordance with the results of a simple least squares estimation, see section 5.2.1.

s_ε	$\hat{c}_s$	$\hat{D}$
%	%	mm^2/year
0.0175	1.33	11.3
0.0200	1.33	11.3
0.0225	1.33	11.3

Table 5.4: *Parameters for the 2-parameter model.*

For $s_\varepsilon = 0.0200$ the following covariance matrix of the unknown parameters, $\mathbf{p} = \left(\hat{c}_s, \hat{D}\right)$ is obtained

$$\mathbf{C_p} = \begin{bmatrix} 0.000740 & -0.00990 \\ -0.00990 & 0.227 \end{bmatrix} \tag{5.9}$$

It is seen that the statistical uncertainty is very small, especially the statistical uncertainty related to the surface concentration is negligible. It can also be seen that the parameters $\hat{c}_s$ and $\hat{D}$ are negatively correlated, $\rho_{\hat{c}_s, \hat{D}} = -0.76$, implying that a high surface concentration and a high transport coefficient are unlikely to occur at the same time.

Lifetime Estimation

On the basis of the parameters shown in table 5.4 and their associated statistical uncertainty, the distribution of the time to initiation of corrosion, T, can now be estimated.

s_ε	μ_T	σ_T
%	years	years
0.0175	29.90	3.15
0.0200	29.91	3.20
0.0225	29.92	3.24

Table 5.5: *Mean value and standard deviation of the lifetime*

The mean and standard deviation of T are shown in table 5.5 where μ_T and σ_T indicates the mean and standard deviation, respectively.

The mean value of the time to initiation of corrosion does not depend on s_ε. However, the standard deviation of the lifetime increases as the standard deviation of the measurement and model uncertainty increases. It is evident that when less accurate information is available the result also becomes less accurate.

As earlier mentioned the mean value of the critical threshold in this analysis is 0.075 %. The result of this probabilistic analysis can, therefore, be compared with the result of the traditional analysis based on $c_{cr} = 0.075$, see section 5.2.1. It is seen that the mean time to initiation of corrosion determined by the probabilistic analysis is the same as the time to initiation of corrosion estimated by the traditional analysis. This is because both computations are based on the same model. The advantage of the probabilistic model is that it also provides an estimate of the uncertainty related to the lifetime. In this case the coefficient of variation of the lifetime is estimated to be about 10 %.

Sensitivity Analysis

The most important stochastic variable in this lifetime estimation is the critical threshold value for initiation of corrosion, c_{cr}. The estimation of the distribution parameters of this variable is solely based on the information shown in table 2.2. It is, therefore, important to investigate the effect of changing the distribution parameters of c_{cr}.

In figures 5.2a and 5.2b, respectively, the mean and standard deviation of the lifetime as functions of the mean value of the critical threshold, c_{cr}, are shown. In this study the coefficient of variation of c_{cr} has been held constant. As expected, both the mean value and standard deviation of the lifetime increases with increasing mean value of the critical threshold. The mean and standard deviation of the lifetime are shown in figures 5.3a and 5.3b, respectively, as functions of the standard deviation of the critical threshold, c_{cr}. The mean value of c_{cr} in this analysis is constant, $\mu_{c_{cr}} = 0.075\%$. It is seen that the mean of the lifetime is invariant towards changes in the standard deviation of c_{cr}. It is also seen that the standard deviation of the lifetime increases with increasing standard deviation of c_{cr}.

The results of the sensitivity analysis are not surprising. The most important observation which can be made on the basis of the analysis is that the uncertainty related to the lifetime only depends on the uncertainty related to the critical threshold, c_{cr}. This observation can be made on the basis of figure 5.3b where it is seen that the standard deviation of the lifetime is a linear function of the standard deviation of the critical threshold.

An extrapolation of the line indicates that when the standard deviation of the critical threshold is negligable also the standard deviation of the lifetime is negligable, i.e. the statistical uncertainty related to the estimated parameters, $\mathbf{p}$, has very little influence on the standard deviation of the lifetime.
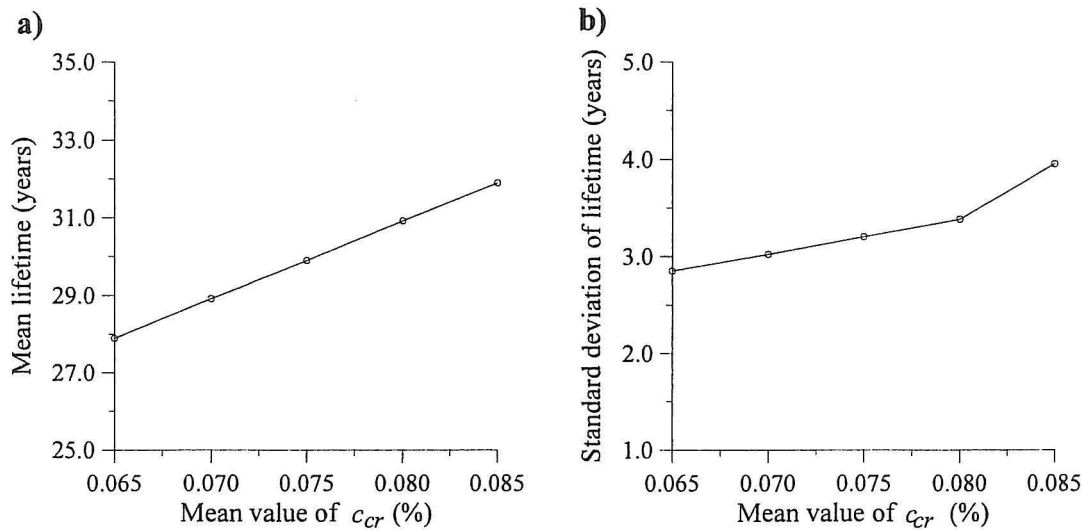
Figure 5.2: *Sensitivity with respect to the mean of c_{cr}.*
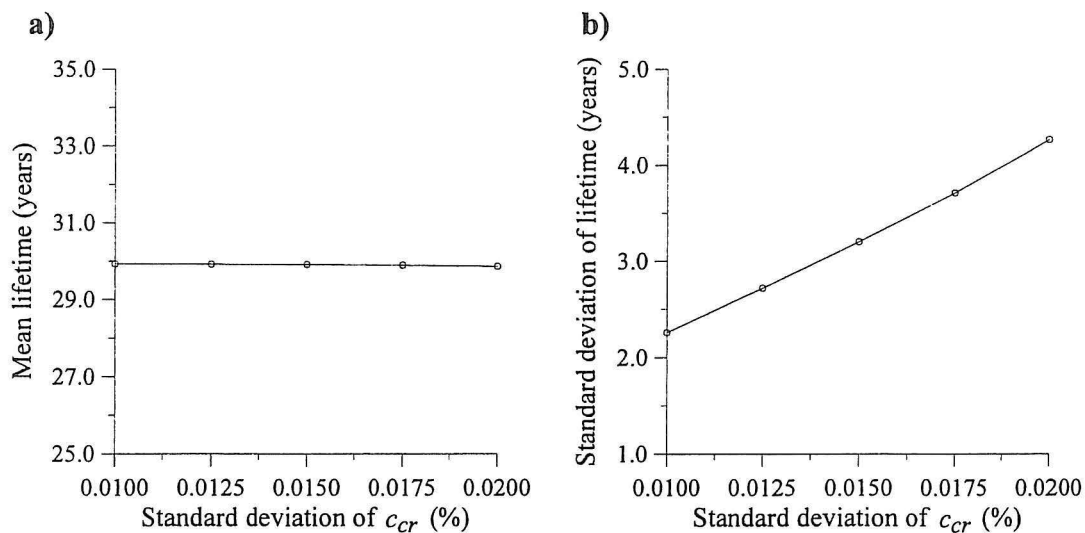
Figure 5.3: *Sensitivity with respect to the standard deviation of c_{cr}.*

5.2.3   3-Parameter Model

The transport coefficient for the outer layer of the structure often has a value different from the transport coefficient for the rest of the structure. This phenomenon can be taken into account by letting the transport coefficient depend on the depth, x_3. In the following a simple model is considered where the low-scale random spatial variation of the transport coefficient is neglected and where the transport coefficient is modelled as

$$\hat{D}(x_3) = \begin{cases} \hat{D}_s & 0 \text{ mm} \leq x_3 \leq 20 \text{ mm} \\ \hat{D}_i & 20 \text{ mm} < x_3 \end{cases} \qquad (5.10)$$

It is now necessary to estimate the parameters, $\mathbf{p} = \left(\hat{c}_s, \hat{D}_s, \hat{D}_i\right)$.

Parameter Estimation

Because the low-scale spatial fluctuation of the transport coefficient is neglected, the parameters can be estimated in the same way as by the 2-parameter model, see section 5.2.2. In table 5.6 the estimated parameters are shown for different values of the standard deviation of the model and measurement uncertainty.

s_ε	$\hat{c}_s$	$\hat{D}_s$	$\hat{D}_i$
	%	mm^2/year	mm^2/year
0.0175	1.33	11.2	8.68
0.0200	1.33	11.2	8.68
0.0225	1.33	11.2	8.68

Table 5.6: *Parameters for the 3-parameter model.*

As for the simple 2-parameter model the parameters do not depend on s_ε. The results indicate that the transport coefficient for the outer layer is larger than the transport coefficient for the inner part of the structure. This can be caused by a larger permeability of the outer layer. However, the effect can also be explained by the fact that the outer layer has lost its ability to bind chloride, thus making the transport of chloride through this layer more efficient.

It is also interesting to notice that $\hat{D}_s$ is almost equal to the value of the transport coefficient estimated on the basis of the 2-parameter model. This indicates that for the 2-parameter model, the transport coefficient has been fitted almost exclusively on the basis of the first few measurements. The last measurements have very little influence on the result due to the relatively large model and measurement uncertainty. In case the transport coefficient is smaller in the inner part of the structure, the assumption that the transport coefficient is constant will be conservative.

For $s_\varepsilon = 0.0200$ the covariance matrix of the parameters, $\mathbf{p}$, is

$$\mathbf{C_p} = \begin{bmatrix} 0.000793 & -0.00975 & -0.00175 \\ -0.00975 & 0.234 & 0.316 \\ -0.00175 & 0.316 & 4.14 \end{bmatrix} \qquad (5.11)$$

It is noticed that the statistical uncertainty related to $\hat{D}_i$ is much larger than the uncertainty related to the other parameters. The large statistical uncertainty originates from the fact that for the measurements in the inner part on the structure, the standard deviation of the model and measurement uncertainty is large in comparison with the measured chloride concentrations. The estimation of $\hat{D}_i$, therefore, is based on very inaccurate information.

Lifetime Estimation

The mean values and standard deviations of the lifetimes estimated on the basis of the 3-parameter model are shown in table 5.7. It is seen that the mean value of the lifetime is larger than the mean values determined on the basis of the 2-parameter model. This is of course due to the fact that $\hat{D}_i$ is significantly smaller than the constant, $\hat{D}$, estimated by the 2-parameter model. However, the standard deviation of the lifetime shows a substantial increase compared to the standard deviation found by the 2-parameter model. This effect is caused by the large statistical uncertainty associated with $\hat{D}_i$.

s_ε	μ_T	σ_T
%	years	years
0.0175	34.59	6.03
0.0200	34.35	6.91
0.0225	34.18	7.87

Table 5.7: *Mean value and standard deviation of the lifetime.*

5.2.4   4-Parameter Model

Now a model where low-scale the random spatial variation of the transport coefficient is taken into account is considered. The mean value of the transport coefficient, $D_0(x)$, is assumed to be constant.

$$\{D(x)\} = \hat{D} + \{D_1(x)\} \tag{5.12}$$

where $\hat{D}$ is a constant. $\{D_1(x)\}$, is modelled as a homogenous zero mean Gaussian field with auto-correlation function

$$\kappa_{D_1 D_1}(d) = \sigma_{D_1}^2 \exp\left(-\frac{d^2}{a^2}\right) \tag{5.13}$$

where σ_{D_1} denotes the standard deviation of the field, d the distance between two points in the 1-dimensional model and a is an unknown constant expressing the correlation length of the field. The unknown parameters now are $\mathbf{p} = \left(\hat{c}_s, \hat{D}, \sigma_{D_1}, a\right)$.

Parameter Estimation

In order to represent the stochastic field the two discretization schemes presented in section 3.7, the midpoint and the local average methods are implemented. In tables 5.8 and 5.9 the estimated parameters are shown for different values of the standard deviation of the model and measurement uncertainty for the midpoint and local average method, respectively

It is seen that there is virtually no difference between the results obtained by the local average method and the midpoint method. Since the midpoint method and the local average method tend to over- and under-represent the variability of the field, respectively,

s_ε	$\hat{c}_s$	$\hat{D}$	σ_{D_1}	a
%	%	mm^2/year	mm^2/year	mm
0.0075	1.41	10.5	1.54	5.69
0.0100	1.40	10.8	1.41	4.77
0.0125	1.38	11.0	1.24	3.72

Table 5.8: *Parameters found by the midpoint method.*

s_ε	$\hat{c}_s$	$\hat{D}$	σ_{D_1}	a
%	%	mm^2/year	mm^2/year	mm
0.0075	1.42	10.5	1.55	5.56
0.0100	1.40	10.7	1.41	4.72
0.0125	1.38	11.0	1.06	3.59

Table 5.9: *Parameters found by the local average method.*

this indicates that a good representation of the stochastic field has been obtained. It is interesting to notice that the standard deviation of $\{D_1\}$ depends on the measurement uncertainty. As s_ε increases, the standard deviation of $\{D_1\}$ decreases. This is explained by the fact that, as s_ε increases, the variability of the measurements is to a larger extent ascribed to the measurement uncertainty than to the variability of the transport coefficient.

It is also interesting to notice that for small values of s_ε the value, $\hat{D}$, lies between the two values of the transport coefficient ($\hat{D}_i$ and $\hat{D}_s$) found by the 3-parameter model, see section 5.2.3. As s_ε increases, only the measurements in the outer layer are important. The value, $\hat{D}$, then approaches the value for the transport coefficient of the outer layer, $\hat{D}_s = 11.2$ mm^2/year which was determined on the basis of the 3-parameter model.

In tables 5.8 and 5.9 it is also seen that the coefficient of variation of the transport coefficient is less than 15 %. This is due to the fact that the experimental results, see table 5.1, lie very close to the solution to the diffusion equation. For other sets of measurements higher coefficients of variation of the diffusion coefficient can be observed. In tables 5.8 and 5.9 it is further seen that the correlation length of $\{D_1\}$ is about 4-5 mm. Taking into account that the measured chloride concentrations are determined as the local average over a length of about 3 mm this correlation length is very short. In fact, the correlation might solely be caused by the local averaging.

For $s_\varepsilon = 0.010$ the covariance matrix of the estimated parameters are

$$
C_p = \begin{bmatrix}
0.00450 & -0.0371 & 0.0104 & 0.156 \\
-0.0371 & 1.061 & -0.120 & -1.62 \\
0.0104 & -0.120 & 0.427 & 1.05 \\
0.156 & -1.62 & 1.05 & 14.6
\end{bmatrix}
\tag{5.14}
$$

The variance of the surface concentration and the mean of the transport coefficient are

much larger than by the 2-parameter model even though s_ε is a factor 2 smaller. This is partly because a larger number of parameters has been included in the model. It might, however, also be because the model provides a poor fit to the measurements.

Lifetime Estimation

In table 5.10 the mean and standard deviation of the lifetime found using the midpoint and local average methods are shown. Again, it is seen that the two methods yield identical results.

	Midpoint		Local average	
s_ε	μ_T	σ_T	μ_T	σ_T
%	years	years	years	years
0.0075	32.83	5.93	32.80	5.94
0.0100	32.44	5.45	32.39	5.45
0.0125	31.61	4.73	31.63	4.73

Table 5.10: *Mean value and standard deviation of the lifetime.*

In figure 5.4 the distribution functions of the lifetime found by the midpoint method are shown for different values of s_ε. It is disturbing to observe that the variability of T decreases with increasing measurement uncertainty. The variability of the lifetime should increase as the measurement uncertainty increases. The reason for this behaviour must be ascribed to the fact that the mean value of the transport coefficient is not constant as assumed. It is therefore difficult to obtain a good fit to the measurements if s_ε is too small.
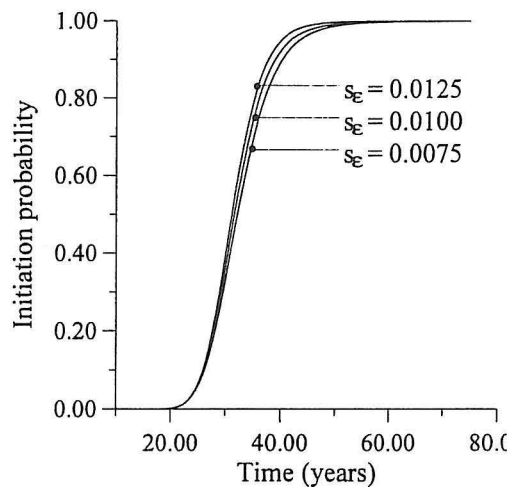

Figure 5.4: *Distribution function of the lifetime.*

5.2.5 5-Parameter Model

The shortcomings of the 4-parameter model can be overcome by letting the mean value be a function of x_3 such that

$$\{D(x_3)\} = \hat{D}(x_3) + \{D_1(x_3)\} \tag{5.15}$$

Analog to the 3-parameter model let $\hat{D}(x_3)$ be given by

$$\hat{D}(x_3) = \begin{cases} \hat{D}_s & 0 \text{ mm} \leq x_3 \leq 20 \text{ mm} \\ \hat{D}_i & 20 \text{ mm} < x_3 \end{cases} \tag{5.16}$$

The standard deviation of $\{D_1(x_3)\}$ is modelled by

$$\sigma_{D_1}(x_3) = VD_0(x_3) \tag{5.17}$$

where V is a constant coefficient of variation. The auto-covariance function is given by

$$\kappa_{D_1 D_1}(x_{3_1}, x_{3_2}) = V^2 D_0(x_{3_1}) D_0(x_{3_2}) \exp\left(-\frac{d^2}{a^2}\right) \tag{5.18}$$

where $d = |x_{3_1} - x_{3_2}|$. The vector of unknown parameters is $\mathbf{p} = \left(\hat{c}_s, \hat{D}_s, \hat{D}_i, \sigma_{D_1}, a\right)$.

Parameter Estimation
The estimated parameters are shown in table 5.11. In contrast to the results obtained by the 4 parameter model it is now observed that $\hat{D}_s$ and $\hat{D}_i$ both are invariant towards changes of s_ε. As for the 4-parameter model it can be observed that the coefficient of variation of the transport coefficient, V, decreases with increasing model and measurement uncertainty.

s_ε	$\hat{c}_s$	$\hat{D}_s$	$\hat{D}_i$	V	a
%	%	mm^2/year	mm^2/year		mm^2/year
0.0075	1.38	3.65	2.77	0.104	3.73
0.0100	1.37	3.66	2.76	0.0973	3.27
0.0125	1.36	3.65	2.76	0.0880	2.81

Table 5.11: Parameters.

For $s_\varepsilon = 0.010$ we find the following covariance matrix of the estimated parameters

$$\mathbf{C_p} = \begin{bmatrix} 0.0246 & -0.0118 & 0.00128 & 0.000160 & 0.109 \\ -0.0118 & 0.528 & 0.0796 & -0.00212 & -0.210 \\ 0.00128 & 0.0796 & 1.360 & 0.0828 & -0.467 \\ 0.000160 & -0.00212 & 0.0828 & 0.00197 & -0.0220 \\ 0.109 & -0.210 & -0.467 & -0.0220 & 12.5 \end{bmatrix} \tag{5.19}$$

Comparing this covariance matrix with the covariance matrix for the 4-parameter model which was determined on the basis of the same value of s_ε, it is seen that the statistical uncertainty on a number of parameters has decreased in spite of the fact that a larger number of parameters has been estimated. This is a sure indication that this model provides a better fit to the data.

Lifetime Estimation

s_ε	μ_T	σ_T
%	years	years
0.0075	34.63	4.78
0.0100	34.78	4.80
0.0125	35.04	4.92

Table 5.12: *Mean value and standard deviation of the lifetime.*

In table 5.12 it is seen that the mean value of the lifetime is constant for all investigated values of s_ε. Further, the standard deviation of the lifetime increases slightly as s_ε increases. The increase, however, is very small. In fact what happens when s_ε is changed is that both the statistical uncertainty and the inherent physical uncertainty changes in such a way that the standard deviation of the lifetime remains nearly constant.

Sensitivity Analysis
As for the 2-parameter model the critical threshold for initiation of corrosion is the most important parameter when determining the lifetime of the structure. A sensitivity analysis with respect to the parameters in the distribution of c_{cr} has, therefore, been performed. In figures 5.5a and 5.5b the sensitivity of the mean and standard deviation of the lifetime, respectively, are shown as a function of the mean of c_{cr}. The coefficient of variation of c_{cr} is held constant.

The sensitivity of the mean and standard deviation of the lifetime, respectively, with respect to changes in the standard deviation of c_{cr} are shown in figures 5.6a and 5.6b. The analyses show the same results as reported by the 2-parameter model. The lifetimes determined on the basis of the 5-parameter model are, however, sligthly less sensitive. This is due to the fact that other variables in this case also contribute to the uncertainty related to the lifetime.

Due to the small scale of fluctuation ($a \approx 3$ mm), modelling the low-scale fluctuation of the transport coefficient requires a relatively large number of stochastic variables. The computational effort involved in the evaluation of the lifetime can, therefore, be reduced considerably if the influence of the low-scale fluctuation can be shown to be negligible. Hence, a computation where the low-scale fluctuation is not taken into account has been performed. All other parameters and their statistical uncertainty remain unchanged. For $s_\varepsilon = 0.0100$ it is found that $\mu_T = 34.74$ years and $\sigma_T = 4.62$ years. By comparing with the results shown in table 5.12 it is seen that the mean remains constant and that neglecting the low-scale spatial variation of the transport leads to a decrease of the standard deviation of only 3.75 %. This clearly indicates that the low-scale fluctuation of the transport

coefficient can be neglected. This result is, however, not surprising since the small correlation length of the transport coefficient implies that it is unlikely to obtain an outcome of $\{D_1\}$ which is extreme. An extreme outcome here means an outcome which leads to a chloride concentration around the reinforcement which is considerably different from the concentration determined by using the mean value of the transport coefficient.

a)   b)
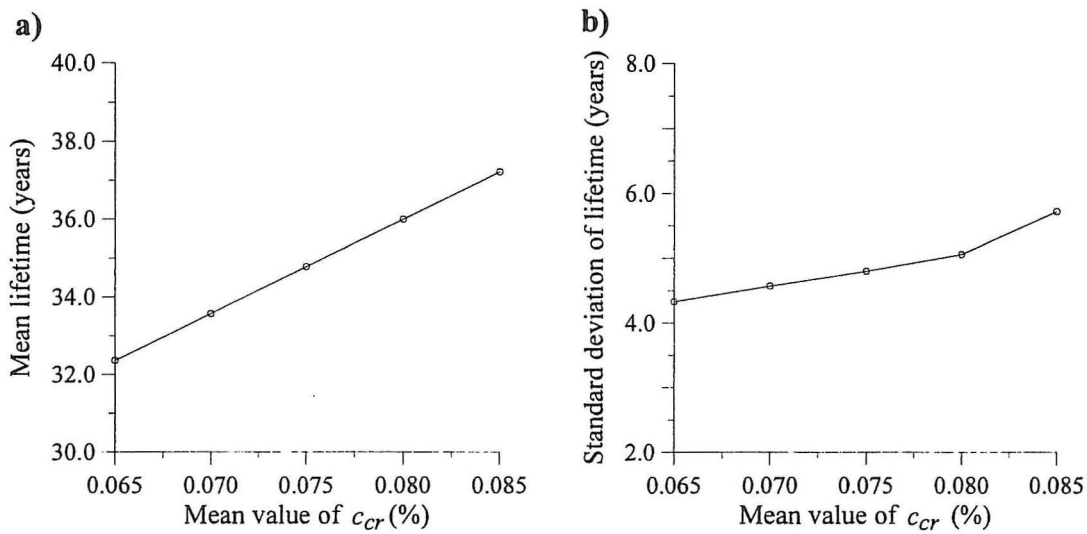
Figure 5.5: *Sensitivity with respect to the mean of c_{cr}.*

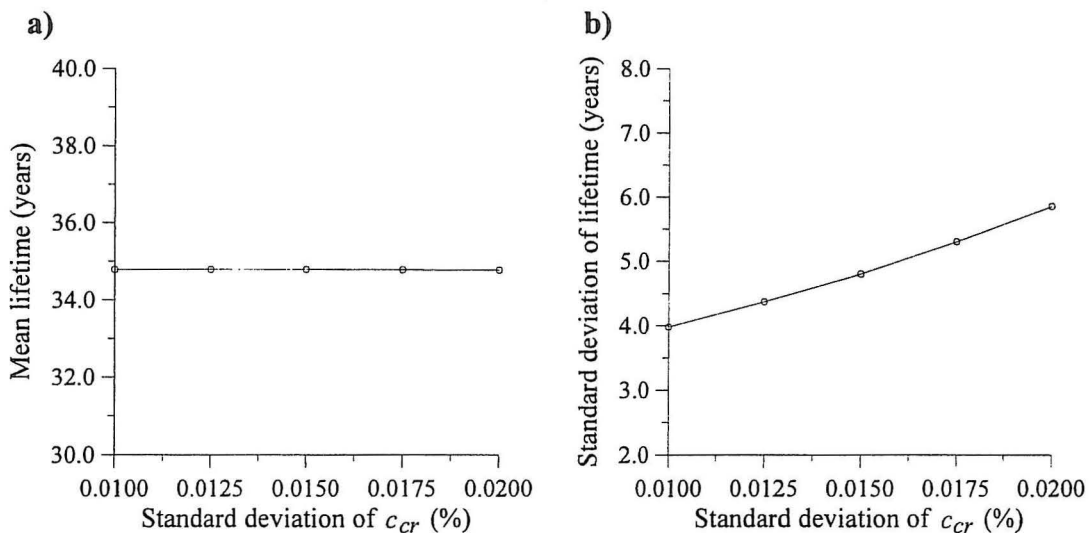a)   b)

Figure 5.6: *Sensitivity with respect to the standard deviation of c_{cr}.*

5.3 Probabilistic Analysis of Several Chloride Profiles

The analysis of a single chloride profile presented in section 5.1 yields an estimate of the time to initiation of corrosion at the point where the measurement was obtained. However,

the purpose of an analysis is usually to determine the probability that corrosion has been initiated at an arbitrary point within a given region. In order to solve this problem it is necessary to take the large-scale random fluctuation of the transport coefficient into account as well as the random spatial fluctuations of the surface concentration, the critical threshold for initiation of corrosion and the cover thickness.

In the following it will be assumed that the variations of the transport coefficient and surface concentration within the area where the measurements are obtained are caused by random variations. Further, because the influence of the low-scale fluctuation of the transport coefficient in section 5.2.5 was shown to be negligible, the low-scale fluctuation of the transport coefficient will not be taken into account. This implies that the models of the transport coefficient and surface concentration presented in section 3.1 now can be formulated in the following way

$$\{D(\mathbf{x})\} = D_0(x_3) + \{D_2(x_1; x_2)\} \tag{5.20}$$
$$\{c_s(\mathbf{x})\} = c_{s_0} + \{c_{s_1}(x_1; x_2)\} \tag{5.21}$$

where D_0 and c_{s_0} describes the means of the transport coefficient and surface concentration, $\{D_2(x_1; x_2)\}$ is a homogenous stochastic field describing the large scale fluctuation of the transport coefficient and and $\{c_{s_1}(x_1; x_2)\}$ is a homogenous stochastic field describing the fluctuation of the surface concentration.

Now the following quantities must be estimated

- The mean value of the surface concentration.
- The standard deviation of the surface concentration.
- The scale of fluctuation of the surface concentration.
- The mean value of the transport coefficient.
- The standard deviation of the large-scale fluctuation of the transport coefficient.
- The scale of fluctuation of the large-scale fluctuation of the transport coefficient.

On the basis of the investigation by Hergenröder mentioned in section 3.1 it is known that the scale of fluctuation for the large-scale fluctuation of the transport coefficient is about 200 - 500 mm. The scale of fluctuation of the surface concentration is assumed to be of the same magnitude. The measurements of the chloride profiles, however, usually are made at a distances much larger than 500 mm. The outcomes of the transport coefficient and surface concentration estimated on the basis of different profiles, therefore, must be considered to be independent. The scales of fluctuation cannot be estimated on the basis of the available data. The fact that the outcomes are independent, however, implies that the means and standard deviations of the surface concentration and transport coefficient can be estimated within the framework of Bayesian statistics relatively easy.

5.3.1   Parameter Estimation

Let the variables be gathered in a r-dimensional stochastic vector $\mathbf{Y} = (Y_1, Y_2, \ldots, Y_r)$. In case the 2-parameter model is implemented $r = 2$ and an outcome of the vector $\mathbf{Y}$ is given

by $\hat{\mathbf{y}}^T = \mathbf{p} = \left(\hat{D}, \hat{c}_s\right)$. The expected value of $\mathbf{Y}$ is $\boldsymbol{\mu}$ and the covariance matrix is $\mathbf{C_{YY}}$. If the surface concentration and transport coefficient are both homogenous Gaussian fields, $\mathbf{Y}$ is a normally distributed vector with density function $f_{\mathbf{Y}}\left(\mathbf{y}|\boldsymbol{\mu}, \mathbf{C_{YY}}\right)$.

It is assumed that the covariance matrix $\mathbf{C_{YY}}$ can be written

$$\mathbf{C_{YY}} = \frac{1}{h}\boldsymbol{\eta}^{-1} \tag{5.22}$$

where $|\boldsymbol{\eta}| = 1$ and h is the so-called mean precision. The relative precision, $\boldsymbol{\eta}$, is assumed to be known. The parameters to be estimated are $\boldsymbol{\mu}$ and h. Further, it is assumed that $\boldsymbol{\mu}$ and h are uncertain and are modelled by stochastic variables. Independent realizations $\hat{\mathbf{y}}_i$, $i = 1, 2, \ldots, n_p$ of the stochastic vector $\mathbf{Y}$ are available where n_p denotes the number of chloride profiles. The following quantities can now be calculated.

$$\mathbf{m} = \frac{1}{n_p}\sum_{i=1}^{n_p}\hat{\mathbf{y}}_i \tag{5.23}$$

$$\mathbf{H} = n_p\boldsymbol{\eta} \tag{5.24}$$

$$\nu = r\left(n_p - 1\right) \tag{5.25}$$

$$v = \frac{1}{\nu}\sum_{i=1}^{n_p}\left(\hat{\mathbf{y}}_i - \mathbf{m}\right)^T\boldsymbol{\eta}\left(\hat{\mathbf{y}}_i - \mathbf{m}\right) \tag{5.26}$$

Raiffa and Schlaifer [2] have shown that the quantities given in eqs. (5.23)-(5.26) are sufficient statistics for the parameters $\boldsymbol{\mu}$ and h. When a set of sufficient statistics exists also a conjugate prior exists, see e.g. Box and Tiao [1]. The conjugate prior for $\boldsymbol{\mu}$ and h is a Normal-Gamma distribution given by

$$f_{\boldsymbol{\mu}h}\left(\boldsymbol{\mu}, h|\mathbf{m}, \nu, \mathbf{H}, v\right) = f_{\boldsymbol{\mu}}\left(\boldsymbol{\mu}|\mathbf{m}, h\mathbf{H}\right)f_h\left(h|\nu, v\right) \tag{5.27}$$

where $f_{\boldsymbol{\mu}}\left(\boldsymbol{\mu}|\mathbf{m}, h\mathbf{H}\right)$ indicates an r-dimensional normal distribution with mean $\mathbf{m}$ and covariance matrix $\left(h\mathbf{H}\right)^{-1}$ and $f_h\left(h|\nu, v\right)$ indicates a Gamma distribution with mean and coefficient of variation, V, given by

$$E\left[h\right] = \frac{1}{v} \tag{5.28}$$

$$V\left[h\right] = \sqrt{\frac{2}{\nu}} \tag{5.29}$$

If a prior Normal-Gamma distribution of $\left(\boldsymbol{\mu}, h\right)$ is assumed with parameters $\left(\mathbf{m}', \nu', \mathbf{H}', v'\right)$ then the posterior distribution of $\left(\boldsymbol{\mu}, h\right)$ will be Normal-Gamma distributed with the parameters

$$\mathbf{m}'' = \left(\mathbf{H}' + \mathbf{H}\right)^{-1}\left(\mathbf{H}'\mathbf{m}' + \mathbf{H}\mathbf{m}\right) \tag{5.30}$$

$$\mathbf{H}'' = \mathbf{H}' + \mathbf{H} \tag{5.31}$$

$$\nu'' = [\nu' + p'] + [\nu + p] - p'' \tag{5.32}$$

$$v'' = \frac{\nu'v' + \mathbf{m}'^T\mathbf{H}'\mathbf{m}' + [v\nu + \mathbf{m}^T\mathbf{H}\mathbf{m}] - \mathbf{m}''^T\mathbf{H}''\mathbf{m}''}{\nu''} \tag{5.33}$$

where p, p' and p'' are the ranks of $\mathbf{H}$, $\mathbf{H}'$ and $\mathbf{H}''$, respectively, and where $\mathbf{H}$, $\mathbf{m}$, v and ν are given by eqs. (5.23)-(5.26).

The predictive distribution of $\mathbf{Y}$ given the prior parameters $(\mathbf{m}', \nu', \mathbf{H}', v')$ and the realizations $\hat{\mathbf{y}}_i$, $i = 1, 2, \ldots, n_p$ is

$$f_{\mathbf{Y}|\hat{\mathbf{y}}}(\mathbf{y}|\hat{\mathbf{y}}) = \int_0^\infty \int_{R^{n_p}} f_{\mathbf{Y}}(\mathbf{y}|\boldsymbol{\mu}, \mathbf{C}_{\mathbf{YY}}) f_{\boldsymbol{\mu}}(\boldsymbol{\mu}|\mathbf{m}'', h\mathbf{H}'') f_h(h|\nu'', v'') \, d\boldsymbol{\mu} dh \tag{5.34}$$

It can be shown that the predictive distribution $f_{\mathbf{Y}|\hat{\mathbf{y}}}(\mathbf{y}|\hat{\mathbf{y}})$ follows a student-t distribution.

5.3.2   Application to Chloride measurements

In case the 2-parameter model is implemented n_p estimates of $\hat{D}$ and $\hat{c}_s$ are obtained by the maximum likelihood method. Simultaneously the maximum likelihood method yields estimates of the uncertainty of these estimates in the form of a covariance matrix $\mathbf{C}_i$ for each profile. The uncertainty related to the estimates, $\hat{\mathbf{y}}_i$, $i = 1, 2, \ldots, n$, is taken into account by modelling each estimate, $\hat{\mathbf{y}}_i$, as a normally distributed stochastic r-dimensional vector with expected value $\hat{\mathbf{y}}_i$ and covariance matrix $\mathbf{C}_i$. The fact that the outcomes, $\hat{\mathbf{y}}_i$, are stochastic variables causes no problems in the implemention of the methodology outlined in the previous section, section 5.3.1. The integration over the random outcomes can be performed by the FORM/SORM-analysis used to estimate the probability that corrosion has been initiated.

5.3.3   Lifetime Estimation

It is now possible to determine the probability that corrosion is initiated at some arbitrary point along the reinforcement in a given region. This probability is given by

$$P_I(t) = 1 - P(c(t, \mathbf{x}) \leq c_{cr}(\mathbf{x}) \ \forall \mathbf{x} \in [\Psi]) \tag{5.35}$$

where $[\Psi]$ denotes all points along the reinforcement.

In order to solve the problem given by eq. (5.35) the reinforcement bars are partitioned into elements small enough to ensure that the chloride concentration and the critical threshold for initiation of corrosion are approximately constant within each element. This discretization naturally depends on the scale of fluctuation of the involved stochastic fields. The probability of corrosion can now be evaluated by

$$P_I(t) = P(\cup_{i=1}^{n_e} c(t, \mathbf{x}_i) \geq c_{cr}(\mathbf{x}_i)) \tag{5.36}$$

where $c(t, \mathbf{x}_i)$ and $c_{cr}(\mathbf{x}_i)$ denotes the chloride concentration and the critical threshold, respectively, within element i and n_e denotes the number of elements. Eq. (5.36) can be solved by a FORM/SORM-analysis of a series system.

5.4 Example: Probabilistic Analysis of Several Chloride Profiles

It will later be convenient to be able to determine the probability that corrosion has been initiated in a 1 × 1 m area. In this example a bridge pier in a marine environment is regarded. The chloride surface concentration is known to be largest in the tidal and splash zone. The investigation is ,therefore, restricted to this area.
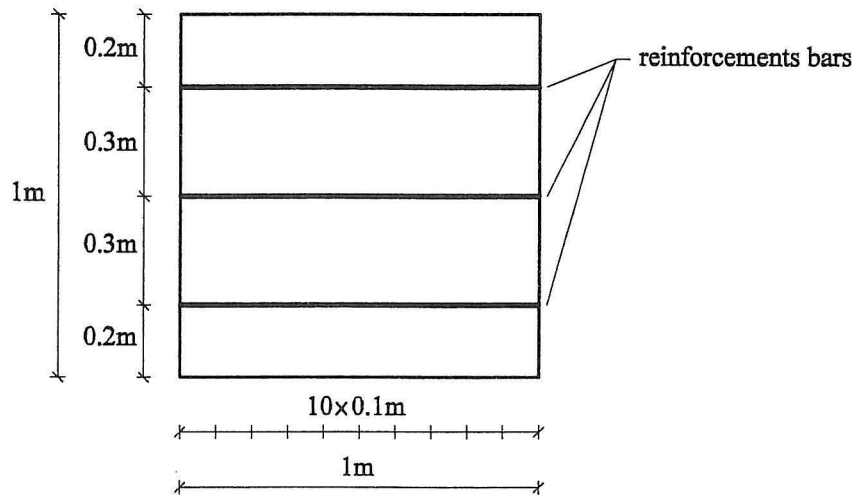

Figure 5.7: *Reinforcement.*

The location of the horizontal reinforcement bars in the given area is shown in figure 5.7. Since the horizontal reinforcement bars have a prescribed cover of 50 mm whereas the vertical bars have a prescribed cover of 70 mm initiation of corrosion in the horizontal reinforcement only is considered here. Each of the three reinforcement bars in figure 5.7 is partitioned into 10 elements of 10 cm. The elements are smaller than 0.5 times the correlation lengths of the stochastic fields, see below. The chloride ingress within each of these elements is assumed to be unidirectional, i.e. it can be described by eq. (5.1).

The following simple model for the cover thickness is implemented

$$\delta\left(x_1, x_2\right) = \delta_0 + A\cos\left(2\pi f\left(x_1 + x_2\right) + \Theta\right) \quad x_1, x_2 \in \{S_g\} \tag{5.37}$$

where δ_0 is the mean thickness of the cover, A is the amplitude of the fluctuation, f is the frequency, *Theta* is a random phase equally distributed in $[0; 2\pi]$ and (x_1, x_2) denotes the coordinates of a point on the surface of the structure. The frequency of the fluctuation is assumed to be $f = 1$ m^{-1}. On the basis of the thickness of the reinforcement bars this is a reasonable assumption. Further, this choice ensures that the result the analysis of the probability of corrosion becomes independent of Θ. Hence, this variable can be neglected in the analysis. It is assumed that the mean of the cover is constant for the given structure. The amplitude, A, is modelled as a Gaussian variable with zero mean. The amplitude is assumed to be independent for different areas of 1 × 1 m. It is, thereby, for a given set of independent measurements of the cover thickness possible to implement Bayesian statistics to estimate the mean of the cover thickness and the standard deviation

of the amplitude, A. For the given structure five measurements of the cover thickness are available. Using the methodology outlined in section 5.3.1 it is found that the mean of the observations is $m = 52, 5$ mm and that the variance is $v = 11, 5$ mm^2.

In this example it is also necessary to take into account the spatial fluctuation of the critical threshold, $\{c_{cr}(\mathbf{x})\}$. Because the structure is located in a marine environment, the humidity is relatively large. Hence, a higher mean value for the critical threshold than in the previous example is used, see section 5.2. The mean value is modelled as a normally distributed variable $c_{cr_0} \sim N(0.1; 0.01)$. The spatial variation is a Gaussian field with zero mean, standard deviation 0.01 and auto-correlation coefficient function

$$\rho_{c_{cr}c_{cr}}(d) = \exp\left(-\frac{d^2}{a_1^2}\right) \tag{5.38}$$

where d denotes the distance between two points and a_1 is a constant expressing the correlation length of the field. As mentioned in section 3.1 the correlation length of $\{c_{cr}(\mathbf{x})\}$ will be about the same as the correlation length of the large-scale fluctuation of the transport coefficient which is about 200-500 mm. The constant a_1 is, therefore, chosen as $a_1 = 350$ mm.

5.4.1   2-Parameter Model

The available data consists of $n_p = 4$ chloride profiles obtained at $t = 10$ years. All measurements have been made at 0.35 m above the mean water level. The distance between the measurements is large enough to ensure that the parameters estimated on the basis of the different profiles are independent.

Implementing the parameter estimation method presented in section 4.1 the following estimates of $\hat{\mathbf{y}}^T = \left(\hat{D}, \hat{c}_s\right)$ and their statistical uncertainty are obtained

$$\hat{\mathbf{y}}_1 = \begin{bmatrix} 20.02 \\ 1.06 \end{bmatrix} \quad \mathbf{C}_1 = \begin{bmatrix} 1.76 & -0.0288 \\ -0.0288 & 6.53 \cdot 10^{-4} \end{bmatrix} \tag{5.39}$$

$$\hat{\mathbf{y}}_2 = \begin{bmatrix} 15.44 \\ 1.03 \end{bmatrix} \quad \mathbf{C}_2 = \begin{bmatrix} 0.899 & -0.0175 \\ -0.0175 & 5.71 \cdot 10^{-4} \end{bmatrix} \tag{5.40}$$

$$\hat{\mathbf{y}}_3 = \begin{bmatrix} 14.78 \\ 1.32 \end{bmatrix} \quad \mathbf{C}_3 = \begin{bmatrix} 0.562 & -0.0172 \\ -0.0172 & 7.28 \cdot 10^{-4} \end{bmatrix} \tag{5.41}$$

$$\hat{\mathbf{y}}_4 = \begin{bmatrix} 18.23 \\ 0.912 \end{bmatrix} \quad \mathbf{C}_4 = \begin{bmatrix} 2.22 & -0.0322 \\ -0.0322 & 6.67 \cdot 10^{-4} \end{bmatrix} \tag{5.42}$$

The transport coefficient is given in mm^2/year and the surface concentration is given in % relative to the dry weight of concrete. The standard deviation of the measurement and model uncertainty is $s_\varepsilon = 0.02$ % for all measurements.

The relative precision of the variables is not known. In the following two models will be investigated

$$\eta_1 = \alpha \begin{bmatrix} \sigma_{c_s}^2 & 0 \\ 0 & \sigma_D^2 \end{bmatrix}^{-1} = 0.8 \begin{bmatrix} 0.2^2 & 0 \\ 0 & 4^2 \end{bmatrix}^{-1} \tag{5.43}$$

$$\eta_2 = \alpha \begin{bmatrix} \sigma_{c_s}^2 & 0 \\ 0 & \sigma_D^2 \end{bmatrix}^{-1} = 1.6 \begin{bmatrix} 0.4^2 & 0 \\ 0 & 4^2 \end{bmatrix}^{-1} \tag{5.44}$$

Compared to the model η_1 the model η_2 assigns larger uncertainty to the surface concentration, c_s.

It is now possible to estimate the parameters μ and h. Applying the methodology outlined in section 5.3.1, using a non-informative prior distribution, the mean values and standard deviations of $\{D(\mathbf{x})\}$ and $\{c_s(\mathbf{x})\}$ can be determined, taking into account that the outcomes, $\hat{y}_i$, themselves are stochastic variables. Because the outcomes, $\hat{y}_i$, themselves are stochastic variables the estimation of the parameters μ and h is performed in the limit state function used in order to evaluate the probability of corrosion, eq. (5.36).

In order to estimate the probability that corrosion has been initiated within the given area knowledge of the auto-correlation coefficient functions of $\{D_2(\mathbf{x})\}$ and $\{c_s(\mathbf{x})\}$ is also necessary. The fields describing the surface concentration and the large-scale fluctuation of the transport coefficient are assumed to be independent. As mentioned the measurements have been performed in such a manner that these auto-correlation coefficient functions cannot be estimated on the basis of the available data. The the auto-correlation coefficient functions given in eqs. (5.45) and (5.46) are considered.

$$\rho_{D_2 D_2}(d) = \exp\left(-\frac{d^2}{a_2^2}\right) \tag{5.45}$$

$$\rho_{C_s C_s}(d) = \exp\left(-\frac{d^2}{a_3^2}\right) \tag{5.46}$$

As in eq. (5.38) the parameters a_2 and a_3 are constants expressing the correlation lengths of the fields. On the basis of prior knowledge the constant a_2 is chosen as $a_2 = a_1 = 350$ mm. As mentioned in section 3.1.1 the correlation length of $\{D_2(\mathbf{x})\}$ can be determined on the basis of measurements of the alkalinity interface in carbonated concrete. However, no measurements are available on the basis of which the correlation length of $\{c_s(\mathbf{x})\}$ can be determined. The spatial variation of the surface concentration is caused by the spatial variation of the spray of sea water. The scale of fluctuation of the spray of sea water is assumed to be about 1000 mm. On this basis the constant a_3 is chosen as $a_3 = 1000$ mm.

In figure 5.8a and 5.8b the Ditlevsen bounds and the Hohenbichler approximation of the probability of corrosion for the 1×1 m area are shown for $\eta = \eta_1$ and $\eta = \eta_2$, respectively.

It is seen that the probability of corrosion obtained on the basis of $\eta = \eta_2$ is smaller than that obtained on the basis of $\eta = \eta_1$. This indicates that the transport coefficient is a more important variable than the surface concentration. The effect on the moments of the lifetime distribution, determined on the basis of the Hohenbichler approximation, however is small. For $\eta = \eta_1$ the mean value is 20.6 years and the standard deviation
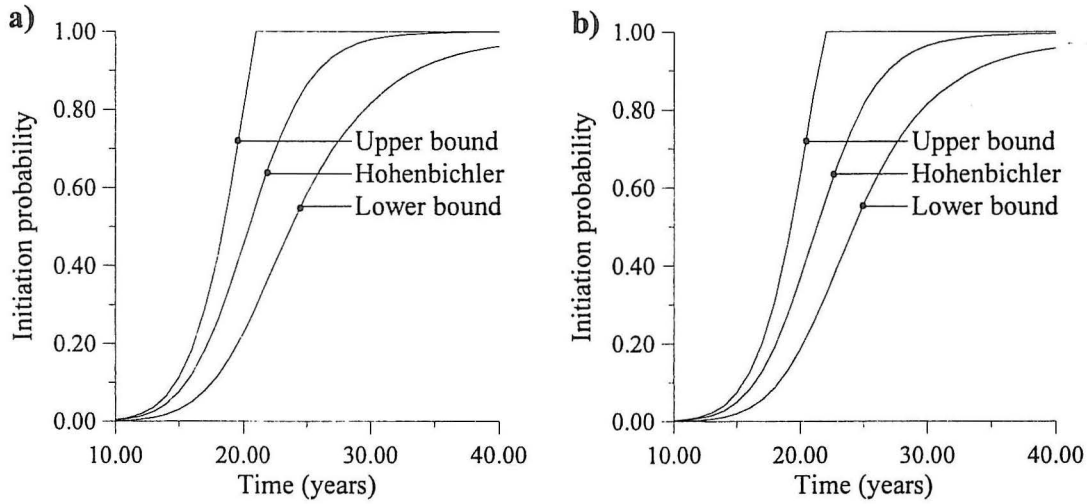
Figure 5.8: *2-parameter model without prior information.*

is 4.29 years. For $\eta = \eta_2$ the mean value is 21.4 years and the standard deviation is 4.50 years. There is only a difference of about 5 % between the mean values, and the coefficients of variation are similar to each other.

The figures 5.8a and 5.8b clearly demonstrate the well-known fact that Ditlevsen bounds only give narrow limits for low probability levels. The present case, concerns estimation of the mean value of the lifetime and the Ditlevsen bounds are then too wide to be of practical use.

The probabilities of corrosion and the moments of the lifetime determined above are based on a very limited data material. The statistical uncertainty, therefore, is significant. The statistical uncertainty can be reduced by using prior information about the parameters. The prior information can be based on experience or experiments where the results cannot be quantified in terms of a surface concentration and a transport coefficient. For the present structure also a large number of dust samples has been made. On the basis of the information from the dust samples the following prior parameters will be used.

$$n' = 5 \tag{5.47}$$

$$\nu' = 8 \tag{5.48}$$

$$\mathbf{m}' = \begin{bmatrix} 18.0 \\ 1.10 \end{bmatrix} \tag{5.49}$$

$$v' = 1.00 \tag{5.50}$$

The probabilities of corrosion determined taking the prior information into account are shown in figures 5.9a and 5.9b for $\eta = \eta_1$ and $\eta = \eta_2$, respectively.

For the model $\eta = \eta_1$ the mean and standard deviation of the time to initiation of corrosion determined on the basis of the Hohenbichler approximation are 19.7 years and 3.66 years, respectively. For the model $\eta = \eta_2$ the mean and standard deviation are 20.7 years and 3.90 years, respectively. The mean values are smaller than those determined without prior information because the prior means of the surface concentration and the
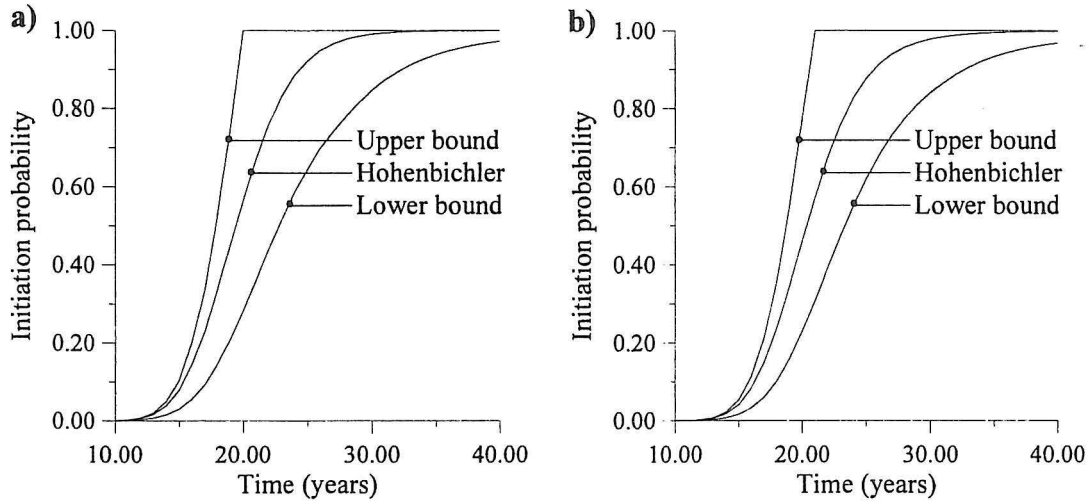
Figure 5.9: *2-parameter model with prior information.*

transport coefficient are larger than the means of the experimental outcomes. However, it is important to notice that a substantial reduction of the coefficient of variation has resulted from taking prior information into account.
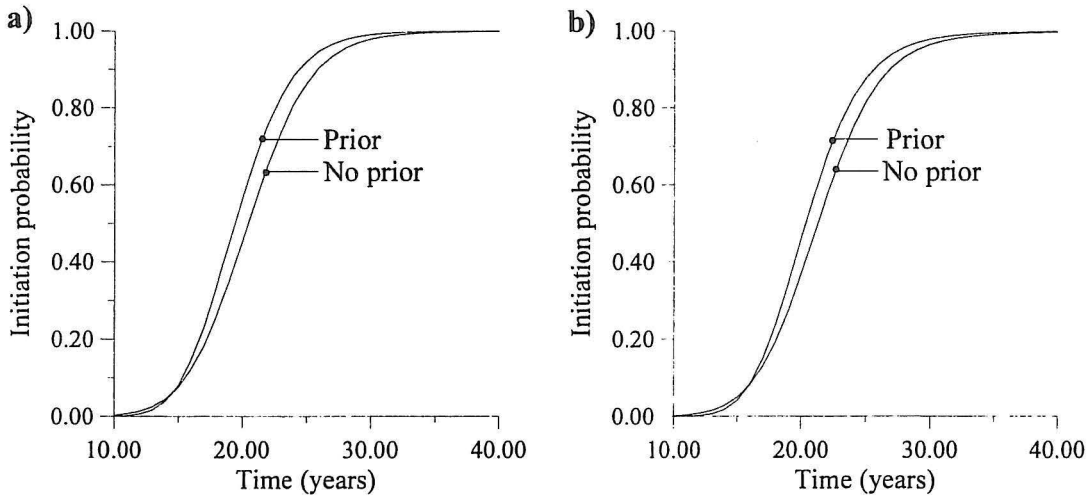
Figure 5.10: *Initiation probabilities for the 1 m^2 area.*

In order to demonstrate more clearly the effect of taking prior information into account the Hohenbichler approximations are shown both with and without prior information in figures 5.10a and 5.10b for $\eta = \eta_1$ and $\eta = \eta_2$, respectively. The figures clearly demonstrate that for low probability levels the probability of corrosion decreases when prior information is taken into account and that for high probability levels the probability of corrosion increases. At some point in between these extremes the two distribution functions cross. This point depends on the prior information.

Sensitivity Analysis

The analysis performed in the previous section, section 5.4.1, was based on a number of assumptions. In order to quantify the importance of these assumptions a number of sensitivity studies has been performed. All the sensitivity studies presented below have been carried out with the model $\eta = \eta_2$, and with prior information included.

First, the effect of changing the correlation lengths of the stochastic fields is investigated. When the correlation length of either the surface concentration, the transport coefficient or the critical threshold for initiation of corrosion is increased also the correlation coefficient between the failure events increases. Therefore, only the effect of changing the correlation lengths of all fields simultaneously is investigated. In figure 5.11 the Hohenbichler approximation for the probability of corrosion is shown for three different combinations of the correlation lengths. Normal correlation signifies the correlation lengths used in the reliability analysis in the previous section, section 5.4.1. Higher and lower correlation signify an increase of 10 % of the correlation lengths and a reduction of 10 % of the correlation lengths, respectively.
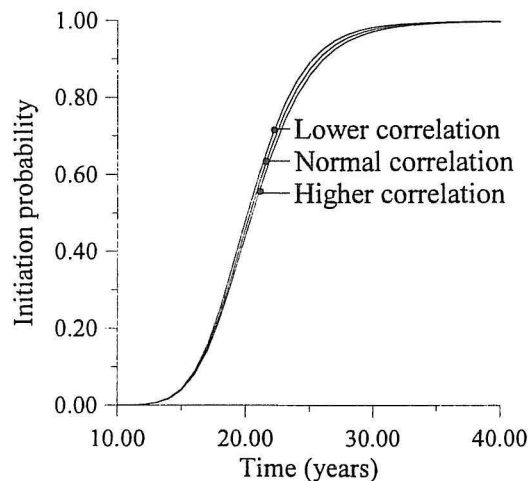

Figure 5.11: *Initiation probabilities for different correlation lengths.*

Figure 5.11 demonstrates that the probability of corrosion increases with decreasing correlation lengths. This is in accordance with our prior knowledge that lower correlation implies a higher probability of obtaining an extreme outcome. It is, however, also seen that the probability of corrosion is relatively insensitive to changes of the correlation lengths. It is, therefore, not necessary to conduct a large number of experiments in order to determine the correlation lengths precisely.

The effort involved in evaluating the initiation probability can be reduced if the number of variables in the problem can be reduced. As earlier mentioned the experimental outcomes, $\hat{y}_i$ $i = 1, 2, \ldots, n_p$ themselves are stochastic variables whose means and covariances are given by eqs. (5.39)-(5.42).

An analysis of the probability of corrosion without taking into account the statistical uncertainty related to the experimental outcomes has been carried out. It must be emphasized that the statistical uncertainty related to the parameters m and v is not neglected in the analysis. The results of this analysis are shown in table 5.13 where also the results

Statistical Uncertainty	Time (*years*)						
	10	15	20	25	30	35	40
Included	$9.57 \cdot 10^{-5}$	0.0405	0.461	0.876	0.978	0.995	0.998
Not included	$8.35 \cdot 10^{-5}$	0.0395	0.461	0.876	0.978	0.995	0.998

Table 5.13: *Effect of statistical uncertainty.*

of the analysis where the statistical uncertainty related to the experimental outcomes was included are shown. The table reveals that the uncertainty related to the experimental outcomes has no effect on the calculated probabilities of corrosion. These variables, therefore, can be replaced by their mean values. The effect of these variables is negligible compared with the effects of the physical uncertainty and the statistical uncertainty related to the model parameters, h and μ.
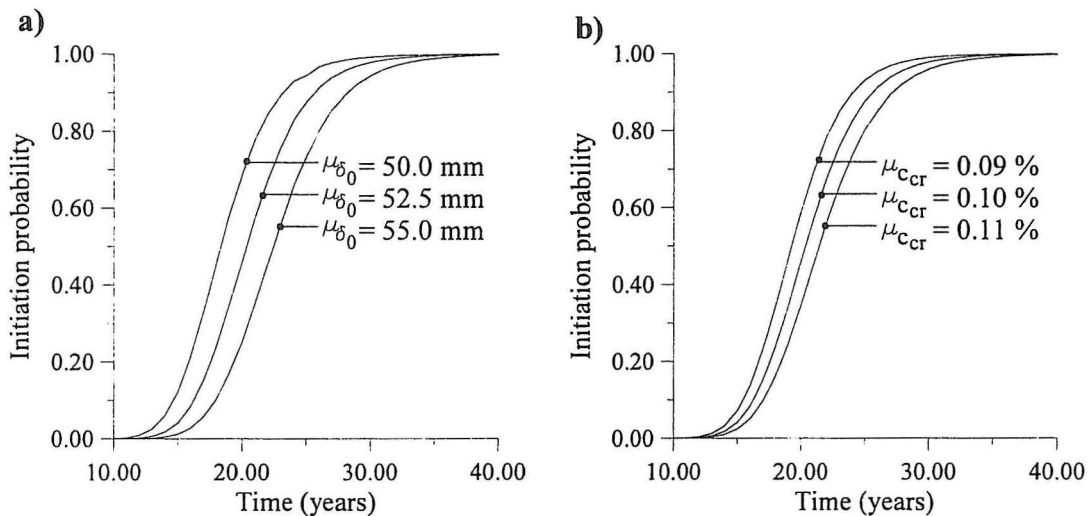

Figure 5.12: *Sensitivity studies.*

In figure 5.12a the probability of corrosion is shown for different mean values of the cover thickness. By the analysis the variance related to the estimate of the cover thickness has been kept constant ($v=11.5$ mm^2). It is seen that the probability of corrosion is very sensitive to changes of the mean of the cover. A reduction of the mean of the cover thickness of 5 % in fact results in a reduction of the mean of the time to initiation of about 10 %. A similar investigation has been carried out with respect to the mean value of the critical threshold for initiation of corrosion. By this analysis the coefficient of variation of the critical threshold value was kept constant. The results are shown in figure 5.12b. The probability of corrosion is also sensitive to changes of the mean of the critical threshold, it is, however, considerably less sensitive to changes of the mean of the critical threshold than to changes of the mean of the cover thickness.

5.4.2   3-Parameter Model

The 3-parameter model presented in section 5.2.3 where the transport coefficient is assumed to depend on the distance from the surface is now implemented. The model is given by eq. (5.10). The following estimates of the outcomes $\hat{\mathbf{y}}^T = \left(\hat{D}_s, \hat{D}_i, \hat{c}_s \right)$ and their statistical uncertainty have been obtained.

$$\hat{\mathbf{y}}_1 = \begin{bmatrix} 22.6 \\ 16.8 \\ 0.991 \end{bmatrix} \quad \mathbf{C}_1 = \begin{bmatrix} 2.13 & -0.465 & -0.0538 \\ -0.465 & 2.96 & 0.0296 \\ -0.0538 & 0.0296 & 1.57 \cdot 10^{-3} \end{bmatrix} \tag{5.51}$$

$$\hat{\mathbf{y}}_1 = \begin{bmatrix} 16.3 \\ 15.0 \\ 0.962 \end{bmatrix} \quad \mathbf{C}_1 = \begin{bmatrix} 1.51 & -0.432 & -0.0367 \\ -0.432 & 1.93 & 0.0193 \\ -0.0367 & 0.0193 & 1.23 \cdot 10^{-3} \end{bmatrix} \tag{5.52}$$

$$\hat{\mathbf{y}}_1 = \begin{bmatrix} 16.5 \\ 12.2 \\ 1.20 \end{bmatrix} \quad \mathbf{C}_1 = \begin{bmatrix} 1.03 & -0.268 & -0.0326 \\ -0.268 & 1.43 & 0.0165 \\ -0.0326 & 0.0165 & 1.26 \cdot 10^{-3} \end{bmatrix} \tag{5.53}$$

$$\hat{\mathbf{y}}_1 = \begin{bmatrix} 20.5 \\ 17.4 \\ 0.836 \end{bmatrix} \quad \mathbf{C}_1 = \begin{bmatrix} 3.75 & -1.04 & -0.0493 \\ -1.04 & 4.52 & 0.0307 \\ -0.0493 & 0.0307 & 9.35 \cdot 10^{-4} \end{bmatrix} \tag{5.54}$$

The transport coefficient is given in mm^2/year and the surface concentration is given in % relative to the dry weight of concrete. The standard deviation of the measurement and model uncertainty is $s_\varepsilon = 0.02$ % for all measurements.

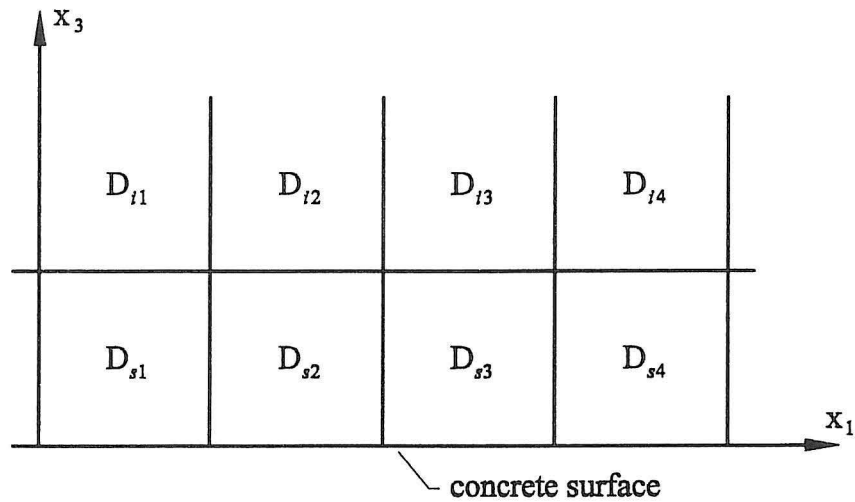**Figure 5.13**: *Stochastic elements.*

The stochastic fields describing the surface concentration and the critical threshold value for initiation of corrosion are modelled in the same way as by the 2-parameter model. It is, however, necessary to use another model for the transport coefficient. In figure 5.13 the stochastic elements are shown. The correlation coefficient between D_{sj} and D_{ij}, see

figure 5.13, is chosen as 0.5. The correlation coefficient matrix for the stochastic variables $(D_{s1}, D_{i1}, D_{s2}, D_{i2}, \ldots)$ can be written as

$$
\rho = \begin{bmatrix}
1 & 0.5 & \rho_{DD}(d) & 0.5\rho_{DD}(d) & \cdots \\
0.5 & 1 & 0.5\rho_{DD}(d) & \rho_{DD}(d) & \cdots \\
\rho_{DD}(d) & 0.5\rho_{DD}(d) & 1 & 0.5 & \cdots \\
0.5\rho_{DD}(d) & \rho_{DD}(d) & 0.5 & 1 & \cdots \\
\vdots & \vdots & \vdots & \vdots & \ddots
\end{bmatrix}
\tag{5.55}
$$

where the auto-correlation coefficient function $\rho_{DD}(d)$ is given by eq. (5.45) and d denotes the distance measured on the surface between two elements. This model is obviously not in accordance with the model formulated in section 5.1.1 where it was argued that the variation of $\{D_2(\mathbf{x})\}$ with the depth was negligible. This would imply that the correlation coefficient between D_{sj} and D_{ij} was one. The data, however, suggests that they are not fully correlated. The correlation coefficient has on the basis of the data been chosen as 0.5.

Again two different models for the relative precision, η, are used

$$
\eta_3 = \alpha \begin{bmatrix}
\sigma_{c_s}^2 & 0 & 0 \\
0 & \sigma_{D_s}^2 & \rho_{D_i D_s}\sigma_{D_s}\sigma_{D_i} \\
0 & \rho_{D_i D_s}\sigma_{D_s}\sigma_{D_i} & \sigma_{D_i}^2
\end{bmatrix}^{-1}
$$

$$
= 1.629 \begin{bmatrix}
0.2^2 & 0 & 0 \\
0 & 4^2 & 0.5 \cdot 4 \cdot 3 \\
0 & 0.5 \cdot 4 \cdot 3 & 3^2
\end{bmatrix}^{-1}
\tag{5.56}
$$

$$
\eta_4 = \alpha \begin{bmatrix}
\sigma_{c_s}^2 & 0 & 0 \\
0 & \sigma_{D_s}^2 & \rho_{D_i D_s}\sigma_{D_s}\sigma_{D_i} \\
0 & \rho_{D_i D_s}\sigma_{D_s}\sigma_{D_i} & \sigma_{D_i}^2
\end{bmatrix}^{-1}
$$

$$
= 2.585 \begin{bmatrix}
0.4^2 & 0 & 0 \\
0 & 4^2 & 0.5 \cdot 4 \cdot 3 \\
0 & 0.5 \cdot 4 \cdot 3 & 3^2
\end{bmatrix}^{-1}
\tag{5.57}
$$

The model η_4 assigns larger uncertainty to the surface concentration, c_s than the model η_3.

In figure 5.14a and 5.14b the initiation probabilities determined on the basis of $\eta = \eta_3$ and $\eta = \eta_4$, respectively, are shown.

It is seen that the probabilities of corrosion are generally smaller than those determined on the basis of the 2-parameter model. This is partly because the transport coefficient in the inner part of the structure is smaller than by the 2-parameter model and partly because the transport coefficients in the surface region and in the inner part are only correlated with a correlation coefficient of 0.5. This makes it more difficult to obtain outcomes of the transport coefficient which leads to a high chloride concentration around the reinforcement. For the model $\eta = \eta_3$ the mean value and standard deviation of the time to initiation of corrosion are 23.6 years and 5.76 years, respectively. For the model $\eta = \eta_4$ the mean and standard deviation are 23.0 years and 7.51 years, respectively. As
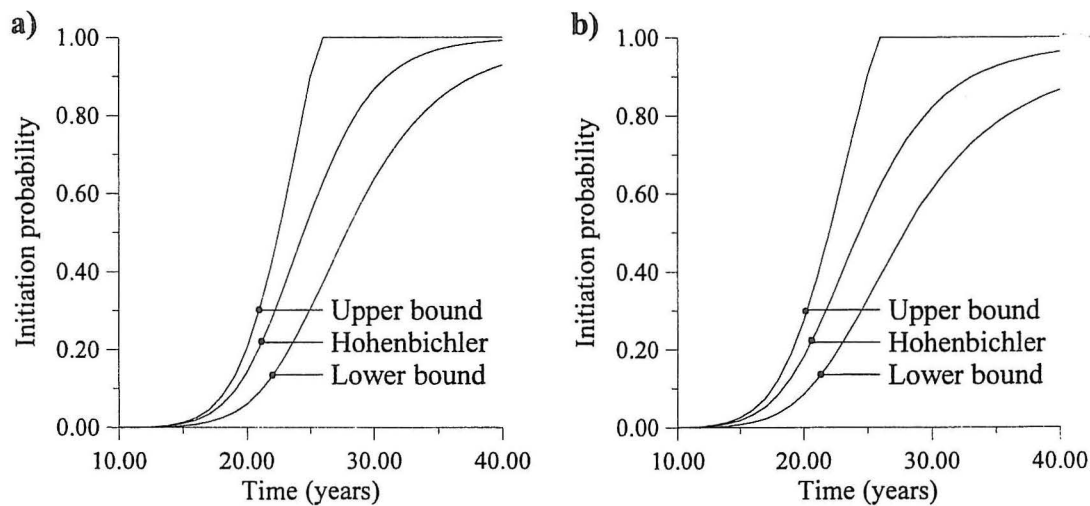
Figure 5.14: *3-parameter model without prior information.*

for the 2-parameter model the mean of the time to initiation of corrosion is not sensitive to changes in the model of the relative precision. However, the standard deviation is substantially larger for the model $\eta = \eta_4$ than for the model $\eta = \eta_3$.
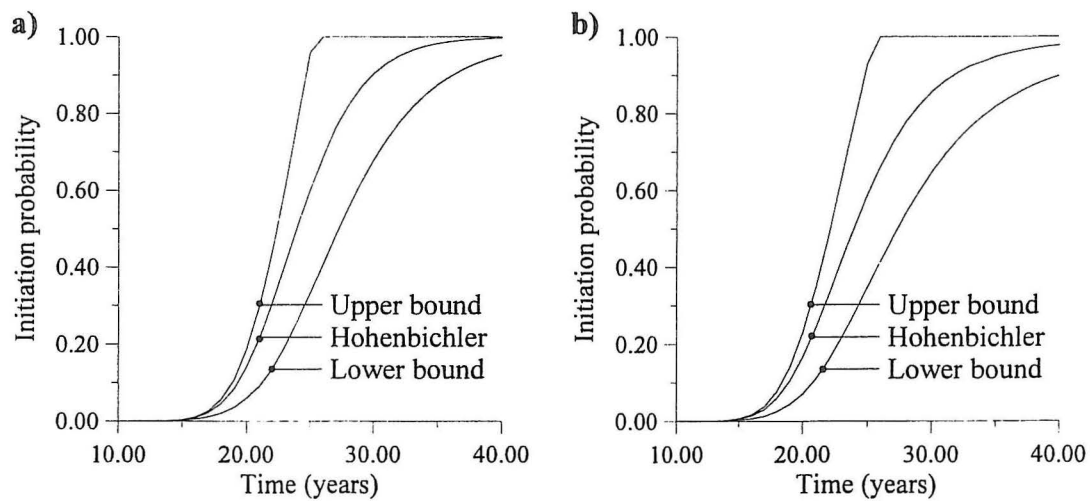
Figure 5.15: *3-parameter model with prior information.*

As by the 2-parameter model, prior information can be taken into account. The following prior parameters are used

$$n' = 5 \tag{5.58}$$

$$\nu' = 12 \tag{5.59}$$

$$m' = \begin{bmatrix} 20.0 \\ 15 \\ 1.10 \end{bmatrix} \tag{5.60}$$

$$v' = 1.20 \tag{5.61}$$

In figures 5.15a and 5.15b the initiation probabilities are shown for $\eta = \eta_3$ and $\eta = \eta_4$, respectively.

Again, it is seen that taking prior information into account leads to a reduction of the uncertainty related to the estimate of the time to initiation of corrosion and that the mean values remain nearly constant. The mean and standard deviation are 24.2 years and 4.37 years, respectively, for $\eta = \eta_3$ and 24.54 years and 5.64 years, respectively, for $\eta = \eta_4$.

Sensitivity Analysis

The sensitivity studies with respect to the mean of the cover thickness, the mean of the critical threshold and the correlation lengths all give the same results as for the 2-parameter model. These findings are, therefore, not shown here. However, the statistical uncertainty related to the maximum likelihood estimates of the surface concentration and the transport coefficient is substantially larger for the 3-parameter model than for the 2-parameter model. Hence, the influence of this uncertainty is investigated. The results are shown in table 5.14.

	Time [years]					
Statistical Uncertainty	15	20	25	30	35	40
Included	0.00326	0.140	0.600	0.904	0.983	0.997
Not included	0.00292	0.138	0.600	0.904	0.983	0.997

Table 5.14: *Effect of statistical uncertainty.*

In table 5.14 it is seen that the effect of the statistical uncertainty related to the experimental outcomes, $\hat{y}$, for very low probability levels only has influence on the calculated probability of corrosion. For higher reliability levels these variables can be replaced by their mean values.

5.5 Summary and Conclusions

In this chapter it has been shown how a single chloride profile can be analyzed. On the basis of a single chloride profile it is possible to estimate the transport coefficient and the surface concentration at the point where the measurement was obtained. By a reliability analysis the time to initiation of corrosion at the given point can be determined. The analysis of a single chloride profile indicates that better results are obtained if the mean of the transport coefficient is modelled as a function of the distance from the surface than if it is modelled as a constant. Further, the analysis shows that the low-scale spatial fluctuation of the transport coefficient can be neglected. However, one must be careful not to draw too general conclusions on the basis of a single example. In fact, analyses of other profiles, not shown here, indicates that in some cases the best results are obtained by letting the transport coefficient be a constant. On the other hand the analyses of

other profiles also indicates that the low-scale random fluctuation transport coefficient in no cases has a significant influence on the problem.

Using Bayesian Statistics an analysis of several chloride profiles has been carried out in order to determine the probability that corrosion has been initiated at an arbitrary point within a given region. The analysis of several profiles indicate that a substantial reduction of the coefficient of variation of the time to initiation of corrosion can be achieved by taking into account prior information obtained on the basis of dust samples. Further, sensitivity studies indicate that the results are insensitive to the correlation lengths of the fields describing the surface concentration, the transport coefficient and the critical threshold for initiation of corrosion. Finally, the sensitivity studies indicate that the most important parameter in the probabilistic model is the mean of the cover thickness.

5.6   References

[1] Box, G. E. P., Tiao, G. C., Bayesian Inference in Statistical Analysis, Addison-Wesley, Reading, MA, USA, 1972.

[2] Raiffa, H. and Schlaifer, R., Applied Statistical Decision Theory. Harvard University Press, Cambridge, Mass., 1961.

[3] Schittkowski, K., User's Guide for the Nonlinear Programming Code NLPQL, Institut für Informatik, Universität Stuttgart.

Chapter 6

Planning of Repair and Maintenance

In Denmark the planning of maintenance and repair of reinforced concrete structures is based on estimates of the time when a given repair strategy must be implemented. These estimates are determined using the available measurements (chloride profiles, dust samples, half-cell measurements etc.) and not least the knowledge and experience of the engineer planning the repair and maintenance. Having determined when the different repair strategies must be implemented it is possible to compare the different strategies with respect to the their cost. For a more detailed description see e.g. Henriksen et al. [6]. Such computations and considerations as the above mentioned are carried out within the framework of a formalized management system. For descriptions of such systems see e.g. Lindbladh [9] and Yañez and Alonso [18]. The major drawback of the traditional method is the lack of a proper statistical analysis of the measurement results. Usually no statistical methods are used in order to take the inherent variability and statistical uncertainty related to the measurements into account. Further, only very simple calculations of the type shown in section 5.2.1 are performed. The estimates of the times when the repair strategies must be implemented are, therefore, often imprecise.

In the following the models and methods presented in the previous chapters are implemented in order to determine the optimal repair and maintenance strategy for a given structure. First, the concept of optimal decisions is introduced and it is shown how optimal decisions can be determined on the basis of an economic decision model. Secondly, different methods for repair and maintenance are presented and finally the methodology is demonstrated in two examples.

6.1 Optimal Decision

The aim of most engineering analysis is to reach some decision on how to solve a given problem. In the present case the aim is to decide which repair and maintenance strategy to apply to a concrete structure subject to chloride ingress. This decision must be based on the available information about the parameters governing the problem. As demonstrated in the previous chapter, chapter 5 these parameters are subject to considerable uncertainty. The purpose of decision analysis is to reach a decision which is in some way optimal considering the given uncertainties.

99

The idea of optimal decisions was developed by von Neumann and Morgenstern [11] who gave a number of axioms for ordering the different decisions in a rational way according to the decision makers preferences. The method is also described in detail in Raiffa and Schlaifer [12] who deals with decision making within a Bayesian framework. Within the field of civil engineering the method has been applied to a number of problems by Benjamin and Cornell [2] and by Ang and Tang [1]. In recent years the method has been applied in conjunction with FORM/SORM-analysis in order to plan repair and maintenance of off-shore structures prone to fatique, see e.g. Madsen et al. [10] and Sørensen and Thoft-Christensen [13]. The method has also been applied within the field of planning of repair and maintenance of concrete structures subject to destructive mechanisms. Sørensen and Thoft-Christensen [14] considered a concrete bridge subject to chloride penetration. However, only a very simple model for the initiation and propagation of corrosion was applied. In recent years a number of works concerned with reliability-based planning of repair of concrete bridges has been published, see e.g. Thoft-Christensen [16], Thoft-Christensen [17] and Frangopol and Hearn [4].

In fact, the application of decision analysis in conjunction with FORM/SORM-analysis has expanded the applicability of decision analysis to more complicated problems where the performance of a structure can be given in terms of a function of several stochastic variables, see e.g. Kroon [8].

A decision maker is faced with the problem of choosing among a finite number of strategies, $\mathbf{a} \in \Omega_\mathbf{a}$, where $\Omega_\mathbf{a}$ denotes the set of available strategies. For a given strategy an outcome of the stochastic variables describing the problem is then selected by nature. For each strategy, $\mathbf{a}$, and outcome of the stochastic variables, $\mathbf{z}$, a given utility, $u(\mathbf{a}, \mathbf{z})$, or cost, $C(\mathbf{a}, \mathbf{z})$, is obtained. In figure 6.1 a so-called *decision tree* is shown. A decision tree is a graphic representation of the problem.

$$\mathbf{a} \in \Omega_\mathbf{a} \qquad\qquad \mathbf{z} \in \Omega_\mathbf{z}$$
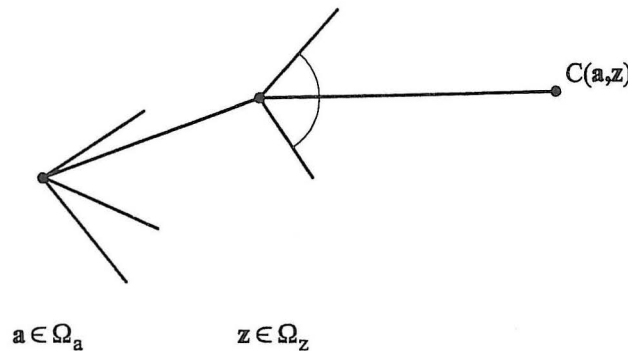
Figure 6.1: *Decision tree.*

The optimal decision is the decision which leads to the maximum expected utility or minimum expected cost. If the cost is considered, the optimal strategy is determined by solving the following optimization problem

$$\left.\begin{array}{ll} \min_\mathbf{a} & E_\mathbf{Z}[C(\mathbf{a}, \mathbf{z})] \\ s.t. & P_f(\mathbf{a}, \mathbf{z}) \leq P_f^{max} \end{array}\right\} \qquad\qquad (6.1)$$

where $E_\mathbf{Z}[C(\mathbf{a}, \mathbf{z})]$ is the expected cost of maintenance and repair, P_f is the probability

of some critical event as collapse of the structure or serviceability failure and P_f^{max} is the maximum allowable value of P_f.

The expected repair cost is estimated from

$$E_{\mathbf{Z}}\left[C\left(\mathbf{a},\mathbf{z}\right)\right] = \sum_{i=T_d}^{T_L} P\left(\text{repair in year } i\right) C_i \qquad (6.2)$$

where T_d denotes the time in years when a decision about the repair strategy is made and T_L denotes the design lifetime of the structure in years. The probability that a given repair strategy is implemented in year i, $P\left(\text{repair in year } i\right)$, depends on the stochastic variables, $\mathbf{Z}$. If the analysis is based solely on prior information it is called a *prior analysis* if information from experiments (chloride profiles) is taken into account it is called a *posterior analysis*. For the repair strategies used in practice (at least in Denmark) the capitalized cost, C_i, related to a repair in year i can be determined on the basis of the following expression

$$C_i = \sum_{j=T_d}^{T_L} C_{i,j} \frac{1}{(1+r)^{j-T_d}} \qquad (6.3)$$

where $C_{i,j}$ is the cost in year j if the repair is performed in year i and r is the real rate of interest.

It might seem questionable to order the decisions according to the expected cost related to these. Especially, if loss of human life is a consequence of failure it might seem unethical to apply an interest rate $r > 0$ to these costs. On this background some researchers argue that it is more reasonable to use some utility function which does not represent monetary values. However, Ditlevsen [3] has argued that using a monetary value for loss of human life and to use a positive interest rate is not unethical.

The major advantage of the probabilistic method is that it provides a framework within which the inherent variability of the measurement results can be taken into account and that it offers the opportunity of updating the results of the analysis on the basis of new information in a rational way. Further, if Bayesian statistic is used, the decision maker can formulate his prior beliefs about the unknown parameters in a rational way.

6.2 Criteria for Repair and Maintenance

Maintenance and repair is carried out in order to ensure that the structure is able to fulfill some design requirements throughout its lifetime. The most important of these requirements is that the structure is able to withstand the loads acting on it with sufficient reliability. However, there are a number of other requirements which e.g. are related to the serviceability of the structure. The requirements can also be related to the visual impression of the structure.

Repair and maintenance could be said to be necessary if the chloride concentration at some point around the reinforcement exceeds the critical threshold, and thus initiates corrosion. However, it must be borne in mind that initiation of corrosion represents no immediate threat to the load-bearing capacity of the structure. Further, for large structures such as

bridge piers, even propagation of corrosion at a single point only has a limited effect on the load-bearing capacity. Therefore, no repair or maintenance is performed in this case. Repair or maintenance will usually be carried out if a given percentage, p, of the surface or part of the structure shows signs of corrosion. This criterion is more related to the visual impression of the structure, than to the ability of the structure to withstand loads. For the purpose of reliability analysis the criterion will be understood in the following way. The surface of a structure or part of a structure is partitioned into fields of 1×1 m. Failure is said to occur when corrosion is initiated in p % of the total number of fields. A similar failure criterion for reinforced concrete structures subject to carbonation has been suggested by Hergenröder [7]. Hergenröder [7] states that failure occurs when 30 % of the reinforcement has been reached by the alkalinity interface.

6.3   Example: Bridge Pier in a Marine Environment

In this example the same pier as in section 5.4 is considered. In section 5.4 the probability that corrosion had been initiated in a 1×1 m area was determined. Now the optimal strategy for maintenance and repair of this pier will be determined. The decision about the repair strategy is made at $T_d = 10$ years and the design lifetime of the pier is $T_L = 50$ years. The available information consists of the measurement results presented in section 5.4. On this basis the decision maker has to decide which of the three different strategies presented below should be applied. All the costs given below are in some monetary unit. It is assumed that the repair is carried out before the probability of any critical event involving loss of human life increases. Therefore, the optimization problem, eq. (6.1) is solved without any restriction on the probability of some critical event.

Strategy 1
By strategy 1 a cathodic protection is applied in the tidal and splash zone. The rest of the surface of the pier up to the height 2.5 m over mean water level is painted. The paint is renewed every 15 years. This strategy is implemented when corrosion has been initiated in an arbitrary point in the tidal and splash zone. In order to determine when corrosion is initiated inspections are carried out each year, beginning five years before the expected time of initiation of corrosion. The cost of these inspections is 25 each year except for the last year before initiation of corrosion where the cost is 100. The cost of the cathodic protection is 1000 and the cost of running the cathodic protection is 20 each year. The cost of painting the surface is 100 every 15 years.

Strategy 2
Strategy 2 is implemented when 5 % of the surface in the splash and tidal zone shows minor signs of corrosion, e.g. small cracks and discolouring of the surface. The repair consists of repairing the minor damages and applying a cathodic protection. As by strategy 1 the costs related to this strategy are the costs of the repair, the costs of an extended inspection programme which starts three years before the expected time of repair and the costs related to the running of the cathodic protection. The cost of repair and installation of the cathodic protection is 2000, the cost of inspection in three years before the repair is 100 each year and the cost of running the cathodic protection is 30 each year.

Strategy 3
The repair consists of a complete exchange of concrete and reinforcement in the corroded areas. The strategy is implemented when 30 % of the surface in the splash and tidal zone shows distinct signs of corrosion, such as cracking and spalling of the cover. The cost related to this strategy are the costs of the repair and the cost of an extended inspection programme which starts three years before the expected time of repair. The cost of repair is 3000 and the cost of inspection in the three years before repair is 200 each year.

6.3.1 Traditional Planning of Repair and Maintenance

On the basis of the values of the surface concentration and transport coefficient given in eqs. (5.39)-(5.42) the time to initiation of corrosion in the points where the measurements were obtained now can be estimated. The estimation is performed using the least squares method outlined in section 5.2.1.

In table 6.1 the estimated times to initiation of corrosion for the four chloride profiles for $c_{cr} = 0.05$ % and for $c_{cr} = 0.10$ %, respectively, are shown. The times in table 6.1 are given in years where $t = 0$ corresponds to completion of the structure.

Profile	$c_{cr} = 0.05$ %	$c_{cr} = 0.10$ %
1	15.8	22.4
2	20.8	29.4
3	19.6	26.9
4	18.6	26.9

Table 6.1: *Estimated time to initiation of corrosion.*

This type of analysis forms the basis for the decision about the repair and maintenance strategy. This analysis does not take into account the variability of the measured parameters, i.e. the transport coefficient and the surface concentration. Further, the variation of the critical threshold value is only taken into account by using two different values in the analysis ($c_{cr} = 0.05$ % and $c_{cr} = 0.10$ %). Another major drawback of the method is that the spatial variation of the surface concentration, the transport coefficient and the critical threshold is not taken into account.

The decison maker assumes that repair strategy 1 must be implemented at $t = 18$ years, that repair strategy 2 must be implemented at $t = 25$ years and that repair strategy 3 must be implemented at $t = 35$ years. In figure 6.2 the cost of repair and maintenance is shown as a function of the real rate of interest, r.

In figure 2.2 it is seen that if the real rate of interest is less than 5 % strategy 1 is optimal. For higher values of r strategy 3 is optimal. Strategy 3 is optimal for high values of r because the costs related to this strategy occour at a much later time than the costs related to the two other strategies. In Denmark $r = 0.07$ is normally used which implies that strategy 3 is the optimal repair and maintenance strategy.

The decision maker can perform a number of studies to determine the sensitivity of the optimal plan to changes of the estimates of the times when the different strategies are
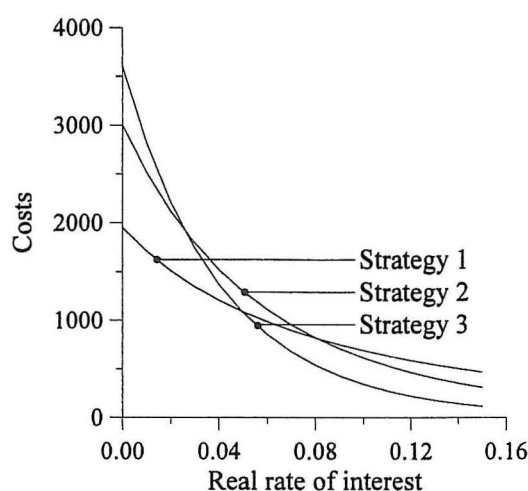
Figure 6.2: *Deterministic calculation of the costs.*

implemented. This is a very simple way of investigating the effect of the uncertainty related to these estimates.

6.3.2 Reliability-Based Planning of Repair and Maintenance

The criteria for implementing a given repair and maintenance strategy are related to the occurrence of corrosion or some signs of corrosion in the tidal and splash zone. The circumference of the considered pier is 20 m and the height of the tidal and splash zone is assumed to be 1 m. The tidal and splash zone can, therefore, be partitioned into 20 elements of 1 × 1 m. In order to determine the mean cost of repair it is necessary to determine the probability that a given repair strategy is implemented at a given time. That is the probability that corrosion has been initiated in a given number of the 20 elements of 1 × 1 m or that some signs of corrosion are visible in a given number of these elements.

In section 5.4 it was demonstrated how the probability that corrosion has been initiated in a 1 × 1 m area can be determined. The method is based on a partitioning of the 1 × 1 m area into smaller elements where the parameters such as the transport coefficient, the surface concentration and the critical threshold for initiation of corrosion are assumed to be constant. The probability that corrosion is initiated in a given element now can be determined by a FORM-analysis and the probability that corrosion is initiated within the 1 × 1 m area is determined by analysing a series system consisting of the individual elements. In order to determine the probability that corrosion has been initiated in a given number of the 1 × 1 m areas, each of the series systems is replaced by an equivalent linear failure element (see section 4.2.2), so that we now have n_a failure elements where n_a denotes the number of 1 × 1 m areas. Under the assumption that the fields describing the transport coefficient, the surface concentration and the critical threshold all are homogenous fields in the considered region all the 1 × 1 m areas will have the same probability of initiation of corrosion implying that the equivalent linear failure elements all have the same reliability index, β_e. The correlations between the equivalent failure elements are determined on

the basis of the fact that only the variables describing the statistical uncertainty and the means of the cover thickness and critical threshold are the same in all failure elements. The effect of the correlations between the surface concentrations in two different 1×1 m areas is not taken into account. This effect is also neglected for the transport coefficient and the critical threshold. This implies that all equivalent failure elements are equally correlated with the correlation coefficient, ρ_e. This makes it possible to determine the probability that a given number of the equivalent elements has entered the failure region analytically, see e.g. Thoft-Christensen and Baker [15]. If N_e denotes the number of equivalent elements. The probability that more than N_f equivalent elements has entered the failure region where $N_f \leq N_e$ is now given by

$$P_R = 1 - \sum_{i=0}^{N_f} \binom{N_e}{i} \int_{-\infty}^{\infty} \left[\Phi \left(\frac{\beta_e + \sqrt{\rho_e} t}{\sqrt{1 - \rho_e}} \right) \right]^{N_e - i} \left[\Phi \left(\frac{-\beta_e + \sqrt{\rho_e} t}{\sqrt{1 - \rho_e}} \right) \right]^i \varphi(t)\, dt \qquad (6.4)$$

where Φ and φ denotes the distribution and density function of the standard Normal distribution, respectively.

For strategy 2 it must be determined when small cracks and discolouring of the surface occur. These signs occour in a given element T_1 years after initiation of corrosion in the given element. By an element is here meant the small area in which the stochastic fields are assumed to be constant, i.e. the element is a part of the 1×1 m area. Based on experience the variable T_1 is modelled as a Normal distribution with mean 7.5 years and coefficient of variation 25 %. The time, T_1, for a given element is independent of T_1 in all other elements.

In order to determine the probability that strategy 3 is used, it is necessary to determine when cracking and spalling of the concrete surface occours. Cracking and spalling will occur in a given element T_2 years after corrosion has been initiated in the given element. Based on experience the variable T_2 is modelled as a Normal distribution with mean 15 years and coefficient of variation 25 %. Also the length of the time period, T_2, for a given element is independent of T_2 for any other element.

As mentioned in section 3.1 very little data is available on the basis of which models for T_1 and T_2 can be formulated. Models such as the above depend on the considered structure as well as the knowledge and beliefs of the model builder. The decision analysis, therefore, should be seen as a tool which can be used in order to support a given decision rather than a method which always yields the optimal solution to a given problem.

It is now possible to determine the probability that a given repair strategy is implemented at a given time. In figures 6.3a, 6.4a and 6.5a the probability that repair is performed is shown for strategy 1, 2 and 3, respectively and for $\eta = \eta_1$. In figures 6.3b, 6.4b and 6.5b the same probabilities are shown for strategy 1, 2 and 3, respectively and for $\eta = \eta_2$. The probabilities shown in figures 6.3, 6.4 and 6.5 are determined on the basis of the 2-parameter model. Also the prior information given in section 5.4.1 is taken into account in this example.

We are now able to determine the expected costs for each of the three repair strategies. In figure 6.6a and 6.6b the expected costs are shown for the three repair strategies as a function of the real rate of interest, r, for $\eta = \eta_1$ and $\eta = \eta_2$, respectively. In figure 6.6 it is seen that there is virtually no difference between the results obtained on the basis
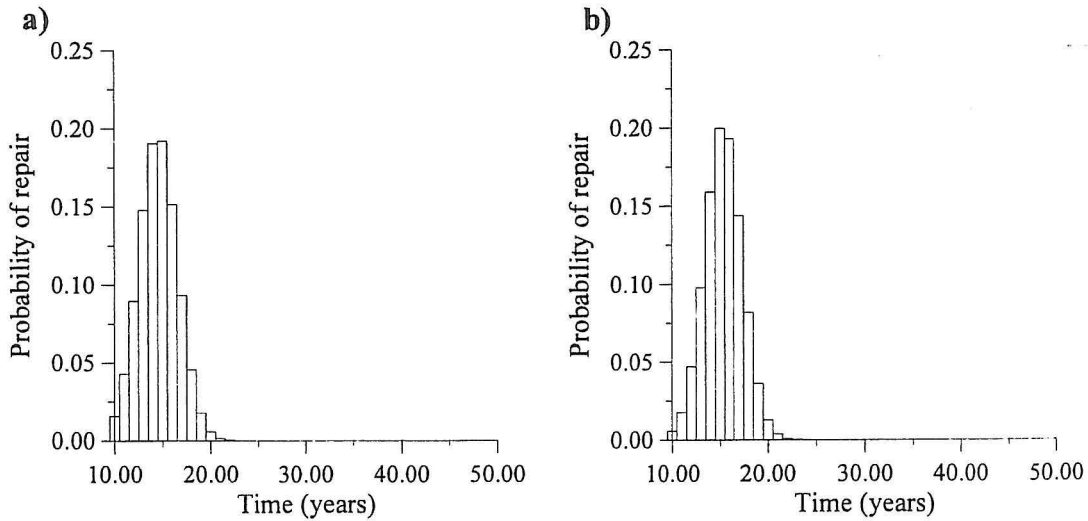
a)

b)

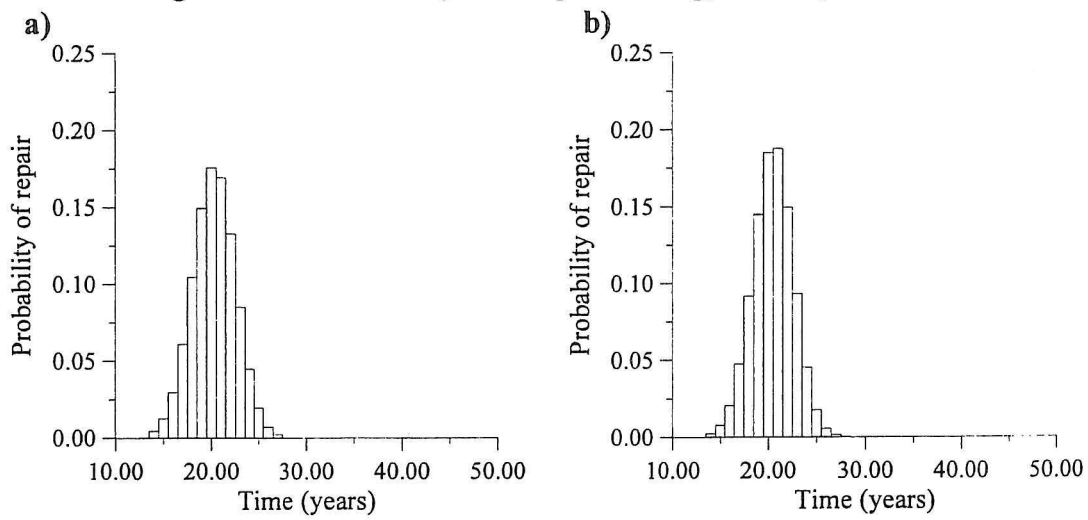**Figure 6.3**: *Probability that repair strategy 1 is implemented.*

a)

b)

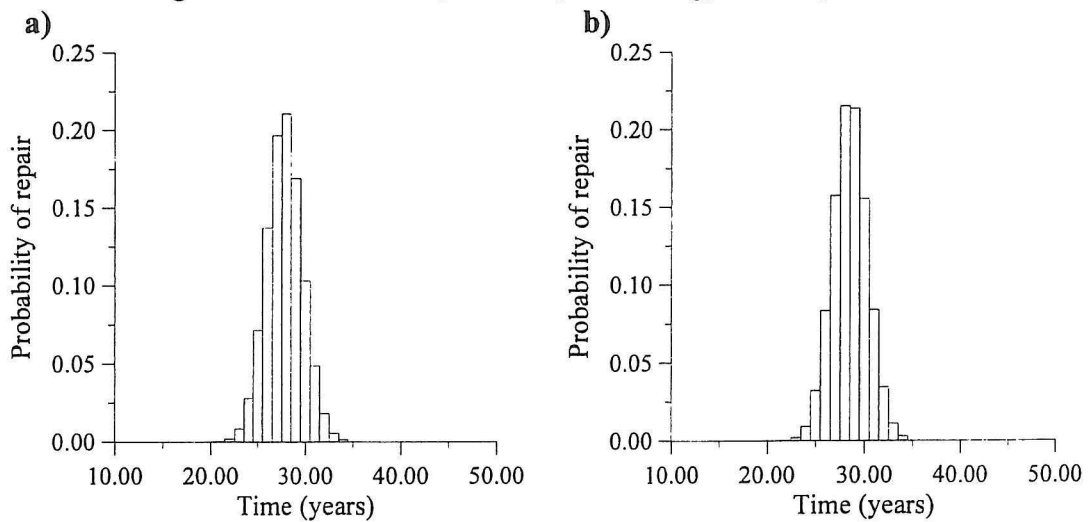**Figure 6.4**: *Probability that repair strategy 2 is implemented.*

a)

b)

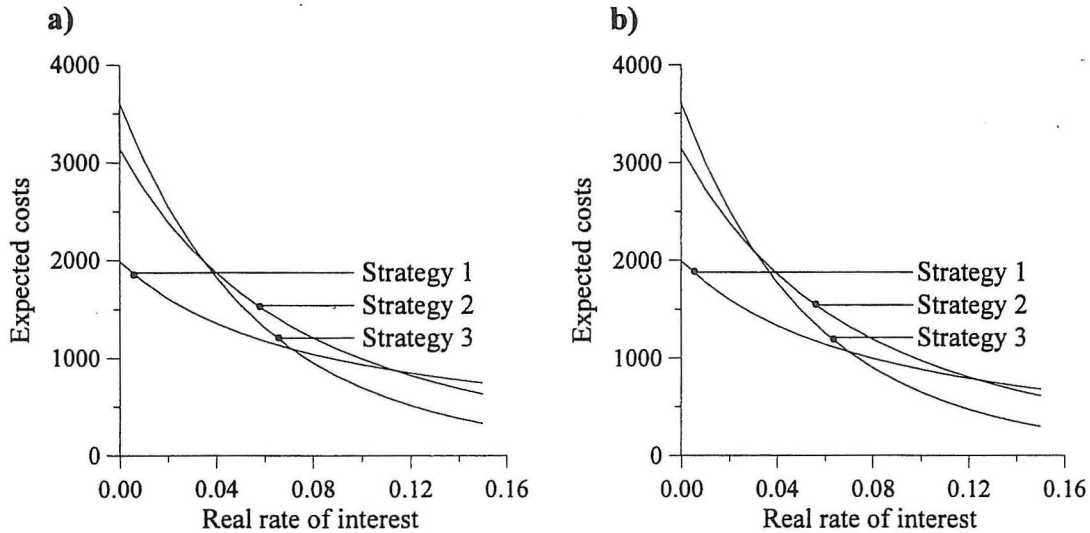**Figure 6.5**: *Probability that repair strategy 3 is implemented.*

Figure 6.6: *Expected costs as a function of r.*

of the two models of η. Further, it is seen that if the real rate of interest is less than 7 %, strategy 1 is the optimal choice. However, for higher rates of interests strategy 3 is optimal. As mentioned $r = 7$ % is normally used in Denmark. For $r = 7$ % the expected cost related to strategy 1 are the lowest.

The same computations can be performed on the basis of the 3-parameter model. The results are shown in figures 6.7a, 6.8a and 6.9a for strategy 1, 2 and 3, respectively, for $\eta = \eta_3$. In the figures 6.7b, 6.8b and 6.9b the results are shown for strategy 1,2 and 3, respectively, for $\eta = \eta_4$.

By comparing the probabilities that a given strategy is implemented determined on the basis of the 3-parameter model (see figures 6.7, 6.8 and 6.9) with the results obtained on the basis of the 2-parameter model (see figures 6.3, 6.4 and 6.5) it is seen that the 3-parameter model indicates that the repair strategies all should be implemented at a later time than determined by the 2-parameter model. This is in good accordance with the results for the 1 × 1 m area investigated in section 5.4 where it was shown that the mean of the time to initiation of corrosion determined by the 3-parameter model is larger than the mean of the time to initiation of corrosion determined by the 2-parameter model.

The expected costs related to the three repair strategies determined on the basis of the 3-parameter model are shown in figures 6.10a and 6.10b for $\eta = \eta_3$ and for $\eta = \eta_4$, respectively. Also for the 3-parameter model the expected cost of repair and maintenance is insensitive towards the model of η. However, on the basis of the 3-parameter model it can be concluded that if the real rate of interest is less than 6 % strategy 1 is optimal. If r is larger than 6 % strategy 3 is optimal.
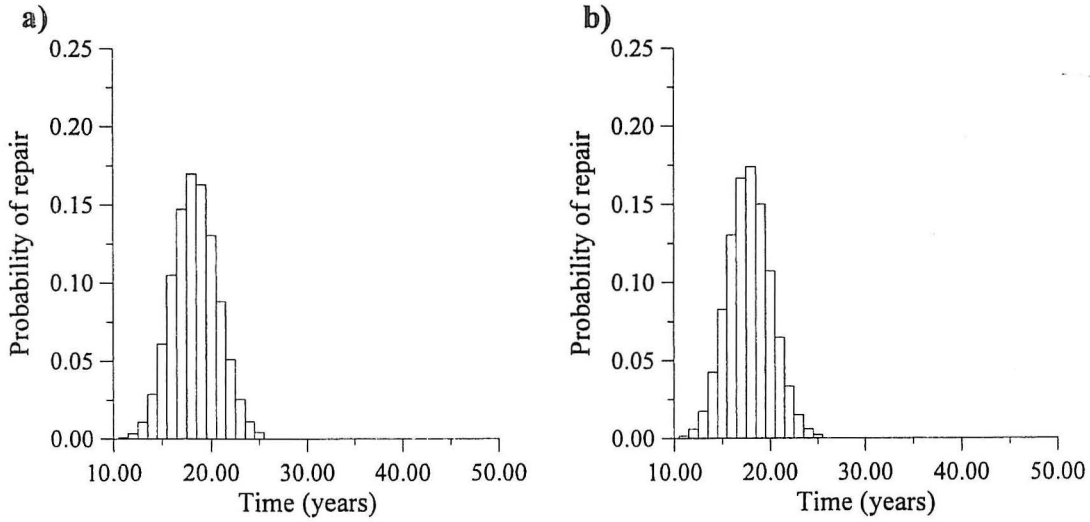
a)

b)

Figure 6.7: *Probability that repair strategy 1 is implemented.*

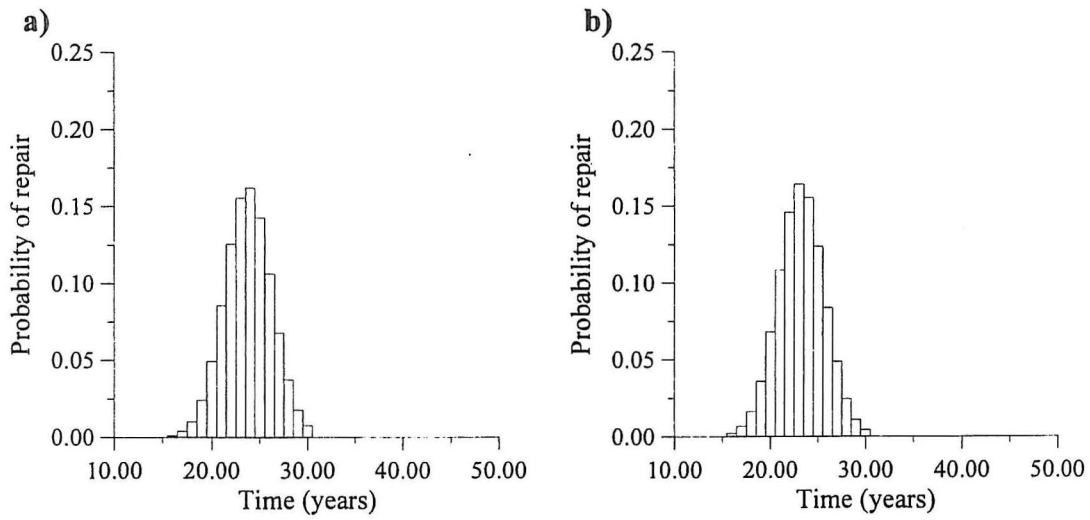a)

b)

Figure 6.8: *Probability that repair strategy 2 is implemented.*
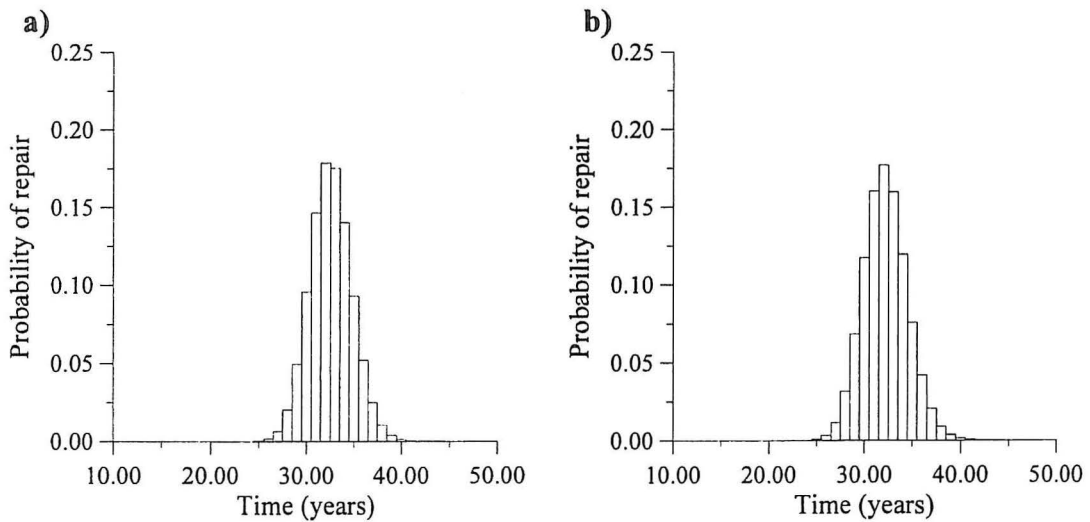
a)

b)

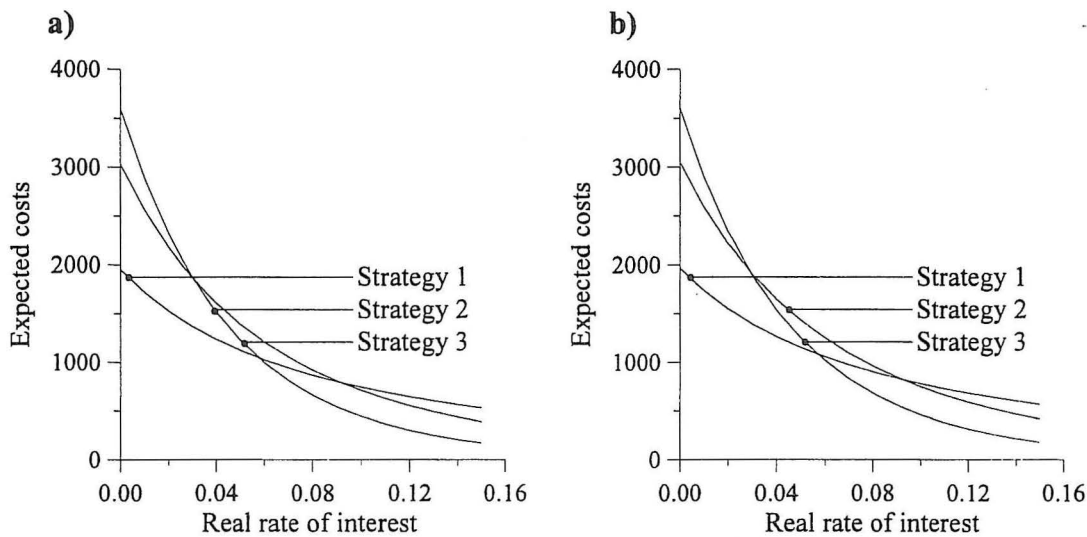**Figure 6.9**: *Probability that repair strategy 3 is implemented.*

Figure 6.10: *Expected costs as a function of r.*

6.4 Example: Large Bridge in a Marine Environment

The previous section was concerned with the planning of repair and maintenance of a single bridge pier. A special repair strategy will be considered for a given pier, only if it is observed that the time to initiation of corrosion in this pier is substantially different from that for all other piers. In general it is necessary to use the same repair and maintenance for all piers of a given bridge. A bridge with ten piers in a marine environment where measurements have shown that none of the piers require a special repair strategy is now considered.

The same three repair and maintenance strategies as in the previous example, section 6.3, are considered. The cost of applying the strategies are n_p times the cost given in section 6.3, where n_p denotes the number of piers. It is, however, necessary to define a new set of criteria for applying the different strategies. A given repair and maintenance strategy can for example be used for the entire bridge at the time when one of the piers is in need of repair. This would e.g. imply that repair strategy 1 has to be implemented before corrosion is initiated in any of the piers. This criterion, however, will be sub-optimal because the repair and maintenance is carried out at a time when the major part of the structure is not yet in need of repair. A more realistic criterion would be to implement a given strategy when a given number of the piers require that the given strategy is implemented. In this example a given repair and maintenance strategy will be implemented when more than three piers require that the given strategy is implemented. The probability that a given pier require that a given strategy is implemented, is determined according to the criteria given in the previous example, see section 6.3.

6.4.1 Evaluation of Failure Criteria

The probability that a given strategy is implemented for a given pier was determined in the previous section, section 6.3. In order to determine the probability that a given

number of piers require a given repair strategy such computations must be made for all piers. Assuming that the event that a given pier requires maintenance is independent of the event that any other pier requires maintenance, the probability that a given number of piers require maintenance can be determined.

In this example it is assumed that the probability that a given pier requires that a given repair and maintenance strategy is implemented is the same for all piers. Further, the values determined in the previous example, see section 6.3, will be used. In that case the probability that N_R out of N_P piers are need of repair where $N_R \leq N_P$ can be determined by

$$P_B = \left(\begin{array}{c} N_P \\ N_R \end{array} \right) P_R^{N_R} (1 - P_R)^{N_P - N_R} \tag{6.5}$$

where the probability that a given pier requires repair, P_R, can be determined by eq. (6.4). In this example the probability that maintenance and repair is performed is equal to the probability that 4 or more piers require repair. In the general case where the probability that a given pier requires that a given repair and maintenance strategy is implemented is not the same for all piers, the evaluation of the probability that the entire bridge requires repair and maintenance cannot be based on the Binomial distribution.

6.4.2   Optimal Repair Strategy

In figures 6.11a and 6.11b the expected cost of repair and maintenance for the entire bridge determined on the basis of the 2-parameter model is shown for $\eta = \eta_1$ and $\eta = \eta_2$, respectively. The expected cost of repair and maintenance for the entire bridge determined on the basis of the 3-parameter model are shown in figures 6.12a and 6.12b for $\eta = \eta_3$ and $\eta = \eta_4$, respectively.

In figures 6.11 and 6.12 it is seen that for the entire bridge the same repair strategy is optimal as for the pier considered in the previous example. This is because the distribution of the time when a given repair strategy is implemented for the pier considered in the previous example is much the same as the distribution of the time when a given strategy is implemented for the entire bridge. The distribution of the time when a given strategy is implemented for the entire bridge, however, depends on the criteria for applying the given strategy. In this example a given strategy for the entire bridge is implemented in case three out of ten piers require that the given strategy is implemented. If for example a given strategy for the entire bridge is implemented when two out of ten piers require that the strategy is implemented different conclusions might be reached, depending on the considered strategies.

6.5   Conclusions

A method for determining optimal repair and maintenance strategies has been presented. The method which determines the optimal strategy by minimizing the expected cost of repair and maintenance is based on traditional decision theory and FORM/SORM-analysis. The method can be implemented in existing bridge management systems because

a)

b)
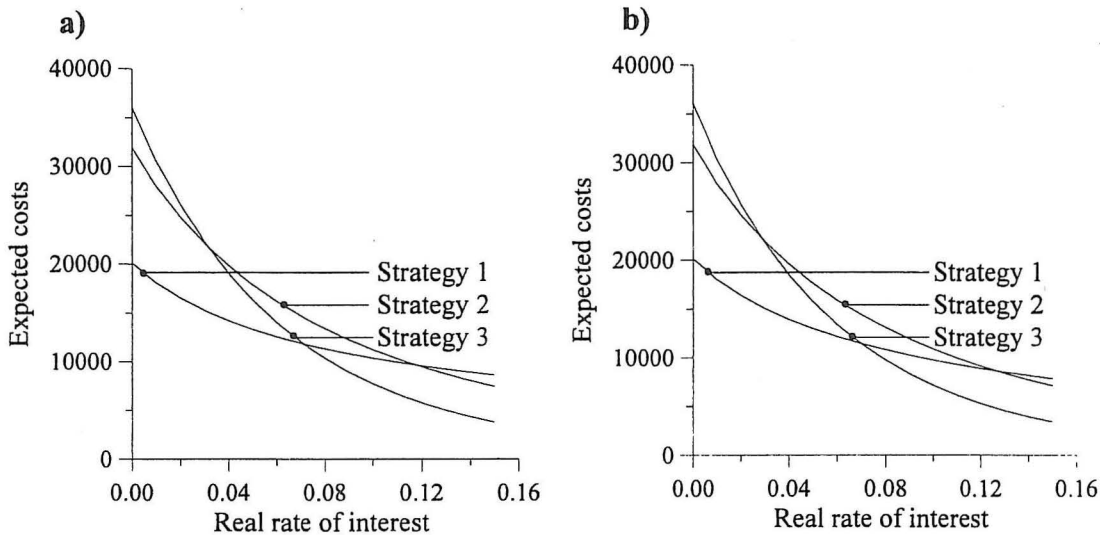
Figure 6.11: *Expected costs as a function of r.*

a)

b)
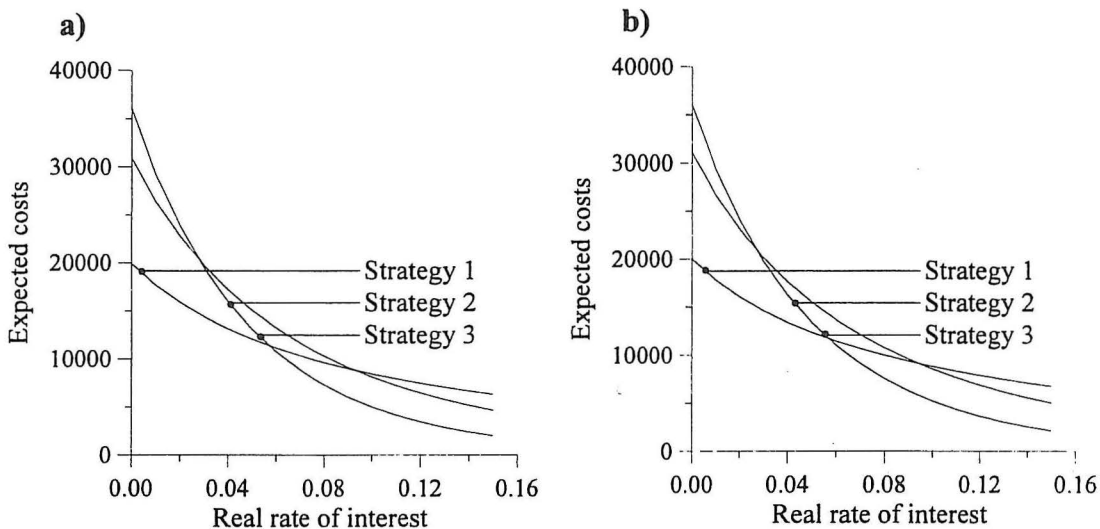
Figure 6.12: *Expected costs as a function of r.*

it is based on measurements of chloride profiles. These measurements are traditionally made before any decision about the repair strategy is made. Further, FORM/SORM-analysis is gaining more wide-spread use and is allready used by consulting engineers in conjunction with reevaluation of existing structures.

In an example the optimal strategy for repair and maintenance of a bridge pier is determined. Initially a traditional analysis is performed which indicates that the optimal strategy is to perform the repair when major signs of corrosion are visible. A decision analysis based on the 2-parameter model gives the result that a preventive repair strategy is optimal. Finally, a decision analysis based on the 3-parameter model gives the same result as the traditional analysis. The different analyses yield different results because they are based on different estimates of the time when the repair strategies are implemented. This only emphazises the need for an accurate method of predicting these times. It is evident that the probabilistic method is more suitable than the traditional approach

because the random variation of the variables can be taken into account in a rational manner. However, also the result of an reliability-based analysis to some extent depends on the prior beliefs of the decision maker. As earlier mentioned the decision analysis, therefore, should be seen as a basis on which to support a given decision rather than a method which always leads to an optimal decision.

6.6 References

[1] Ang, A., Tang, W. H., Probability Concepts in Engineering Planning and Design, Vol. II Decision, Risk and Reliability, Wiley, New York, 1984.

[2] Benjamin, J. R., Cornell, C. A., Probability, Statistics and Decision ofr Civil Engineers, McGraw-Hill, 1970.

[3] Ditlevsen, O., Risk Acceptance Criteria in the Light of Decision Analysis, 2nd WEGEMT Graduats School, Accidental Loadings on Marine Structures: Risk and Response, Technical University of Denmark, 24-29 April, 1995.

[4] Frangopol, D. M., Hearn, G., Managing the Life-Cycle Satety of Deteriorating Bridges, in: Casas, J. R., Klaiber, F. W., Mari, A. R., (eds.) Recent Advances in Bridge Engineering, CIMNE, Barcelona, 1996, pp. 38-55.

[5] Gollwitzer, S., Rackwitz, R., Equivalent Components in First-Order Systems Reliability, Reliability Engrg, 5, 1983, pp. 99-115.

[6] Henriksen, C., Stoltzner, E., Lauridsen, J., Kloridbetinget korrosion, Vejdirektoratet, Broområdet, 1991, in danish.

[7] Hergenröder, M., Zur statistischen Instandhnatungsplannung für bestehende Bauwerke bei Karbonatiserung des Betons and möglicher Korrosion der Bewehrung, Berichte aus dem Konstruktiven Ingenieurbau, TU München, 4/92, 1992. In german.

[8] Kroon, I. B., Decision Theory Applied to Structural Engineering Problems, Ph.D.-thesis, Structural Reliability Theory Paper No. 132, Dept. of Building Technology and Structural Engineering, Aalborg University, Denmark, 1994.

[9] Lindbladh, L., Bridge Management within the Swedish National Road Administration, in: Harding, J. E., Parke, G. A. R., Pyall, M. J., (eds.), Bridge Management, Inspection, Maintenance , Assesment and Repair, Elsevier Applied Science, London, 1990, pp. 51-62.

[10] Madsen, H. O., Sørensen, J. D., Olesen, R., Optimal Inspection Planning for Fatigue Damage of Offshore Structures, Proc. ICOSSAR89, San Francisco, 1989, pp. 2099-2106.

[11] Von Neumann, Morgenstern, Theory of Games and Economical Behaviour, Princeton University Press, 1943.

[12] Raiffa, H., Schlaifer, R., Applied Statistical Decision Theory, Harvard University Press, Cambridge, Mass., 1961.

[13] Sørensen, J. D., Thoft-Christensen, P., Integrated Reliability-Based Optimal Design of Structures, in: Thoft-Christensen, P., (ed.), Reliability and Optimization of Structural Systems, IFIP WG 7.5 Conference, Springer-Verlag, 1987, pp. 385-398.

[14] Sørensen, J. D., Thoft-Christensen, P., Inspection Strategies for Concrete Bridges, in: Thoft-Christensen, P. (ed.), Reliability and Optimization of Structural Systems 88, Springer Verlag, IFIP WG 7.5 Conference, Springer-Verlag, 1988, pp. 325-336.

[15] Thoft-Christen, P., Baker, M. J., Structural Reliability Theory and Its Applications, Springer-Verlag, Berlin, 1982.

[16] Thoft-Christensen, P., Advanced Bridge Management Systems, Structural Engineering Review, 7, 1995, pp. 151-163.

[17] Thoft-Christensen, P., Bridge Managemant Systems. Present and Future, in: Casas, J. R., Klaiber, F. W., Mari, A. R., (eds.) Recent Advances in Bridge Engineering, CIMNE, Barcelona, 1996, pp. 13-37.

[18] Yañez, M. A., Alonso, A. J., The State of the Bridge Management System in the State National Highway Network of Spain, in: Casas, J. R., Klaiber, F. W., Mari, A. R., (eds.) Recent Advances in Bridge Engineering, CIMNE, Barcelona, 1996, pp. 99-114.

Chapter 7

Reliability-Based Planning of Experiments

The probabilistic model formulated in chapter 3 can be used as a basis for determining optimal experiment plans. An optimal experiment plan is a plan which ensures that the optimal amount of information from the experiments is obtained at the lowest cost. The outcomes of the experiments can be used to verify the selected model as well as to plan additional experiments if the information obtained still shows too large scatter.

The concept of optimal experiment planning has mainly been developed within the field of *linear theory*. If the experiment outcomes are known to be a linear function depending on some unknown parameters, so-called *factorial plans* can be implemented. The factorial plans ensure that the variances of the estimated parameters are minimized and that the parameters are independent, see e.g. Box and Draper [2] and Myers [12]. Factorial plans can also be developed within the framework of Bayesian statistics, see e.g. Pilz [13] or Box and Tiao [3]. It is evident that the factorial plans ensures that the optimal amount of information is gained from the experiments, however, no economic considerations are taken into account.

Also within the field of life testing and accelerated life testing of machines and structural components optimal experiment plans have been developed. In this case the lifetime of a given component is assumed to follow a given distribution whose parameters depend on some applied stress level. A well-known example is steel structures subject to cyclic loads. The logarithm of the lifetime is often assumed to be normally distributed. The mean is modelled as a linear function of the logarithm of the amplitude of the stress and the coefficient of variation of the lifetime is assumed to be constant.

Chernoff [5] already formulated the basic concepts of optimal plans for life testing. He introduced the concept of locally optimal designs, i.e. designs which are optimal if the parameters were known. Then the outcome of a future experiment can be determined in terms of a probability distribution function accounting for the inherent variability of the test item. It seems somewhat self-contradictory to assume that the parameters are known. However, Chernoff [5] argues that, if a sensitivity study shows that the design is nearly optimal for a sufficiently large range of parameters around the given values such a plan would be satisfactory in practical applications.

Chernoff [5] defines the optimal plan as the plan which minimizes the sum of variances

of the parameters (so-called A-optimality). A number of similar optimality critera has later been proposed. They are all based on some functional of the accuracy of the parameter estimates as expressed by the parameter covariance matrix, e.g. the trace (A-optimality), the determinant (D-optimality), the maximum eigenvalue (E-optimality) or some quadratic form (C-optimality), see Pilz [13]. The cost of the experiments is not taken into account. Further, all these optimality critera fail to take into account the influence of the parameters on the reliability of a given element/system. Clearly, it is more important to reduce the variability of a parameter with a large influence on the reliability of the component/system than to reduce the variability of a parameter with less influence.

A number of different life models has been investigated by e.g. Escobar and Meeker [6], Meeker and Nelson [11] and Mann [10]. In these works the optimal experiment plans are determined by minimizing the variance of the mean lifetime at some working stress. Clearly, this leads to simple reliability oriented experiment plans. Bayesian reasoning have also been used to determine optimal plans for life tests, see. e.g. Chaloner [4] who considers a linear model with normally distributed observations.

In a recent work Sørensen et al. [15] suggest a criterion involving directly the experiment cost and the economic consequences when using experiment results for predictions of the performance of the object under consideration. Moreover, they suggested to determine optimal plans by using Bayesian decision theory (see e.g. Raiffa and Schlaifer [14]) thus enabling incorporation of prior information. This approach has also been discussed in more detail in Kroon [8]. For applications of this method see e.g. Faber et al. [7] and Kroon et al. [9].

7.1   Rational Planning of Measurements

The problem of rational planning of new measurements/experiments can be treated on different levels of complexity from simple 'deterministic' cost-benefit analysis combined with experience to solving complicated optimization problems based on decision theory.

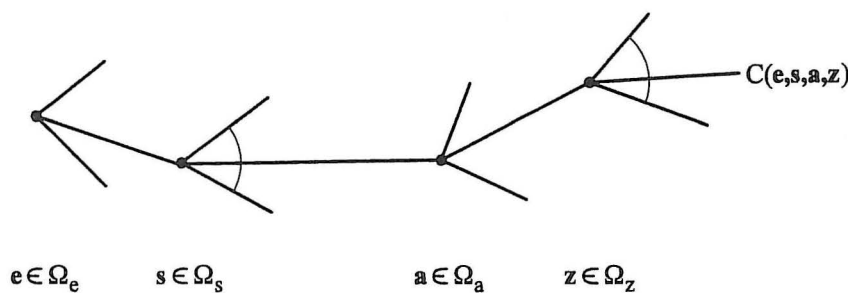$$e \in \Omega_e \qquad s \in \Omega_s \qquad \qquad a \in \Omega_a \qquad z \in \Omega_z$$

Figure 7.1: *Decision tree related to planning of measurements.*

In figure 7.1 a decision tree is shown with the basic four levels of decisions/realisations, namely

1. At the first level the decisions related to planning of measurements are made. For

example the number of new measurements is determined. The measurement planning variables are denoted e and the set of available decisions is denoted Ω_e.

2. The observations of the measurements are obtained at the second level. The observation obtained by the measurement being planned is not known at the time of planning and are therefore modelled by stochastic variables denoted **S** with the admissible range Ω_s .

3. On the basis of the observations it must be decided which action to take. This decision is made by the user/owner and is denoted a. The action could typically be time and type of a repair. The set of possible actions is denoted Ω_a.

4. At the fourth level some realisation is observed. Typically this realisation is related to observation of some critical event, for example failure. The uncertainties related to the loads (environment) and resistances are modelled by the stochastic variables **Z** with the admissible range Ω_Z. The limit state function

$$g(\mathbf{e}, \mathbf{S}, \mathbf{a}, \mathbf{z}) = 0 \tag{7.1}$$

is used to model a critical event. The critical event can also be given in terms of a union of intersections of a number of events. The critical event describes the state of the structure. The structure can be in a safe region where all requirements are fulfilled or in some other state where it it is not able to fulfill one or more of the required performance criteria. Each of these states can be associated with a given cost.

Corresponding to the decisions by the 'user' e and a and the realisations by nature of **S** and **Z** a utility (or alternatively a cost) is obtained. If only the costs denoted $C(\mathbf{e}, \mathbf{S}, \mathbf{a}, \mathbf{Z})$ are considered, the optimal decisions e* and a* can be obtained by solving the following optimization problem (*extended form of analysis*), see Raiffa and Schlaifer [14] and Benjamin and Cornell [1]

$$C^* = \min_{\mathbf{e}} E_{\mathbf{S}|\mathbf{e}}[\ \min_{\mathbf{a}} E''_{\mathbf{Z}|\mathbf{S}}[C(\mathbf{e}, \mathbf{S}, \mathbf{a}, \mathbf{Z})]\ ] \tag{7.2}$$

where $E_{\mathbf{S}|\mathbf{e}}[-]$ is the expectation with respect to the joint density function for **S** in the chosen experiment plan e and $E''_{\mathbf{Z}|\mathbf{S}}[-]$ is the expectation with respect to the updated joint density function of **Z** given **S**.

In some cases the optimization problem can be formulated by (*normal form of analysis*)

$$C^* = \min_{\mathbf{e}}\ \min_{\mathbf{d}} E'_{\mathbf{Z}}[E_{\mathbf{S}|\mathbf{e},\mathbf{z}}[C(\mathbf{e}, \mathbf{d}(\mathbf{S}), \mathbf{Z})]\ ] \tag{7.3}$$

where $\mathbf{d}(\mathbf{S})$ is a decision rule specifying the action a to be taken directly on the basis of observations of **S**. $E'_{\mathbf{Z}}[-]$ is the expectation with respect to the prior density function of **Z**. $E_{\mathbf{S}|\mathbf{e},\mathbf{z}}[-]$ is the expectation with respect to the joint density function for **S** in the chosen experiment plan e and for given **Z**. The normal form of analysis can be used when it is possible to formulate a decision rule. Otherwise the extensive form of analysis has to be used.

From a computational point of view (7.3) is generally much easier to solve than (7.2) since the minimization with respect to the action a is inside the expectation with respect to **S**.

The cost function is assumed to be written

$$C(\mathbf{e}, \mathbf{S}, \mathbf{a}, \mathbf{Z}) = C_M(\mathbf{e}) + C_R(\mathbf{e}, \mathbf{S}, \mathbf{a}, \mathbf{Z}) + C_F I[g(\mathbf{e}, \mathbf{S}, \mathbf{a}, \mathbf{Z}) \leq 0] \qquad (7.4)$$

where C_M is the cost of the measurements, C_R is the costs of the actions to be performed on the basis of the observed measurements and C_F is the cost of failure. The indicator function $I[.]$ is equal to one if failure occurs and equal to zero if the component or system is safe. In order to determine the expected value of C it is necessary to evaluate the probability of failure, $P(g(\mathbf{e}, \mathbf{S}, \mathbf{a}, \mathbf{Z}) \leq 0)$.

The probability of failure updated on the basis of the measurement results, $\hat{\mathbf{s}}$, for the experiment plan $\mathbf{e}$ and design $\mathbf{a}$ is estimated by

$$P_f'' = P(g(\mathbf{e}, \hat{\mathbf{s}}, \mathbf{a}, \mathbf{Z}''(\hat{\mathbf{s}})) \leq 0) \qquad (7.5)$$

where $\mathbf{Z}''(\hat{\mathbf{s}})$ denotes the updated stochastic variables $\mathbf{Z}$. In section 5.3.1 it is described how $\mathbf{Z}$ can be updated by Bayesian methods. P_f'' can be estimated by FORM/SORM-analysis.

As mentioned above the planning of the new measurements can be made on different levels of complexity. Here four levels are considered:

Level 1 Planning of Experiments

An optimization problem is formulated with $\mathbf{e}$ as optimization variables and where the measurement costs are minimized with a constraint on the probability of some critical event

$$\left.\begin{array}{ll} \min_{\mathbf{e}} & C_M(\mathbf{e}) \\ s.t. & P_f''(\mathbf{e}) \leq P_f^{\max} \end{array}\right\} \qquad (7.6)$$

where $P_f^{\max}$ is the maximum acceptable probability of the critical event. This optimization problem is solved with choices of measurement results $\hat{\mathbf{s}}$ which have the same physical variability as the already known measurements, see example below.

Level 2 Planning of Experiments

The expected cost of measurements and actions (repairs) is minimized with a constraint on the probability of some critical event

$$\left.\begin{array}{ll} \min_{\mathbf{e}} \min_{\mathbf{a}} & C_M(\mathbf{e}) + E_{\mathbf{Z}}[C_R(\mathbf{e}, \hat{\mathbf{s}}, \mathbf{a}, \mathbf{Z})] \\ s.t. & P_f''(\mathbf{e}, \hat{\mathbf{s}}, \mathbf{a}) \leq P_f^{\max} \end{array}\right\} \qquad (7.7)$$

This optimization problem can be solved with the same choices of measurement results $\hat{\mathbf{s}}$ as at level 1. The decision on measurement planning is then taken by comparing the expected cost of actions C_R to the costs of measurements C_M of different experiment plans (including no measurements). If only optimal repair planning is to be made, this can be done by solving eq. (7.7) with $\mathbf{a}$ as the only optimization variables. This is the problem which was solved in chapter 6.

Level 3 Planning of Experiments

The measurement plan $\mathbf{e}$ and the actions $\mathbf{a}$ are chosen such that the expected cost of measurements, actions (repairs) and failure is minimized:

$$\left.\begin{array}{ll} \min_{\mathbf{e}} \min_{\mathbf{a}} & C_M(\mathbf{e}) + E_{\mathbf{X}}[C_R(\mathbf{e}, \hat{\mathbf{s}}, \mathbf{a}, \mathbf{Z})] + C_F P_f''(\mathbf{e}, \hat{\mathbf{s}}, \mathbf{a}) \\ s.t. & P_f''(\mathbf{e}, \hat{\mathbf{s}}, \mathbf{a}) \leq P_f^{\max} \end{array}\right\} \qquad (7.8)$$

The constraint is not needed and can in principle be deleted. This optimization problem can also be solved for different measurement plans $\mathbf{e}$ and with choices of measurement results as indicated above.

Level 4 Planning of Experiments

The full optimization problem (7.2) or (7.3) formulated on the basis of decision theory is solved and the results are used in combination with experience to select the optimal measurement plan $\mathbf{e}$. The numerical methods used in order to solve the full optimization problem requires a large number of evaluations of the utility function. Hence, the method can only be applied if the evaluation of the utility function can be performed with relative ease.

7.2 Visual Inspection

As mentioned in section 2.3 the visual inspection can only reveal whether the structure shows signs of corrosion. If a visual inspection of a given structure at the time $t = t_m$ reveals no visible signs of corrosion the probability that visible signs of corrosion occur at at later time, $t > t_m$, can be updated. The following events are introduced

$$\begin{array}{lll} \{C\} & : & \text{Visible signs of corrosion at } t = t_m \\ \{C_T\} & : & \text{Visible signs of corrosion at } t > t_m \\ \{D\} & : & \text{Detection of corrosion at } t = t_m \end{array}$$

$$(7.9)$$

First consider the case where the probability that visible signs of corrosion have occurred at $t = t_m$ given no signs have been detected is negligible, i.e. $P\left(C|\overline{D}\right) = 0$. The probability that visible signs of corrosion have occurred at $t = t$ given that no signs have occurred at $t = t_m$ is

$$P\left(C_T|\overline{C}\right) = \frac{P\left(C_T\right) - P\left(C\right)}{1 - P\left(C\right)} \qquad (7.10)$$

where it has been used that the probability of corrosion is an increasing function of time, t.

This expression can be used to gain some understanding of the effect of performing the visual inspection. The expression, eq. (7.10), shows that in order for the visual inspection to have any effect, the probability that minor signs of corrosion have occurred at the time $t = t_m$, $P\left(C\right)$, must be relatively high.

If it is not assumed that $P\left(C|\overline{D}\right) = 0$, the updated probability of corrosion at $t > t_m$ can be determined on the basis of

$$
\begin{aligned}
P\left(C_T|\overline{D}\right) &= \frac{P\left(C_T \cap C \cap \overline{D}\right)}{P\left(\overline{D}\right)} + \frac{P\left(C_T \cap \overline{C} \cap \overline{D}\right)}{P\left(\overline{D}\right)} \\
&= P\left(C|\overline{D}\right) + \frac{P\left(C_T|\overline{C} \cap \overline{D}\right) P\left(\overline{C} \cap \overline{D}\right)}{P\left(\overline{D}\right)} \\
&= P\left(C|\overline{D}\right) + P\left(C_T|\overline{C} \cap \overline{D}\right) P\left(\overline{C}|\overline{D}\right)
\end{aligned} \tag{7.11}
$$

where $P\left(C_T|\overline{C} \cap \overline{D}\right) = P\left(C_T|\overline{C}\right)$ can be determined on the basis of eq. (7.10). In eq. (7.11) it is seen that it only makes on sense to perform a visual inspection if the probability of corrosion at $t = t$, $P\left(C_T\right)$, is larger than $P\left(C|\overline{D}\right)$.

Maintenance and repair of a given structure can be carried out when signs of corrosion are visible. If the distribution function of the time to occurrence of visual signs of corrosion is known, i.e. the distribution function of the time when the maintenance and repair is carried out is known, this distribution can be updated on the basis of a visual inspection.

7.2.1   Example: Effect of Visual Inspections

The bridge pier analyzed in the example in section 6.3 is also considered in this example. Further, since repair strategy 2 is implemented when minor signs of corrosion occur, the distribution of the time when signs of corrosion are visible is equal to the distribution of the time when repair strategy 2 must be implemented. In the following example the 2-parameter model and $\eta = \eta_1$ is used. The probability that no signs of corrosion are visible at $t = t_m$ given that no signs of corrosion have been detected is assumed to be $P\left(\overline{C}|\overline{D}\right) = 0.95$.

Figure 7.2a shows the probability that minor signs of corrosion occur in a given year (the same as figure 6.4a). Figure 7.2b shows the probability that minor signs of corrosion occur in a given year given no signs of corrosion were detected at a visual inspection of the structure at $t_m = 20$ years. In figure 7.2 it is seen that even though a visual inspection at $t_m = 20$ years has revealed no signs of corrosion, the probability that signs will occur after 20 years is still very large. The results of the inspection, in fact, have only increased the mean of the distribution with a few years. In conclusion, the visual inspection has very little influence on the distribution of the time to initiation of corrosion.

Alternatively, the results of the inspection can be used as information in the Bayesian analysis of the chloride profiles. Since no signs of corrosion has occurred it is likely that the transport coefficient and surface concentration has lower values than the ones measured earlier. The prior distribution of these parameters can then be changed accordingly and a new analysis can be carried out.
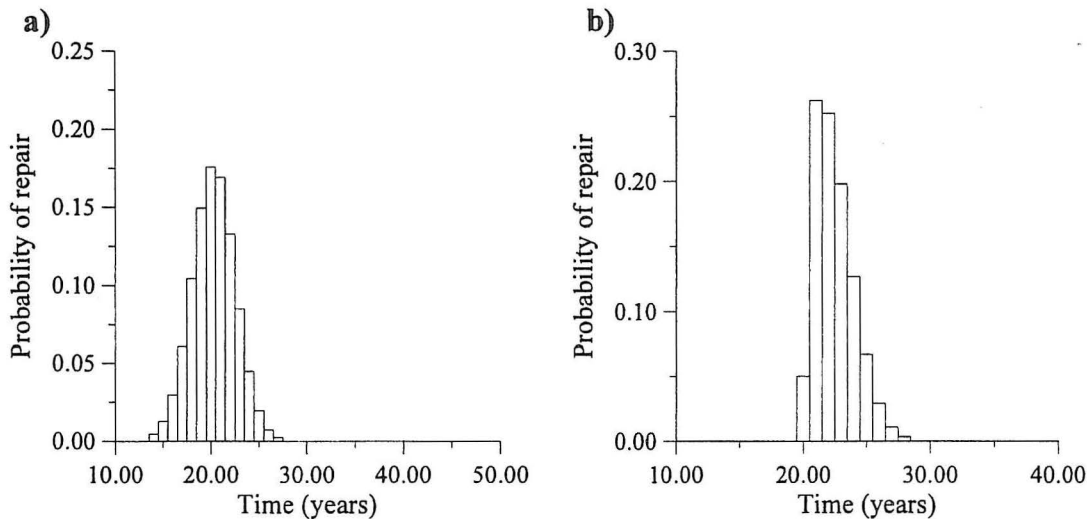
Figure 7.2: *Probability of corrosion given no signs have been detected at $t = 20$ years.*

7.3 Half-Cell Measurements

As outlined in section 2.3 half-cell measurements are used to detect corrosion in reinforced concrete structures. On the basis of the results of half-cell measurements, the probability of corrosion can be updated as well as the estimates of the times when the different maintenance and repair strategies must be implemented. In section 2.3 it was also mentioned that the results of a half-cell measurement performed at the time $t = t_m$ are interpreted in the following way:

$$P \,(\text{corrosion has occurred at } t = t_m | V < -350\text{mV}) \;=\; 0.9 \qquad (7.12)$$
$$P \,(\text{no corrosion has occurred at } t = t_m | V > -200\text{mV}) \;=\; 0.9 \qquad (7.13)$$

where V denotes the measured potential. It is important to emphazise that the probabilities of corrosion given in eqs. (7.12) and (7.13) are based on the information from the half-cell measurements only, and that no other information is taken into account. Using a linear interpolation between these values it is possible to construct a curve which gives the probability of corrosion as a function of the measured potential, see figure 7.3.

When performing half-cell measurements a large number of measurements with distances from 100 mm - 500 mm is performed. On the basis of the measurements a map of the measured potentials in the given structure can be made. On the basis of the map the areas with the largest probability of corrosion can be identified. As mentioned in section 2.3 the cover is often removed in these areas in order to perform a visual inspection of the reinforcement. This assures that, given corrosion has been initiated, it is very likely to be detected. However, it is difficult on the basis of the half-cell measurements to demonstrate that corrosion has not been initiated. If for example all measurements from a given structure show that the potential is larger than -200 mV and N_m measurements has been performed, the probability that corrosion has not been initiated in any of the points covered by the investigation is
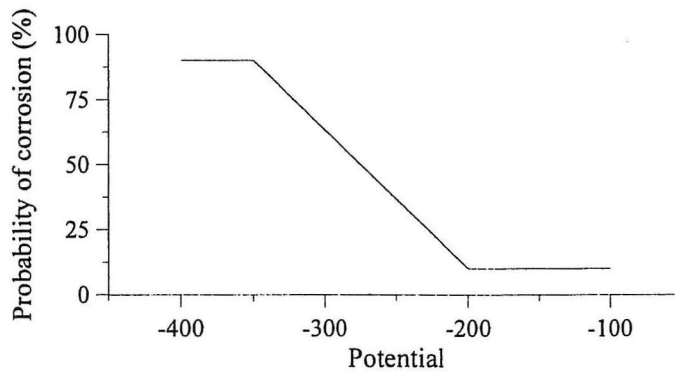
Figure 7.3: *Probability of corrosion af a function of the potential.*

$$P \text{ (No corrosion in any of the points)}$$
$$= \prod_{i=1}^{N_m} P \text{ (No corrosion at point } i\text{)} \tag{7.14}$$

if the occurrence of corrosion at two different points are independent events and if all measurement results are independent. It is evident that P (No corrosion at point i) cannot exceed 0.9. Further, the total number of measurements is large (up to several thousand). This implies that the probability that corrosion has not been initiated at any point, determined by eq. (7.14), will be very low.

It is obvious that the expression, eq. (7.14), cannot be used in order to determine the probability that corrosion has not been initiated at any point. In general the occurrence of corrosion at two different points are not independent events. However, this simple example indicates that it is difficult on the basis half-cell measurements to determine the probability that corrosion has not been initiated. There are, in fact, no rules for the interpretation of the results which take into account the number of measurements and the distance between the measurements.

Even if it is possible on the basis of half-cell measurements to establish that corrosion has not been initiated, the value of this information is limited. It is only possible to perform an updating along the lines demonstrated in the previous section 7.2.1 where the effect of a visual inspection was taken into account. Half-cell measurements seem to be more applicable for demonstrating that corrosion has been initiated than it has not been initiated.

7.4   Dust Samples

So far the dust samples have only been used in order to formulate a prior distribution for the transport coefficient and the surface concentration, see section 5.4.1. However, the dust samples can in principle also be used in order to estimate a surface concentration and transport coefficient. It must, however, be remembered that the dust samples are
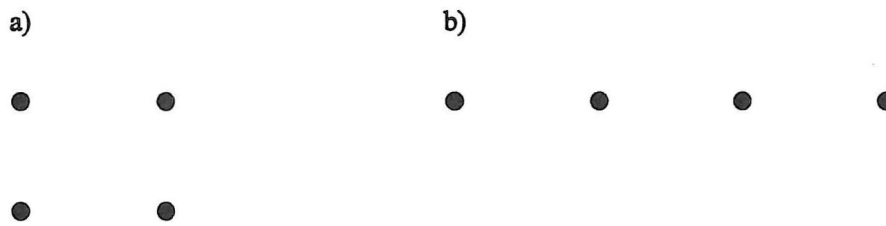
a)   b)

Figure 7.4: *Arrangement of boreholes for dust samples.*

obtained from several boreholes. It is important that the distance from the individual boreholes is not too large and that the boreholes are arranged in a suitable manner. For example, the arrangement of the boreholes shown in figure 7.4**a** is to be preferred from the arrangement shown in figure 7.4**b**.

On the basis of the dust samples it is possible to determine the chloride concentration as a function of the distance from the surface. However, for a given sample it is only possible to estimate the concentration at 3 or 4 different depths. Therefore, it is only possible to use the 2-parameter model for the dust samples. Further, the measurement uncertainty related to the dust samples is much higher than the measurement uncertainty related to the chloride profiles implying that the estimated parameters are subject to a larger scatter. The major advantage of the dust samples over the chloride profiles is the ease by which the measurements can be performed and the low cost of performing the measurements.

If the dust samples allow for the estimation of a surface concentration and a transport coefficient, the planning of this type of experiment can be performed according to the method for chloride profiles outlined in the next section.

7.5   Chloride Profiles

As earlier mentioned the estimation of the time to initiation of corrosion in a reinforced concrete structure is usually based on information gained from chloride profiles. The planning of this type of measurements is, therefore, treated in more detail in the following. It is show how level 1, 2 and 3 planning of the experiments can be performed and the level 4 planning is discussed.

7.5.1   Level 1 Planning of Experiments

Inspections of concrete structures subject to chloride ingress are usually carried out at some fixed time interval, T_I. If the engineer is able to show a sufficiently small probability of corrosion in the next time interval, no decision about the type of repair and maintenance strategy has to be made. This decision can be postponed until after the next inspection. If the decision can be postponed, new information from the next inspection can be taken into account and possibly form the basis of a more detailed model. E.g. the variation of the transport coefficient as a function of time can be taken into account.

The problem can be formulated in the following way

$$\min \quad C_M(\mathbf{e}) \tag{7.15}$$

$$s.t. \quad P_I''(t_m + T_I, \mathbf{e}, \hat{\mathbf{s}}) \leq P_I^* \tag{7.16}$$

where $C_M(\mathbf{e})$ denotes the cost related to the experiments and P_I^* is an upper bound for the probability of corrosion at the time $t_m + T_I$, where t_m denotes the time where the measurements are made.

The cost related to the measurements is modelled by

$$C_M(\mathbf{e}) = C_I + C_e n_{new} \tag{7.17}$$

where C_I is the fixed cost related to the measurements, C_e denotes the cost of a single measurement and n_{new} denotes the number of new experiments. Using this simple model of the experiment cost, the optimal plan is the plan with the lowest number of measurements for which $P_I''(t_m + T_I, \mathbf{e}, \hat{\mathbf{s}}) \leq P_I^*$.

The calculation of the probability of corrosion will be based on the assumption that the parameters $\boldsymbol{\mu}$ and h are known. In order to determine the effect of the new measurements it is necessary to know the joint distribution of the statistics v and $\mathbf{m}$ for the given values of h and $\boldsymbol{\mu}$ and for a given number of new experiments, n_{new}. The definition of these parameters is given in section 5.3.1. Raiffa and Schlaifer [14] have shown that the joint distribution is given by

$$f_{\mathbf{MV}}(\mathbf{m}, v | n_{new}, \nu_{new}, h, \boldsymbol{\mu}) = f_{\mathbf{M}}(\mathbf{m} | \boldsymbol{\mu}, n_{new} h \boldsymbol{\eta}) f_V(v | h, \nu_{new}) \tag{7.18}$$

where $f_{\mathbf{M}}(\mathbf{m} | \boldsymbol{\mu}, n_{new} h \boldsymbol{\eta})$ is a normal distribution with mean $\boldsymbol{\mu}$ and covariance matrix $(n_{new} h \boldsymbol{\eta})^{-1}$ and $f_V(v | h, \nu_{new})$ is a Gamma-distribution with mean and coefficient of variation given by

$$E[v] = \frac{1}{h} \tag{7.19}$$

$$V[v] = \sqrt{\frac{2}{\nu_{new}}} \tag{7.20}$$

The probability of corrosion as a function of the experiment plan, $\mathbf{e}$, i.e. for a given number of new measurements, and as a function of the outcomes of the measurements, $\hat{\mathbf{s}}$, can be evaluated by

$$P_I''(t_m + T_I, \mathbf{e}, \hat{\mathbf{s}}) = \int_{\Omega_\mathbf{m}} \int_{\Omega_v} P_I''(t_m + T_I, \mathbf{e}, \hat{\mathbf{s}} | \mathbf{m}, v) f_{\mathbf{MV}}(\mathbf{m}, v | n_{new}, \nu_{new}, h, \boldsymbol{\mu}) \, d\mathbf{m} dv \tag{7.21}$$

where $P_I''(t_m + T_I, \mathbf{e}, \hat{\mathbf{s}} | \mathbf{m}, v)$ is the probability that corrosion has been initiated at the time $t_m + T_I$ in the given structure for a given outcome of $\mathbf{m}$ and v and $\Omega_\mathbf{m}$ and Ω_v denote the admissible ranges of $\mathbf{m}$ and v, respectively. If the example described in section 6.3

is considered the probability $P_I''(t_m + T_I, \mathbf{e}, \hat{\mathbf{s}}|\mathbf{m}, v)$ can be determined on the basis of eq. (6.4) where the reliability index, β_e, depends on $\mathbf{m}$ and v. The distributions of h and μ is updated on the basis of the experimental outcomes according to the rules given in section 5.3.1.

Naturally, the parameters μ and h are not known. It is, therefore, necessary to perform a sensitivity analysis in order to quantify the sensitivity of the optimal plan towards changes of the parameters. If the plan is not sensitive it can be considered to be optimal.

The computation of the probability of corrosion at the time $t = t_m + T_I$ for a given set of parameters $\mathbf{m}$ and v, $P_I''(t_m + T_I, \mathbf{e}, \hat{\mathbf{s}}|\mathbf{m}, v)$, can be performed in the way outlined in section 6.3. The probability of corrosion is equal to the probability that maintenance strategy 1 introduced in section 6.3 is implemented.

The integration in eq. (7.21) can be performed in a number of ways

- Gauss integration.
- Conditional sampling.
- Nested FORM/SORM
- Response surface method.

The most simple way to perform the integration is probably Gauss integration. However, it is a well-known fact that the efficiency of the Gauss integration decreases rapidly with the dimension of the integral. In the present case the integral has 3 or 4 dimensions depending on whether the 2- or 3-parameter model is used. If 6 Gauss points are used for each variable this corresponds to 216 and 1296 calculations of $P_I''(t_m + T_I, \mathbf{e}, \hat{\mathbf{s}}|\mathbf{m}, v)$ for the 2- and 3-parameter model, respectively.

The integral can also be solved using conditional sampling. By conditional sampling the integration indicated in eq. (7.21) is performed using Monte Carlo simulation. However, the number of simulations must be large enough to ensure that the uncertainty related to the estimated failure probabilities is insignifigant. Only if this criterion is met it is possible to solve the optimization problem given in eq. (7.16). If the number of simulations necessary to obtain this accurracy is too large the method is inefficient.

The FORM/SORM-analysis is basically a method for numerical integration and it can be applied to solve arbitrary integrals if these have been reformulated in a suitable way, see section 4.4. The method only gives an approximate value for the integral. However, as mentioned in section 4.4 the method is likely to be very efficient.

The integral can also be solved on the basis of some approximation of $P_I''(t_m + T_I, \mathbf{e}, \hat{\mathbf{s}}|\mathbf{m}, v)$ as a function of the integration variables. Such an approximation can be determined by a response surface method. In order to use this method for the integration, it is necessary to obtain a very accurate approximation of the function $P_I''(t_m + T_I, \mathbf{e}, \hat{\mathbf{s}}|\mathbf{m}, v)$. It is, however, difficult to obtain an accurate approximation because the integration region is very large.

7.5.2 Example: Level 1 Planning of Experiments

The bridge pier considered in section 6.3 is also investigated in this example. The maintenance and repair strategy 1 considered in the example in section 6.3 is implemented

when corrosion is initiated. The time to initiation of corrosion for a given outcome of $\mathbf{m}$ and v, therefore, can be determined in the way outlined in section 6.3.2.

Using the methodology presented above the effect of performing additional experiments is investigated. The experiments are performed at $t_m = 10$ years and it is assumed that a new inspection of the bridge will be carried out in 5 years, i.e. $T_I = 5$ years. It is now necessary to determine the probability that corrosion has been initiated at $t = t_m + T_I = 15$ years as a function of the number of new experiments. The optimal number of experiments is the number which ensures that the probability that corrosion has been initiated at $t = 15$ years is sufficiently small.

In the following only the 2-parameter model introduced in section 5.4.1 is investigated. It is assumed that the new experiments reproduces the mean values of the parameters determined on the basis of the previous experiments, that is

$$h = \frac{1}{v} = 2.191 \tag{7.22}$$

$$\mu = \mathbf{m} = \begin{bmatrix} m_1 \\ m_2 \end{bmatrix} = \begin{bmatrix} 17.28 \\ 1.079 \end{bmatrix} \tag{7.23}$$

for $\boldsymbol{\eta} = \boldsymbol{\eta}_1$ and

$$h = \frac{1}{v} = 2.147 \tag{7.24}$$

$$\mu = \mathbf{m} = \begin{bmatrix} m_1 \\ m_2 \end{bmatrix} = \begin{bmatrix} 17.28 \\ 1.079 \end{bmatrix} \tag{7.25}$$

for $\boldsymbol{\eta} = \boldsymbol{\eta}_2$.

These parameters are determined on the basis of the experiment outcomes given in eqs. (5.39)-(5.42). The uncertainty related to the outcomes is not taken into account. According to the sensitivity analysis shown in section 5.4.1 the error made by disregarding this uncertainty is negligible.

In figures 7.5a and 7.5b the probability of corrosion is shown as a function of the number of new experiments for $\boldsymbol{\eta} = \boldsymbol{\eta}_1$ and $\boldsymbol{\eta} = \boldsymbol{\eta}_2$, respectively. The results in figure 7.5 have been determined by conditional sampling. The number of samples is 250 and the coefficients of variation of the estimated probabilities are all about 10 %.

In figures 7.6a and 7.6b the results of the same example are shown again. The failure probabilities have been evaluated by Gauss integration. For each of the variables 6 Gauss points have been used. The number of evaluations of the conditional probability of corrosion is 216. The numerical effort required to obtain the results shown in figure 7.6 is of the same magnitude as for the conditional sampling. By a comparison of the figures 7.5 and 7.6 it is seen that virtually identical results are obtained. However, it must be kept in mind that the results obtained by Gauss integration are not subject to any statistical uncertainty. Depending on the number of Gauss points used for the integration the result may be subject to some numerical error. In the present case where 6 Gauss points have been used for each variable this error is assumed to be negligible. The Gauss integration, therefore, seem to be the most suitable of the two methods.
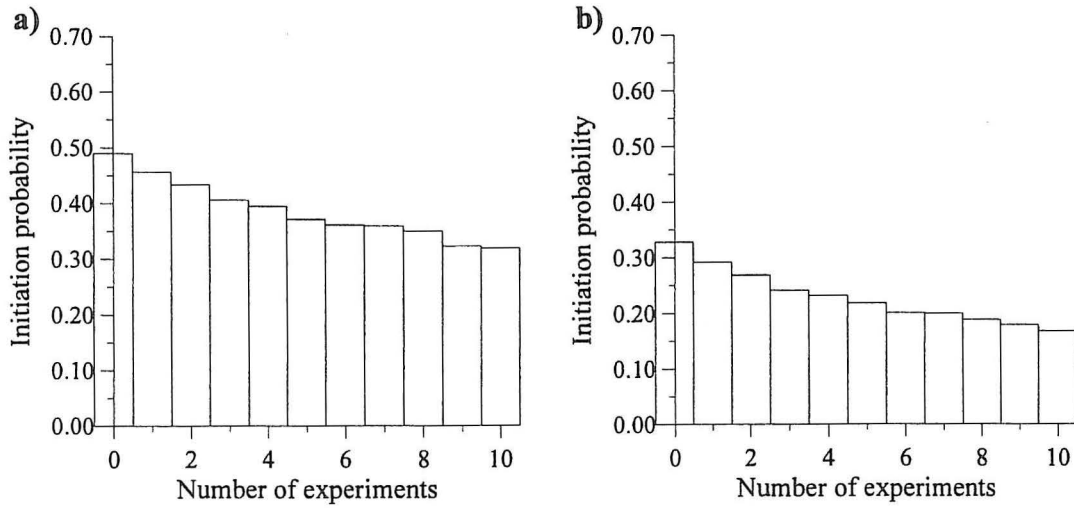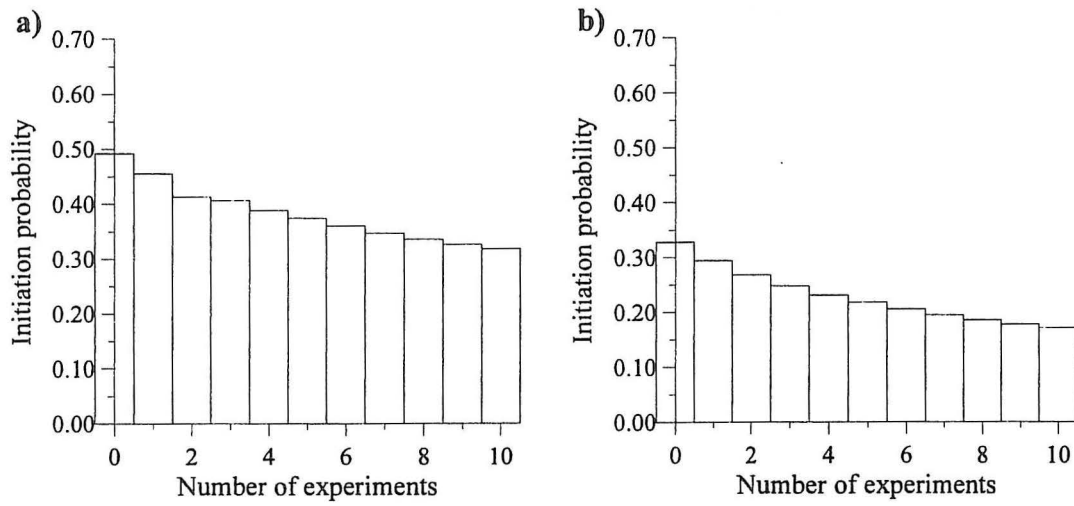
Figure 7.5: *Conditional sampling.*
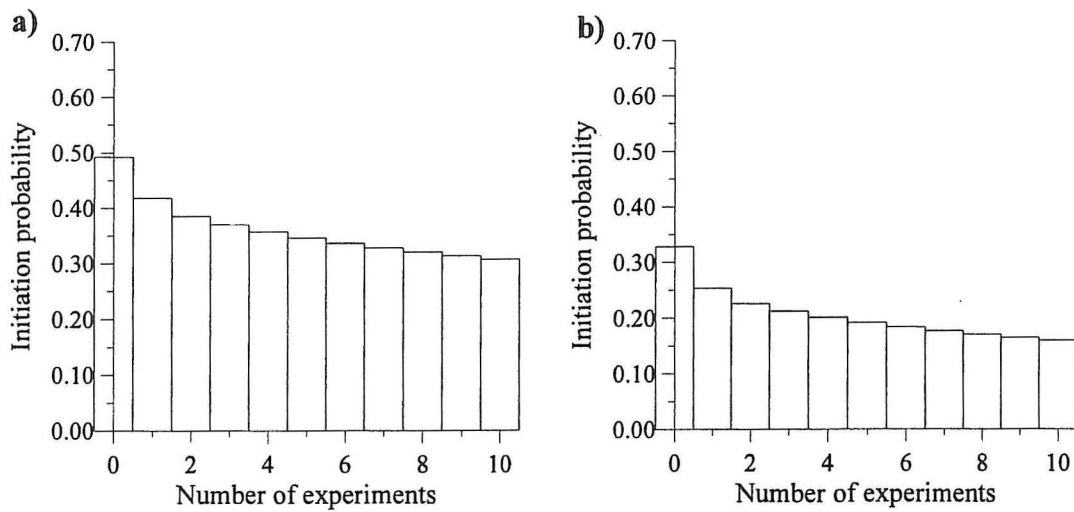

Figure 7.6: *Gauss integration.*

Figure 7.7: *Nested FORM.*

The same computations have also been performed by nested FORM. The results are shown in figures 7.7a and 7.7b for $\eta = \eta_1$ and $\eta = \eta_2$, respectively. The limit state function is

$$g = u_a - P_I'' \left(t_m + T_I, \mathbf{e}, \hat{\mathbf{s}} | \mathbf{m}, v \right) \tag{7.26}$$

where u_a is an auxiliary standard normally distributed variable. It typically requires 15-20 evaluations of $P_I'' \left(t_m + T_I, \mathbf{e}, \hat{\mathbf{s}} | \mathbf{m}, v \right)$ in order to evaluate the probability of corrosion by nested FORM. This implies that the method is about 10-15 times faster than Gauss integration. However, by comparing the results in figure 7.7 with the results in figure 7.6 it is seen that the nested FORM has a tendency to underestimate the failure probabilities. This behaviour can be improved by using SORM analysis which, however, requires a larger number of evaluations of the conditional probability of corrosion, $P_I'' \left(t_m + T_I, \mathbf{e}, \hat{\mathbf{s}} | \mathbf{m}, v \right)$. It is also important to notice that as n_{new} increases the results obtained by nested FORM become more accurate and for n_{new} approaching infinity the result is exact. When n_{new} approaches infinity the conditional probability of corrosion is a constant and the limit state function is linear. The fact that the estimated probabilities are too low for small values of n_{new} and exact for large values of n_{new} implies that the difference $\Delta P_I \left(n_{new} \right) = P_I \left(n_{new} \right) - P_I \left(n_{new} - 1 \right)$ is underestimated by nested FORM.

If it is assumed that $\eta = \eta_2$ and it it can be accepted that the probability of corrosion at $t = 15$ years is 0.2, the optimal number of new experiments is $n_{new} = 7$. The fairly high probability of corrosion can be accepted because initiation of corrosion causes no immediate threat to the load-bearing capacity of the pier. If, on the other hand, it is believed that $\eta = \eta_1$, it would not be possible to perform enough experiments to reach the acceptable level. Further, if the 3-parameter model is believed to be correct, the probability of corrosion at $t = 15$ years is 0.043 and 0.067 for $\eta = \eta_3$ and $\eta = \eta_4$, respectively, without any additional experiments. Unfortunately, this indicates that the optimal decision is very sensitive to changes of η and to a large extent depends on the chosen model of chloride ingress. It is, therefore, possible to reach virtually any result, depending on the beliefs of the model builder.

Sensitivity Analysis

The computations made above in section 7.5.2 are based on known values of the parameters h and $\boldsymbol{\mu}$. These parameters, however, are subject to uncertainty. Hence, it is necessary to investigate the effect of changing the parameters. One the basis of the four experiment outcomes shown in eqs. (5.39)-(5.42) the standard deviations of the parameters $\boldsymbol{\mu}$ and h are determined. In the following only the case $\eta = \eta_2$ is considered.

In figures 7.8a and 7.8b the probability of corrosion is shown as a function of n_{new} for $\mu_1 = m_1 - \sigma_{\mu_1}$ and for $\mu_1 = m_1 + \sigma_{\mu_1}$, respectively, where σ_{μ_1} denotes the standard deviation of μ_1 and where m_1 denotes the mean value of μ_1 (the transport coefficient). The results of the sensitivity analysis with respect to μ_2 (the surface concentration) are shown in the figures 7.9a and 7.9b where the values $\mu_2 = m_2 - \sigma_{\mu_2}$ and $\mu_2 = m_2 + \sigma_{\mu_2}$, respectively, have been used. The results shown in figure 7.10a were obtained on the basis of $h = \frac{1}{v} - \sigma_h$ and the results shown in figure 7.10b were obtained on the basis of $h = \frac{1}{v} + \sigma_h$. By the sensitivity analysis only the parameters stated above have been changed. All other variables remain unchanged.
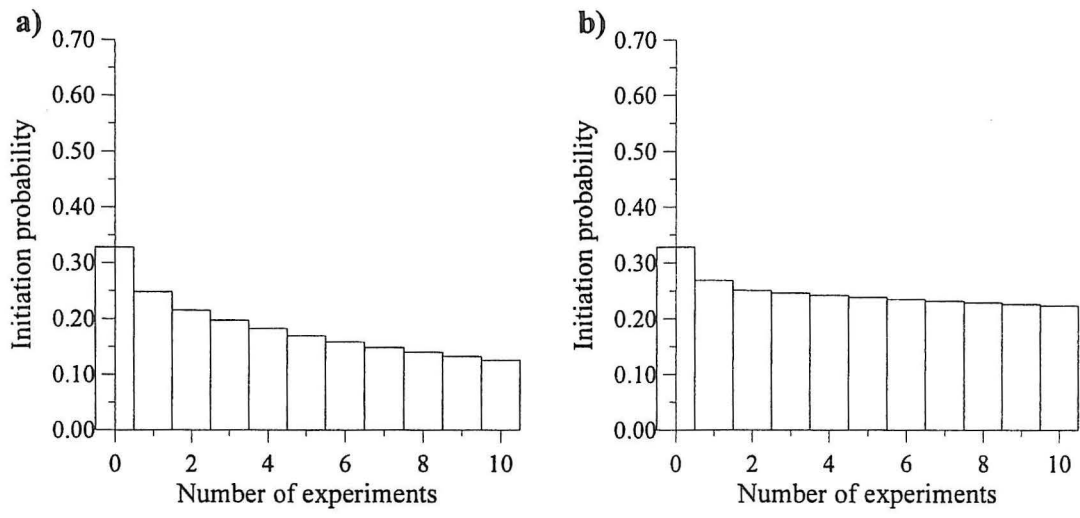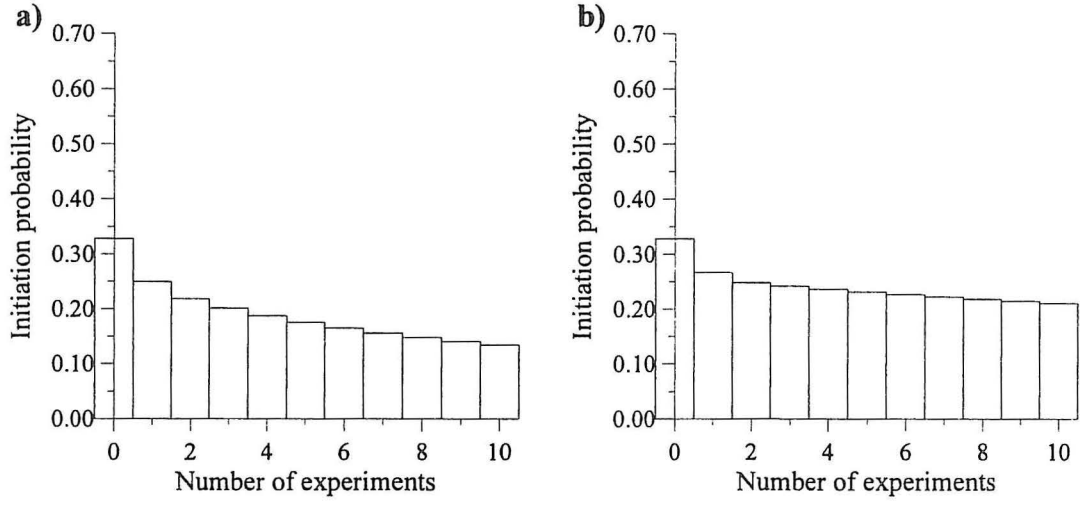
Figure 7.8: *Sensitivity with respect to m_1.*

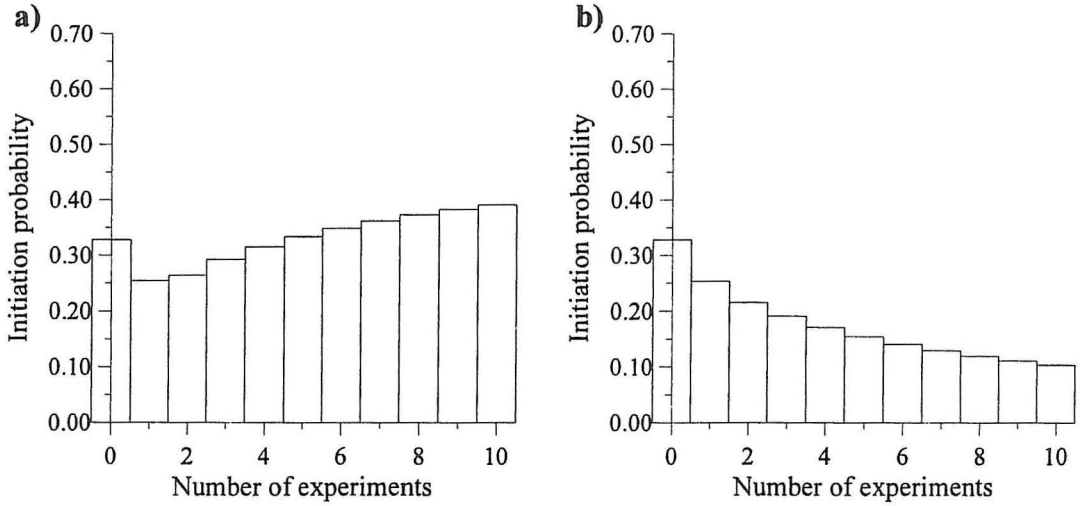Figure 7.9: *Sensitivity with respect to m_2.*

Figure 7.10: *Sensitivity with respect to h.*

The computations are performed by FORM-analysis because this is the most efficient method. For the sensitivity analysis the absolute values of the results are not important. It is more important to compare the results relative to each other. The results obtained on the basis of a FORM-analysis are sufficiently accurate to facilitate this comparison.

The sensitivity analysis reveals that the results are very sensitive to changes of the values of h and μ. Especially if a false value of h is chosen erroneous results are obtained. In fact, the suggested method is only applicable if the uncertainty related to the parameters h and μ is small. However, if so it seems unnecessary to perform additional experiments.

In conclusion, the level 1 planning of experiments as presented in this section is of little practical interest. As demonstrated the results to a large extent depends on the model builder. Further, the optimal plan is very sensitive towards changes of the parameters μ and h.

7.5.3 Level 2 Planning of Experiments

A level 2 optimal plan is determined by minimizing the expected cost of measurements and maintenance under the condition that the probability of some critical event is lower that an upper limit. In the present case, however, the different repair strategies all are associated with different critical events (see section 6.3). Also, it seems unlogical to impose some upper limit on the probability of these events since they are believed to have no influence on the probability of loss of human life. In fact, the probability of loss of human life is believed to be constant until the time when repair is performed. The repair is performed in order to prevent increasing probability of loss of human life.

In the following the optimal experiment plan and repair strategy, therefore, will be defined as the ones which minimize the expected total cost, $E[C_T]$, without restrictions on the probability of any critical event. The expected total cost is determined as

$$E[C_T] = C_M(\mathbf{e}) + E_\mathbf{Z}[C_R(\mathbf{e}, \hat{\mathbf{s}}, \mathbf{a}, \mathbf{Z})] \qquad (7.27)$$

7.5.4 Example: Level 2 Planning of Experiments

Level 2 planning of experiments is now implemented in order to determine the optimal experiment plan and maintenance method for the bridge pier considered in section 6.3 and in the previous section, 7.5.2. The same three maintenance strategies as in section 6.3 are considered and the same economic model for the maintenance strategies is used. The real rate of interest is chosen as $r = 0.07$.

The expected cost of maintenance for a given experiment plan and maintenance strategy is computed in the way outlined in section 6.3. The necessary computations of the probability that a given maintenance strategy is implemented when a given number of new experiments has been performed again is based on the assumption that the parameters μ and h are known. The values of the parameters μ and h are given in eq. 7.25. Further, the same problem as in the previous section is considered, i.e. the 2-parameter model is implemented, however only the model $\eta = \eta_2$ is considered.

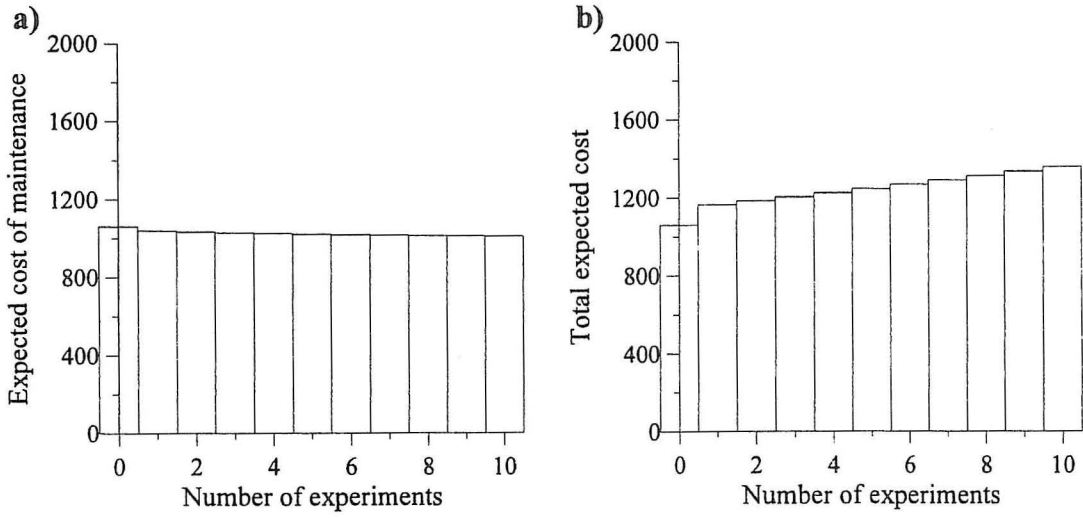The probability that a given repair and maintenance strategy is implemented as a function
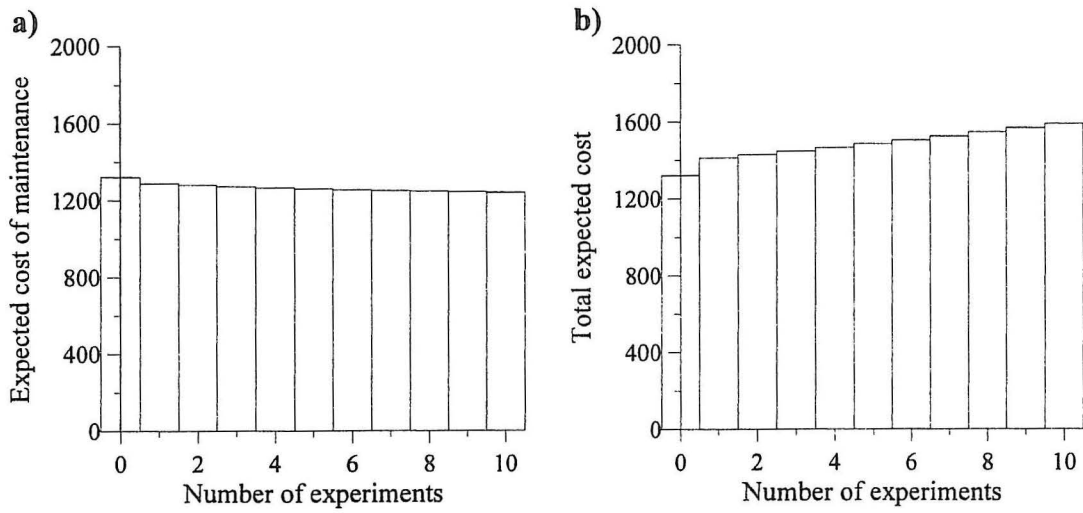
Figure 7.11: *Maintenance strategy 1.*
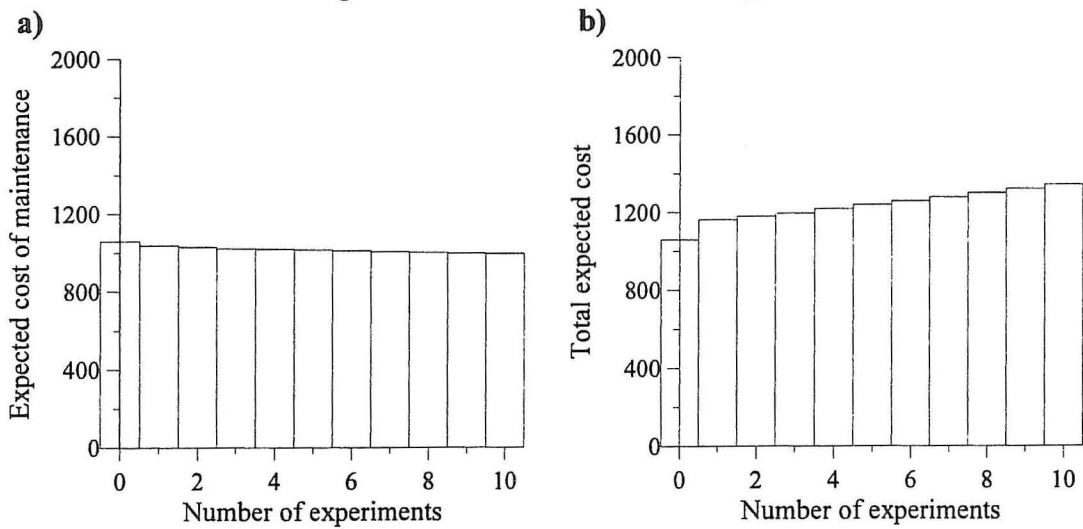

Figure 7.12: *Maintenance strategy 2.*

Figure 7.13: *Maintenance strategy 3.*

of the experimental plan, i.e. the number of new experiments, is determined in the way the probability of corrosion as a function of the number of new experiments was determined in the previous section, see eq. (7.21). Since a large number of computations has to be made the probability that a given maintenance strategy is implemented is determined by FORM-analysis.

The cost of measurements is determined on the basis of the model given in eq. 7.17. The initial cost is $C_I = 100$ and the cost of a measurement is $C_e = 25$.

In figures 7.11a, 7.12a and 7.13a $E_{\mathbf{Z}}[C_R(\mathbf{e}, \hat{\mathbf{s}}, \mathbf{a}, \mathbf{Z})]$, the expected cost of repair and maintenance, is shown, as a function of the number of new experiments for repair strategy 1, 2 and 3 respectively. The total expected cost, $E[C_T]$, as a function of the number of new experiments is shown in figures 7.11b, 7.12b and 7.13b for repair strategy 1, 2 and 3 respectively.

In figures 7.11, 7.12 and 7.13 it is seen that the optimal decision is to perform no additional experiments and to implement repair strategy 1. In other words, by performing additional measurements it is not possible to obtain a reduction of the cost of maintenance of the same size as the cost of the additional measurements.

The expected cost of maintenance and repair is very sensitive towards changes of the mean of the time when a maintenance and repair strategy is implemented and less sensitive towards changes of the standard deviation. Further, the effect of additional experiments is a reduction of the standard deviation of the time when a repair and maintenance strategy must be implemented. The mean value remains approximately constant. Therefore, the expected cost of repair and maintenance remains almost constant independently of the number of new experiments. In conclusion, the result of the level 2 analysis is not surprising.

Due to the computational effort involved in performing the computations for reaching the above conclusion no sensitivity analysis has been performed. However, the figures 7.11a, 7.12a and 7.13a indicate that the reduction of the cost of maintenance obtained by performing additional measurements must be several magnitudes larger in order to make additional measurements optimal. It is not likely that such a large reduction of the maintenance cost can be obtained even if substantially different values of μ and h were used in the analysis. A sensitivity analysis with respect to the real rate of interest, r, will show the same result as the analysis in section 6.3.

The present example indicates that if no decision rule, $\mathbf{d}(\mathbf{S})$, specifies the action to be taken on the basis of the experimental results or if no critical event is taken into account, the effect of the new measurements is negligible.

7.5.5   Level 3 Planning of Experiments

Level 3 planning of measurements is just like the level 2 planning except that the expected cost of failure is added to the expected total cost. The expected cost of failure is given by $C_F P_f(\mathbf{e}, \hat{\mathbf{s}}, \mathbf{a}, \mathbf{Z})$, see eq. (7.8). This now leaves the problem of defining the failure event and determining the probability of failure. Failure could be defined as collapse of the structure. As earlier mentioned, see section 6.3, the probability of structural failure is believed not to change significantly prior to the repair of the structure. The expected cost

of failure in that case is constant and the level 3 planning of the measurements will lead to the same result as the level 2 planning of measurements. As an alternative a monetary loss can be ascribed to the implementation of a given maintenance strategy. If we consider the above example it seems logical to ascribe a high cost to the implementation of strategy 3 since strategy 3 is implemented when distinct signs of corrosion have occurred, a lower cost to strategy 2 because strategy 2 is implemented when minor signs of corrosion have occurred and no cost to strategy 1, because strategy 1 is implemented before any signs of corrosion are visible. In this way it is possible to ascribe some monetary value to the visual impression of the structure. Depending on the value of the visual impression of the structure this methodology might lead to another optimal maintenance plan than the one determined above, in section 7.5.4.

7.5.6 Level 4 Planning of Experiments

For the example considered in the previous sections the evaluation of the probability that a given maintenance strategy is implemented is very time consuming in terms of CPU-time. Since a level 4 planning of measurements requires an even larger number of evaluations the effort required in order to use this method is excessive. Further, the implementation of level 4 planning of measurements is difficult because it requires that an optimization is performed within an optimization. This poses very strict demands on the accuracy of the inner optimization. Finally, as argued in the level 2 planning of measurements, the optimum found by this method is believed to be very stable towards changes in the parameters. This means that the level 4 planning of experiments would lead to the same result.

7.6 Measurements of Cover Thickness

The planning of the number of measurements of the cover thickness can be performed in the same manner as the planning of the number of chloride profiles.

7.6.1 Example: Measurements of Cover Thickness

In figure 7.14 the probability of corrosion is shown as a function of time for different numbers of additional measurements of the cover thickness. The computations are based on the 2-parameter model and $\eta = \eta_2$. It has been assumed that the new measurements reproduces the parameters estimated on the basis of the original experiments, $m = 52.5$ mm and $v = 11.5$ mm^2, see section 5.4. In other words, the values of the sufficient statistics m and v remain constant as the number of experiments is increased. It is seen that the effect of performing additional measurements of the cover thickness is negligible.

It must, however, be emphasized that an analysis of the above type only investigates the effect of reducing the statistical uncertainty related to the parameters in the probabilistic model. The effect of a change of the mean values of the parameters is not investigated. As demonstrated in section 5.4.1 the probability of corrosion in a 1 × 1 m area is very sensitive towards changes of the mean of the cover thickness. This sensitivity analysis indicates
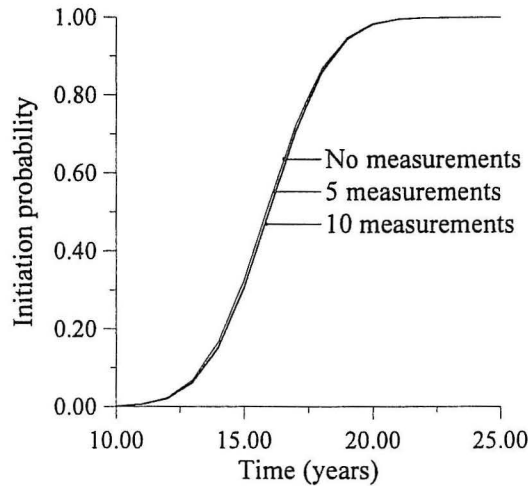
Figure 7.14: *Effect of measurements of the cover thickness.*

that if additional experiments lead to a change of the mean of the cover thickness, these measurements should be performed.

7.7   Summary and Conclusion

In the present chapter the problem of optimal planning of experiments was considered. It has been shown how optimal plans can be determined on the basis of decision analysis and how the analysis can be carried out at different levels of complexity. It is shown that visual inspections and half-cell measurements only have a limited effect on the estimated times when maintenance and repair of a given structure must be carried out. More detailed analyses are carried out in order to determine the optimal number of measurements of chloride profiles. First the number of measurements necessary to ensure that the probability of corrosion at a given time is sufficiently low is determined. However, the experiment plan determined on this basis is very sensitive to the model of chloride ingress and to a large extent depends on the values of the model parameters which were assumed to be known by this analysis. Further, an analysis has been carried out where the optimal plan was determined by minimizing the expected cost of the measurements and the maintenance and repair. This analysis showed that no additional measurements are necessary and that the optimal maintenance and repair strategy determined in section 6.3 is optimal. Further, it is argued that this result is insensitive to changes of the model parameters. However, the computational effort involved in the computations of the optimal experiment plan is excessive. The duration of the computations of the expected cost of measurements and maintenance and repair is about 10 days on a Silicon Graphics Workstation for a given repair strategy. This makes the method less attractive.

Instead of performing the experiment planning on the basis of decision analysis as suggested in the present chapter, the experiment plan can be determined on the basis of sensitivity studies such as these performed in section 5.4.1. On the basis of sensitivity studies the most important variables can be identified. If the cost of performing the exper-

iments, needed in order to estimate the important parameters more precisely, is known, an experiment plan can be determined on this basis.

7.8 References

[1] Benjamin, J. R., Cornell, C. A., Probability, Statistics and Decision for Civil Engineers, McGraw-Hill, 1970.

[2] Box, G. E. P., Draper, N. R., Emperical Model-Building and Response Surfaces, Wiley, New York, 1987.

[3] Box, G. E. P., Tiao, C. T., Bayesian Inference in Statistical Analysis, Wiley, New York, 1992.

[4] Chaloner, K., Optimal Bayesian Experimental Design for Linear Models, The Annals of Statistics, 12, 1984, pp. 283.300.

[5] Chernoff, H., Locally Optimal Designs for Estimating Parameters, Ann. Math. Stat., 24, 1953, pp. 586-602.

[6] Escobar, L. A., Meeker, W. Q., Planning Accelerated Life Test with Type II Censored Data, Journ. Stat. Compt. Simul., 23, 1986, pp. 273-297.

[7] Faber, M. H., Sørensen, J. D., Kroon, I. B., Optimal Fatigue Testing - a Reassesment Tool, IABSE Colloquium, Copenhagen, Denmark, 1993, IABSE Report 67, pp. 61-68.

[8] Kroon, I. B., Decision Theory Applied to Structural Engineering Problems, Ph.D.-thesis, Structural Reliability Theory Paper No. 132, Dept. of Building Technology and Structural Engineering, Aalborg University, Denmark.

[9] Kroon, I. B., Sørensen, J. D., Faber, M. H., Rational Planning of Offshore On-Site Measurements, Proceedings of the 4th International Offshore and Polar Engineering Conference, (ISOPE-94), Vol. IV, Osaka, Japan, 1994, pp. 500-504.

[10] Mann, N. R., Design of Over-Stress Life-Test Experiments when the Failure Times have the Two-Parameter Weibull Distribution, Technometrics, 14, 1972, pp. 437-451.

[11] Meeker, Q. M., Nelson, W., Optimum Accelerated Life-Tests for the Weibull and Extreme Value Distributions, IEEE Transactions on Reliability, R-24, 1975, pp. 321-332.

[12] Myers, R. H., Response Surface Methodology, Allyn and Bacon, Boston, 1971.

[13] Pilz, J., Bayesian Extimation and Experimental Design in Linear Models, Teubner-Text zur Mathematik, Band 55, Leipzig, 1983.

[14] Raiffa, H., Schlaifer, R., Applied Statistical Decision Theory, Harvard University Press, Cambridge, Mass., 1961.

[15] Sørensen, J. D., Faber, M. H., Kroon, I. B., Risk Based Optimal Fatique Testing, in: Lin, Y. K., (ed.), Probabilistic Mechanics and Structural and Geotechnical Reliability, ASCE, Denver, 1992, pp. 523-526.

Chapter 8

Summary and Conclusions

On the basis of the methods, models and examples presented in the present thesis a number of conclusions can be reached. First, a brief summary of the thesis is given in this chapter where also a number of the conclusions are presented. Then the most important conclusions are emphazised.

8.1 Summary

In the industrialized world an increasing percentage of the highway authority budgets is spent on rehabilitation of reinforced concrete structures. The main reasons for the increasing cost are material deterioration due to environmental factors, poor design and poor workmanship. Further, the number of old structures is steadily increasing, which in itself increases the need for rehabilitation. In Denmark chloride-initiated corrosion is the most common reason for deterioration of reinforced concrete structures. This mechanism, therefore, has been chosen as an example of how such deterioration can be described by a probabilistic model. Such a model can be used to determine the optimal strategy for maintenance and repair of a given structure and to determine an optimal plan for additional measurements.

In chapter 1 a short presentation of the problem is given together with a description of the purpose of probabilistic models. Further, the main objectives of the project are identified. The main objectives are to

- Formulate a probabilistic model for chloride ingress and initiation of corrosion.
- Investigate numerical methods for determining the chloride concentration in a given structure.
- Estimate the parameters in the probabilistic model on the basis of measurements.
- Determine the probability that corrosion is initiated in a given structure on the basis of the probabilistic model and the estimated parameters.
- Determine the optimal repair and maintenance strategy for a given structure.
- Determine optimal experimental plans for performing measurements.

In chapter 2 a description is given of the microstructure of concrete and the principles and reactions involved in its formation. The porosity and permeability of hardened concrete

and their dependence on a number of factors are described. The main issues of the chapter are: chloride ingress and chloride-initiated corrosion. Different models of chloride ingress are discussed and it is concluded that the chloride ingress can be described with sufficient accuracy by the diffusion equation. In order to use this expression to predict the chloride concentration in a given structure the surface concentration and the ability of the concrete to transport chloride, the transport coefficient, must be estimated. Normally the transport coefficient is assumed to be constant. However, a variation of the transport coefficient with time and/or position can be taken into account. In chapter 2 it is further, stated that corrosion is initiated when the chloride concentration at some point around the reinforcement exceeds a critical threshold value.

A probabilistic model of chloride ingress is presented in chapter 3 where also different formulations of the finite element method which can be used to solve the diffusion equation are given. The transport coefficient is modelled as a sum of three parts. The parts represent a mean value, a fast fluctuating spatial variation (correlation length 3-5 mm) and a slower spatial variation (correlation length 200-500 mm). In a similar manner the surface concentration, the cover thickness and the critical threshold for initiation of corrosion are modelled as a sum of two parts where the first represents the mean value and the second a random spatial variation. The estimation of the probability that corrosion has been initiated in a given region can be based on a stochastic finite element analysis. It is concluded that the midpoint method and the local average method are the methods best suited to solve the given problem. Further, different finite element formulations of the diffusion equation are compared on the basis of an example. The example indicates that the most efficient and accurate solution of the diffusion equation is obtained by using the standard finite element method formulation where the chloride concentration in the elements is approximated by the use of shape functions. This formulation ensures that the chloride concentration is continuous over the element boundaries. However, the flux vector is not continuous over the element boundaries.

In chapter 4 various methods to estimate the parameters in the probabilistic model are presented together with the methods to determine the probability that corrosion has been initiated at a given time. These calculations are performed using FORM/SORM-analysis.

The estimation of the parameters in the probabilistic model is performed on the basis of so-called chloride profiles. A chloride profile is a series of measurements of the chloride concentration as a function of the distance from the surface of the structure. In chapter 5 it is shown how an analysis of such a profile can be performed in order to estimate the probability that corrosion is initiated at a given time at the point where the measurement was made. The analysis of a chloride profile indicates that the best results are obtained by modelling the mean value of the transport coefficient as a function of the distance from the surface of the structure. However, one must be careful not to reach too general conclusions on the basis of a single example. In fact, it is not always an advantage to take the spatial variation of the mean of the transport coefficient into account because this increases the number of unknown parameters and thereby the statistical uncertainty. A sensitivity analysis shows that the low-scale spatial fluctuation of the transport coefficient can be neglected. This makes the estimation of the probability of corrosion much more efficient because the number of stochastic variables needed to model the problem decreases significantly. In chapter 5 it is further shown how the analysis of several chloride profiles

can be carried out such that the spatial variation of the variables over a larger area can be taken into account. On this basis it is possible to perform an analysis where the probability that corrosion has been initiated at an arbitrary point within a given region can be determined. This analysis is performed by partitioning the considered area into smaller elements in which the considered variables are assumed to be constant. The probability that corrosion has been initiated can now be determined by the analysis of a series system. A sensitivity analysis indicates that the most important variables are the thickness of the cover and the critical threshold for initiation of corrosion.

In chapter 6 it is demonstrated how the probabilistic model can be used to determine the optimal strategy for maintenance and repair of a structure subject to chloride ingress. The optimal strategy for maintenance and repair is determined by minimizing the expected cost of maintenance and repair throughout the lifetime of the structure. In an example the optimal strategy for maintenance and repair of a pier of a coastal bridge is determined. It is shown that the optimal strategy is sensitive towards changes in the estimates of the times when the different strategies must be implemented. If the different strategies must be implemented relatively soon in relation to the time when the optimal strategy is determined it is optimal to implement a strategy which prevents initiation of corrosion. If an analysis shows that the strategies must be implemented at a later time it is optimal to wait until relatively severe signs of corrosion are visible and then perform a repair. These conclusions are based on a real rate of interest of 7 %. If the real rate of interest is low (less than about 4 %) it is always optimal to use a strategy which prevents corrosion.

When additional measurements are performed it is possible to determine the time when corrosion is initiated or the time when a given strategy must be implemented with larger accuracy. This might lead to a reduction of the expected cost of repair and maintenance. However, the cost of performing the measurements naturally increases. It is, therefore, of interest to determine the optimal number of measurements. This problem is considered in chapter 7. It is shown that visual inspections and half-cell measurements only have a very limited effect on the estimates of the times when the given maintenance and repair strategies must be implemented. The optimal number of measurements of chloride profiles is determined on the basis of decision theory. On the basis of a simple model it is determined how many measurements it is necessary to perform in order to ensure that the probability that corrosion is initiated at a given time is lower than a given value. However, it is shown that this plan is very sensitive towards changes in the measurement results. An analysis is performed where the optimal plan is determined by minimizing the expected cost of the measurements and of maintenance and repair. The considered example indicates that it is not necessary to perform additional experiments. Further, it is argued that the optimum is not sensitive towards changes of the measurement results. However, due to the computational effort involved it has not been possible to perform a sensitivity analysis. The computational effort involved is excessive because it is necessary to perform a large number of computations of the probability that corrosion has been initiated at a given time. As earlier mentioned this computation involves an analysis of a series system. However, the example indicates that the number of measurements normally performed is sufficient to plan the maintenance and repair of a given structure.

8.2   Main Conclusions

On the basis of the above summary it can be concluded that the main objectives stated above and in the introduction have been reached. Further, it can be concluded that the computations necessary to solve the given problems can be performed within the framework of FORM/SORM-analysis which implies that similar analyses can be performed by practising engineers with knowledge of these methods.

One of the most important conclusions which can be drawn on the basis of the present work is that in order to determine the time to initiation of corrosion in a given structure, it is necessary to use data from measurements on the given structure. In chapter 5 a comparison is made of the results obtained on the basis of measurements from a given structure and the results obtained on the basis of measurements from a large number of different structures. It is shown that a substantial reduction of the standard deviation of the time to initiation of corrosion is obtained when only measurements from the considered structure are taken into account.

Another important conclusion is that it is necessary to take the random spatial variation of the transport coefficient, the surface concentration, the critical threshold for initiation of corrosion and the cover thickness into account when calculating the probability that corrosion has been initiated at an arbitrary point within a given region. This is seen by comparing the probability that corrosion has been initiated in a 1 × 1 m area (see section 5.4) with the probability that corrosion has been initiated somewhere on the entire structure (see section 6.3). Hence, the size of the given structure plays an important role in the investigation of the probability that corrosion has occurred at an arbitrary point in the structure.

It has been demonstrated that the probabilistic model of chloride ingress and initiation of corrosion can be applied to determine cost-optimal plans for repair and maintenance of a given structure. However, it is important that the criterion for applying a given strategy for maintenance and repair is formulated in a way suitable for reliability analysis. It is, however, difficult to determine optimal experimental plans for additional measurements. The major problem is the numerical effort involved in the necessary computations. This problem can perhaps be overcome by reformulating the probabilistic model such that the effort involved in computing the probability of corrosion decreases. The problem, however, will soon disappear with the advance of faster computers.

As mentioned in the introduction there has been some discussion in recent years about the physical model describing chloride ingress in concrete. In this view it must be emphasized that the methodology presented in the present thesis can be applied to any model of chloride ingress which is based on the diffusion equation. The effect of chloride binding, the variation of the mean value of the transport coefficient with the position and the variation of the transport coefficient with time can be taken into account. However, it is important to use a model which can fit the observed data and a model where the parameters can be given a physical interpretation. Further, it must be noted that the model is based on the assumption that a connected system of capillary pores and microcracks exist. If the system of capillary pores and microcracks is not connected, chloride can only penetrate to a certain depth. For a given structure it is, however, difficult to show that no connected system of pores and cracks exists.

An important aspect in future work concerned with corrosion of the reinforcement is to formulate a more detailed model for the cover thickness than the one used in the examples herein (see section 5.4). This is particularly important because the cover thickness has been shown to be the most important variable in the model, see section 5.4.1. Further, in order to determine the load-bearing capacity of a given structure as a function of time a model for propagation of corrosion must be formulated. Finally, it is important to notice that probabilistic models can be used in order to model other destructive mechanisms in reinforced concrete. The present model can for example easily be reformulated such that it can be used in order to model carbonation. Future work within the field will also be concerned with a number of other destructive mechanisms such as alkali-aggregate reactions and freeze-thaw action. In fact, probabilistic models of destructive mechanisms are sure to attract much attention in the future both within the research programmes mentioned in section 1.1 and in other connections.

Appendix A

Program Modules

In the following brief descriptions of the programme modules used for the evaluation of the results of the examples shown in the main report are given. A part of the modules originate from existing programmes and another part has been developed with the purpose of solving the given problem. The modules which have been developed, therefore, should only be considered as "research code".

The major part of the modules has been programmed in FORTRAN77. However, a few modules have been programmed in MATLAB. The modules programmed in MATLAB have all been implemented in conjunction with the FEM-program FEMLAB which was also programmed in MATLAB.

A.1 Existing Modules

PRADSR This module solves probability integrals of the type shown in eq. (4.9) by FORM-analysis. The module performs the transformation from u- to z-space and locates the β-point. The user must supply a limit state function written in FOR-TRAN and a data-file specifying the probabilistic model. The module has formed the basis for the computations of the probability that corrosion has been initiated in a given point.

HOHENB The module computes the Hohenbichler approximation to the multidimensional standard normal distribution, see Hohenbichler [4]. The module is used in all examples where system reliability is considered.

ODBOUN On the basis of a vector of β-values for the elements in a system and a matrix specifying the correlations between the failure events this module computes the Ditlevsen bounds for the failure probability, see Ditlevsen [2]. The module is only used in order to determine the bounds for the probability that corrosion has been initiated in a 1 m by 1 m area. See section 5.4.

NLPQL This optimization program solves general nonlinear optimization problems. For a more detailed description see section 4.5. The module has been used in comjunction with the maximum likelihood parameter estimation in section 5.2.

COLSOL For a given stiffness matrix and load vector this module solves the FEM-equations. The module is based on the skyline redection method and is, therefore, very efficient, see Bathe [1]. The module is used in the FEM-program FEMAN, see section A.2

FEMLAB The FEMLAB environment consists of a number of modules programmed in MATLAB which can be used to solve FEM-problems. For a detailed description of the modules see Hededal and Krenk [3]. The modules are used in the example in section 3.8.

A.2   Own Modules in FORTRAN

FEMAN This module is a finite element program used to determine the chloride concentration in a given point at a given time. The module solves the 1-dimensional diffusion problem. The module COLSOL mentioned above, see section A.1, has been used to solve the FEM-equation. The module FEMAN has been used in when the diffusion equation could not be solved analytically.

LIKECA The likelihood of obtaining a given set of observed outcomes of the chloride concentration is determined by this module. The module uses PRADSR, see section A.1, in order to solve probability integrals with equality constraints. The module is used in order to analyse a single chloride profile, see section 5.2.

YDIFPS The module performs the differentation of the standard normal distribution function necessary in order to evaluate the probability integrals with equality constraints, see section 4.2.3. The module is used with the above mentioned LIKECA.

FAILEL This module contains the limit state function for the reliability program PRADSR, see section A.1. The limit state function describes the critical event, e.g. that the chloride concentration around the reinforcement exceeds the critical threshold value.

ALPVEC For a given system this module determines an equivalent reliability index and α-vector. Further, it determines the correlation coefficient between different systems. The module is used when determining the probability that corrosion has been initiated in a given number of 1 m by 1 m areas, see section 5.4.

A.3   Own Modules in MATLAB

DIFDRV The main module for solving 2-dimensional diffusion problems within the framework of FEMLAB, see section A.1. The module arranges the input and calls a module that determines the stiffness matrix on the basis of a simulated outcome of the field describing the transport coefficient. Further, it calls modules which determine the mass matrix and load vector and it performs the time-integration.

KEFLUX3P This module determines an element stiffness matrix for a 3-node element describing diffusion in 2 dimensions. The stiffness matrix is determined by the flux-based method described in section 3.5.4.

KEHY3P This module determines an element stiffness matrix for a 3-node element describing diffusion in 2 dimensions. The stiffness matrix is determined by the hybrid method described in section 3.5.3.

COVMAT On the basis of the coordinates for the Gauss-points used to evaluate the local stiffness matrices and the auto-covariance function of the transport coefficient this module determines the covariance matrix for the variables describing the transport coefficient in the Gauss-points. Further, an outcome of the variables is generated.

A.4 References

[1] Bathe, K.-J., Finite Eelemt Procedures in Engineering Aanlysis, Prentice-Hall, New Jersey, 1982.

[2] Ditlevsen, O., Narrow Reliability Bounds for Structural Systems, Journ. Struc. Mech., 7, pp. 171-200, 1979.

[3] Hededal, O., Krenk, S., FEMLAB, Matlab Toolbox for The Finite Element Method, Version 1.0, Aalborg University, 1995.

[4] Hohenbichler, M., An Asymptotic Formula for the Probability of Intersections, Berichte zur Zuverlässigheitstheorie der Bauwerke, SFB 96, 69, Technical University of Munich, pp.21-48, 1984.

[5] Schittkowski, K., User's Guide for the Nonlinear Programming Code NLPQL, Institut für Informatik, Universität Stuttgart.

Appendix B

Notation

$\mathbf{a}$	arbitrary vector
$\mathbf{a}$	action, repair strategy
a, a_1, a_2, a_3	correlation length
a_i	coordinate of local node 1 in element i
A	amplitude of the fluctuation of the cover thickness
b_i	coordinate of local node 2 in element i
$\mathbf{B}_c$	derivatives of the shapefunctions, $\mathbf{N}_c$ with respect to $\mathbf{x}$
c	chloride concentration in a given point
$\dot{c}$	derivative of the chloride concentration with respect to time
$\overline{\mathbf{c}}$	nodal values of the concentration
c_0	initial concentration
c_{cr}	critical threshold for initiation of corrosion
$\{c_{cr}(\mathbf{x})\}$	stochastic field describing the critical threshold for initiation of corrosion
c_{cr0}	mean value of the critical threshold for initiation of corrosion
$\{c_{cr1}(\mathbf{x})\}$	stochastic field describing the fluctuation of the critical threshold for initiation of corrosion around the mean
$\hat{c}_i$	measured chloride concentration
c_s	surface concentration in a given point
$\hat{c}_s$	surface concentration estimated on the basis of a chloride profile
$\{c_s(\mathbf{x})\}$	stochastic field describing the surface concentration
$c_{s0}(\mathbf{x})$	mean value function of the surface concentration
$\{c_{s1}(\mathbf{x})\}$	stochastic field describing the fluctuation of the surface concentration around the mean
$\mathbf{C}$	covariance matrix
$C_{D_i D_j}$	covariance between the transport coefficient in the stochastic elements i and j
C_i	cost if the repair is performed in year i
$C_{i,j}$	cost in the year j if the repair is performed in the year i
C_e	cost of a measurement
C_F	cost of failure
C_I	fixed cost of measurements
C_M	cost of performing measurements

C_R	cost of performing repairs
d	distance between two points
$\mathbf{d}$	decision rule
D	transport coefficient
D_s	transport coefficient in the outer layer of a structure
D_i	transport coefficient in the inner part of a structure
$\hat{D}$	value of the transport coefficient estimated on the basis of a chloride profile
$\mathbf{D}(\mathbf{x})$	constitutive matrix as a function of the position
$\mathbf{D}_0(\mathbf{x})$	mean value function of the constitutive matrix
$\{\mathbf{D}_1(\mathbf{x})\}$	matrix whose elements are stochastic fields with a low scale of fluctuation
$\{\mathbf{D}_2(\mathbf{x})\}$	matrix whose elements are stochastic fields with a high scale of fluctuation
$D_0(\mathbf{x})$	mean value function of the transport coefficient
$\{D_1(\mathbf{x})\}$	stochastic field with low scale of fluctuation
$\{D_2(\mathbf{x})\}$	stochastic field with high scale of fluctuation
$\mathbf{e}$	experimental plan
$E[.]$	mean value of $[.]$
$\mathbf{E}$	mass matrix
f	frequency of the fluctuation of the cover thickness
$f(x)$	stochastic field
$f_i(\mathbf{v})$	constraints in optimization problem
$f_{\mathbf{X}|\mathbf{P}}(\mathbf{x}|\mathbf{p})$	joint density function of $\mathbf{X}$ given the parameters $\mathbf{P}$
$g(\mathbf{u})$	limit state function
h	mean precision
$\mathbf{H}$	sufficient statistic for the covariance
$\mathbf{I}$	identity matrix
K	observed event
$\mathbf{K}$	stiffness matrix
$\mathbf{K}_0$	mean value of the stiffness matrix
$\mathbf{K}_1$	deviations of the stiffness matrix from the mean
l	characteristic length
$l(\hat{\mathbf{x}}|\mathbf{p})$	likelihood function for the outcomes $\hat{\mathbf{x}}$ given the parameters $\mathbf{p}$
$\mathbf{m}$	sufficient statistic for the mean
M	event corresponding to failure
n	number of nodes in a FEM-element
n_e	number of equality constraints in an optimization problem
n_f	number of failure modes
n_{new}	number of new measurements
n_p	number of chloride profiles
n_q	number of constraints in an optimization problem
$\mathbf{n}$	unit vector normal to the surface
N_e	number of equivalent failure elements
N_f	number of equivalent elements that have failed
N_P	number of bridge piers

N_R	number of bridge piers for which a given repair and maintenance strategy must be implemented
$\mathbf{N}_c$	shape functions for c
$\mathbf{N}_\mathbf{q}$	shape functions for $\mathbf{q}$
$O\,(\mathbf{v})$	object function
p	parameter in the probabilistic model of limit state function
$P\,(.)$	probability of the event (.)
$\mathbf{P}$	vector of unknown parameters
P_B	probability that repair is implemented for a bridge
P_f	failure probability
P_I	probability of initiation of corrosion
P_R	probability that a given repair and maintenance strategy is implemented
$\mathbf{q}$	chloride flow vector
$\overline{\mathbf{q}}$	matrix containing the nodal flow vectors
q_n	flux normal to the surface
r	real rate of interest
$\mathbf{R}$	load vector
s	sum of squares
s_ε	standard deviation of measurement uncertainty
S	surface of an element
$\mathbf{S}^e$	local stiffness matrix determined by the hybrid method
S_g	part of the surface with known surface concentration
S_q	part of the surface with known flux
$\mathbf{S}$	observations
t	time
t_m	time when a visual inspection is performed
T	length of a time period
T_1	initiation period
T_2	probagation period
T_d	time when the decision of repair strategy is made
T_L	lifetime
T_s	time when signs of corrosion occur
$\mathbf{U}$	vector of standard normal distributed variables
$\mathbf{u}^*$	design point
$\mathbf{v}$	optimization variables
$v_{i,l}$	lower limit for the ith optimization variable
$v_{i,u}$	upper limit for the ith optimization variable
$V\,[.]$	coefficient of variation of [.]
w	weight function
$\mathbf{W}_{0_i},\ \mathbf{W}_{1_i},\ \mathbf{W}_{0_i}$	weighted integrals
w/c	water-cement ratio
$x\,,\mathbf{x}$	position
$\mathbf{Z}$	vector of stochastic variables
$\hat{\mathbf{z}}$	observation of the stochastic vector $\mathbf{Z}$
$\boldsymbol{\alpha}$	unit vector form origin to the β-point in u-space

β_i	reliability index of failure mode i
β_e	equivalent reliability index
γ_j	relative position of the centre of gravity of $\frac{1}{D}$ along side j
	in a hybrid element
δ	thickness of the cover in a given point
$\{\delta(\mathbf{x})\}$	stochastic field describing the cover thickness
δ_0	mean value of the cover thickness
$\{\delta_1(\mathbf{x})\}$	stochastic field describing the fluctuation of the cover thickness
	around the mean
ε	measurement uncertainty
η	relative precision
Θ	random phase
$\kappa_{D_1 D_1}$	autocovariance function of the field D_1
$\kappa_{D_2 D_2}$	autocovariance function of the field D_2
μ_{D_i}	mean value of the transport coefficient in stochastic element i
ν	degrees of freedom
ξ	local coordinate in FEM-element
Ξ	Hessian matrix
Π	total energy
ρ_{DD}	auto-correlationcoefficient function of the field D
ρ_e	correlation coefficient between equivalent elements
$\boldsymbol{\rho}$	correlation coefficient matrix
σ	standard deviation
$\varphi(\mathbf{u})$	standard normal density function
$\Phi(\mathbf{u})$	standard normal distribution function
$\Omega_{\mathbf{p}}$	admissable range of $\mathbf{p}$

Superscripts

e	indicates an element matrix
max	maximum allowable value
T	transpose
$\prime$	prior distribution
$\prime\prime$	posterior distribution
$\hat{}$	an outcome

Appendix C

Resume in Danish/Resume på Dansk

I den industrialiserede verden benyttes en stigende andel af vejmyndighedernes budgetter på rehabilitering af eksisterende armerede betonkonstruktioner. Dette skyldes at betonkonstruktioners bæreevne reduceres med tiden som følge af en række destruktive mekanismer. Endvidere stiger antallet af gamle konstruktioner, hvilket i sig selv forøger behovet for rehabilitering. I Danmark er chlorid-initieret korrosion af armeringen den mest udbredte nedbrydningsmekanisme. Denne mekanisme er derfor blevet udvalgt som et eksempel på, hvorledes nedbrydningsmekanismer kan beskrives ved hjælp af en probabilistisk model. En sådan model kan anvendes til at planlægge vedligeholdelse og reparation af en given konstruktion samt til at planlægge nye forsøg.

I kapitel 1 er givet en præsentation af problemet, samt en kort redegørelse for formålet med probabilistiske modeller. Endvidere er formålene med projektet blevet identificeret. Formålene med projektet er at

- Formulere en probabilistisk model for chloridindtrængning og initiering af korrosion.
- Undersøge numeriske metoder til bestemmelse af chloridkoncentrationen i en given konstruktion.
- Estimere parametrene i den probabilistiske model på grundlag af målinger.
- Bestemme sandsynligheden for, at korrosion er initieret i en given konstruktion på grundlag af den probabilistiske model og de estimerede parametre.
- Bestemme den optimale strategi for vedligeholdelseselse og reparation for en given konstruktion.
- Bestemme en optimal plan for at udføre nye målinger, således at der opnås yderligere information, som kan anvendes i forbindelse med estimeringen af sandsynligheden for, at korrosion er blevet initieret.

I kapitel 2 er der indledningsvis givet en kort redegørelse for betons mikrostruktur samt en beskrivelse af principperne og reaktionerne vedrørende hærdningen af beton. Den hærdede betons porøsitet og permeabilitet og disses afhængighed af en række faktorer er beskrevet. Hovedvægten i kapitlet er lagt på emnerne: chloridindtrængning og chlorid-initieret korrosion. Forskellige modeller for chloridindtrængning diskuteres, og det konkluderes, at

chloridindtrængningen med tilstrækkelig nøjagtighed kan beskrives ved diffusionsligningen. For at benytte dette udtryk til bestemmelse af chloridconcentrationen i en given konstruktion må overfladekoncentrationen samt betonens evne til at transportere chlorid (transportkoefficienten) estimeres. Normalt antages transportkoefficienten at være konstant; men dennes variation med tiden og/eller stedet kan også tages i regning. I kapitel 2 redegøres endvidere for, at korrosion initieres, når chloridkoncentrationen omkring armeringen overskrider en grænseværdi.

Den probabilistiske model for chloridindtrænging præsenteres i kapitel 3, hvor også forskellige elementmetodeformuleringer, som kan anvendes til løsning af diffusionsligningen sammenlignes. Transportkoefficienten modelleres som en sum af tre led. Leddene repræsenterer middelværdien, en hurtigt fluktuerende stedslig variation (korrelationslængde 3-5 mm) og en langsommere stedslig fluktuation (korrelationslængde 200-500 mm). På lignende vis modelleres både overfladekoncentrationen, den kritiske grænse for initiering af korrosion samt dæklagstykkelsen som en sum af to led, hvor det første repræsenterer middelværdien og det andet en tilfældig stedslig fluktuation. Bestemmelsen af sandsynligheden for, at der i et givet område initieres korrosion, må baseres på en analyse med stokastisk elementmetode. Det konkluderes, at midtpunktsmetoden og den lokale middels metode er bedst egnede til at løse det givne problem. Endvidere sammenlignes på grundlag af et eksempel forskellige elementmetodeformuleringer af diffusionsligningen. Eksemplet indikerer, at diffusionsligningen kan løses mest effektivt og nøjagtigt ved at benytte den normale elementmetodeformulering, hvor chloridkoncentrationen i de finitte elementer approksimeres vha. formfunktioner, og som sikrer, at chloridkoncentrationen er kontinuert over elementgrænserne uden dog at sikre kontinuitet af fluxvektoren.

I kapitel 4 præsenteres de beregningsmetoder, som skal anvendes til af estimere parametrene i den probabilistiske model samt til at bestemme sandsynligheden for, at der til et givet tidspunkt er initieret korrosion. Til disse beregninger anvendes FORM/SORM-analyse da disse efterhånden er ved at finde anvendelse blandt praktiserende ingeniører.

Estimeringen af parametrene i den probabilistiske model sker på grundlag af såkaldte chloridprofiler, hvor chloridkoncentrationen er målt som en funktion af afstanden til betonens overflade. I kapitel 5 er der vist, hvorledes en analyse af et sådant profil kan gennemføres. På grundlag af en sådan analyse er det muligt at estimere, hvornår der vil opstå korrosion i det punkt hvor målingen blev foretaget. Analysen af et chloridprofil viser, at det er fordelagtigt at modellere middelværdien af transportkoefficienten som en funktion af afstanden til betonens overflade. Der kan dog ikke foretages helt generelle konklusioner på et enkelt eksempel, og generelt er det ikke sikkert, at det er fordelagtigt at tage en stedslig variation af middelværdien i regning, da dette medfører en forøgelse af antallet af ukendte parametre og dermed den statistiske usikkerhed. En sensitivitetsanalyse af en analyse af et enkelt chloridprofil viser, at den hurtige fluktuation af transportkoefficienten kan negligeres, uden at dette har indflydelse på sandsynligheden for korrosion. Dette gør bestemmelsen af tiden til initiering af korrosion væsentligt simplere. Der er i kapitel 5 endvidere redegjort for, hvorledes en analyse af flere chloridprofiler kan gennemføres således at variablenes variation over et større område tages i regning. På dette grundlag er det muligt at gennemføre en analyse til at bestemme sandsynligheden, for at der på et givet tidspunkt er initieret korrosion i et vilkårligt punkt i et givet område. Denne analyse foregår ved at inddele det givne område i mindre elementer hvor der ikke er no-

gen tilfældig stedslig variation af de stokastiske variable. Sandsynligheden for at der er initieret korrosion i et vilkårligt punkt i det samlede område kan nu bestemmes ved en analyse af et seriesystem. På grundlag af et eksempel kan det konkluderes, at de vigtigste variable i denne analyse er tykkelsen af dæklaget samt den kritiske grænse for initiering af korrosion.

I kapitel 6 er det demonstreret, hvorledes den probabilistiske model kan benyttes til at bestemme den optimale strategi til vedligeholdelse og reparation af en konstruktion udsat for chloridindtrængning. Den optimale plan for vedligeholdelse og reparation bestemmes ved at minimere de forventede udgifter til vedligeholdelse og reparation gennem konstruktionens levetid. I et eksempel bestemmes den optimale plan for vedligeholdelseelse og reparation af en bropille på en kystbro. Det vises, at den optimale plan er følsom over for ændringer i estimaterne for, hvornår de givne strategier implementeres. Hvis de forskellige strategier skal implementeres på et forholdsvis tidligt tidspunkt, er det optimalt at anvende en strategi, som forhindrer, at korrosion initieres. Hvis det derimod forudses, at strategierne skal implementeres på et senere tidspunkt, er det optimalt at anvende en strategi, hvor der først foretages en reparation, når forholdsvis store skader er synlige.

Når der gennemføres yderligere målinger af en konstruktions tilstand, er det muligt med større nøjagtighed at forudse, hvornår korrosion initieres, eller hvornår en given strategi for vedligeholdelse og reparation skal anvendes. Dette kan medføre en reduktion af udgifterne ved vedligeholdelse og reparation; men har naturligvis også til følge, at udgifterne til målingerne stiger. Dette problem er undersøgt i kapitel 7. Det vises, at effekten af at foretage en visuel inspektion af konstruktionen samt at foretage EKP-målinger kun har ringe indflydelse på estimaterne af, hvornår en given strategi skal implementeres. Planlægningen af antallet af målinger af chloridprofiler gennemføres på grundlag af beslutningsteori. Ved en simpel model bestemmes antallet af forsøg, som det er nødvendigt at gennemføre for at sikre, at sandsynligheden for korrosion til et givet tidspunkt er lavere end en given værdi. Det viser sig dog, at denne plan er meget følsom over for ændringer i måleresultaterne. Der gennemføres også en analyse, hvor de samlede udgifter i forbindelse med målingerne samt konstruktionens vedligeholdelseelse minimeres. Det givne eksempel viser, at det ikke er nødvendigt at udføre yderligere forsøg. Endvidere argumenteres der for, at dette optimum er meget insensitivt over for de forudsatte måleresultater. Det har dog på grund af beregningernes omfang ikke været muligt at gennemføre nogen egentlig sensitivitetsanalyse. Beregningernes omfang er stort, idet det er nødvendigt at foretage mange beregninger af sandsynligheden for, at der forekommer korrosion i et givet område. Denne beregning involverer som før nævnt en analyse af et seriesystem. Eksemplet indikerer dog, at de måleprogrammer, som normalt gennemføres, har et tilstrækkeligt omfang. Det vil sige, at antallet af målinger er tilstrækkeligt til at planlægge konstruktionens vedligeholdelse og reparation.

Kapitel 8 indeholder en sammenfatning og en sammenfatning af de konklusioner som er blevet nået gennem projektet, og som også er blevet nævnt her. Den overordnede konklusion er, at det gennem projektet er lykkedes at nå de mål, som blev opstillet indledningsvis. De nødvendige beregninger til bestemmelse af en optimal forsøgsplan er dog meget omfattende. Endvidere kan det konkluderes at beregningerne, som er gennemført i projektet, alle kan udføres ved hjælp af velkendte FORM/SORM-teknikker og derfor kan anvendes af praktiserende ingeniører med kendskab til disse metoder.

STRUCTURAL RELIABILITY THEORY SERIES

PAPER 133: H. U. Köylüoğlu, S. R. K. Nielsen & A. Ş. Çakmak: *Stochastic Dynamics of Nonlinear Structures with Random Properties subject to Random Stationary Excitation.* ISSN 0902-7513 R9520.

PAPER NO. 134: H. U. Köylüoğlu, S. R. K. Nielsen & A. Ş. Çakmak: *Solution of Random Structural System subject to Non-Stationary Excitation: Transforming the Equation with Random Coefficients to One with Deterministic Coefficients and Random Initial Conditions.* ISSN 0902-7513 R9429.

PAPER NO. 135: S. Engelund, J. D. Sørensen & S. Krenk: *Estimation of the Time to Initiation of Corrosion in Existing Uncracked Concrete Structures.* ISSN 0902-7513 R9438.

PAPER NO. 136: H. U. Köylüoğlu, S. R. K. Nielsen & A. Ş. Çakmak: *Solution Methods for Structures with Random Properties subject to Random Excitation.* ISSN 0902-7513 R9444.

PAPER NO. 137: J. D. Sørensen, M. H. Faber & I. B. Kroon: *Optimal Reliability-Based Planning of Experiments for POD Curves.* ISSN 0902-7513 R9455.

PAPER NO. 138: S.R.K. Nielsen & P.S. Skjærbæk, H.U. Köylüoğlu & A.Ş. Çakmak: *Prediction of Global Damage and Reliability based upon Sequential Identification and Updating of RC Structures subject to Earthquakes.* ISSN 0902-7513 R9505.

PAPER NO. 139: R. Iwankiewicz, S. R. K. Nielsen & P. S. Skjærbæk: *Sensitivity of Reliability Estimates in Partially Damaged RC Structures subject to Earthquakes, using Reduced Hysteretic Models.* ISSN 0902-7513 R9507.

PAPER NO. 140: R. C. Micaletti, A. Ş. Çakmak, S. R. K. Nielsen & H. U. Köylüoğlu: *Error Analysis of Statistical Linearization with Gaussian Closure for Large Degree-of-Freedom Systems.* ISSN 1395-7953 R9631.

PAPER NO 141: H. U. Köylüoğlu, S. R. K. Nielsen & A. Ş. Çakmak: *Uncertain Buckling Load and Reliability of Columns with Uncertain Properties.* ISSN 0902-7513 R9524.

PAPER NO. 142: S. R. K. Nielsen & R. Iwankiewicz: *Response of Non-Linear Systems to Renewal Impulses by Path Integration.* ISSN 0902-7513 R9512.

PAPER NO. 143: H. U. Köylüoğlu, A. Ş. Çakmak & S. R. K. Nielsen: *Midbroken Reinforced Concrete Shear Frames Due to Earthquakes. - A Hysteretic Model to Quantify Damage at the Storey Level.* ISSN 1395-7953 R9630.

PAPER NO. 144: S. Engelund: *Probabilistic Models and Computational Methods for Chloride Ingress in Concrete.* Ph.D.-Thesis. ISSN 1395-7953 R9707.

PAPER NO. 145: H. U. Köylüoğlu, S. R. K. Nielsen, Jamison Abbott & A. Ş. Çakmak: *Local and Modal Damage Indicators for Reinforced Concrete Shear Frames subject to Earthquakes.* ISSN 0902-7513 R9521

PAPER NO. 146: P. H. Kirkegaard, S. R. K. Nielsen, R. C. Micaletti & A. Ş. Çakmak: *Identification of a Maximum Softening Damage Indicator of RC-Structures using Time-Frequency Techniques.* ISSN 0902-7513 R9522.

STRUCTURAL RELIABILITY THEORY SERIES

PAPER NO. 147: R. C. Micaletti, A. Ş. Çakmak, S. R. K. Nielsen & P. H. Kirkegaard: *Construction of Time-Dependent Spectra using Wavelet Analysis for Determination of Global Damage.* ISSN 0902-7513 R9517.

PAPER NO. 148: H. U. Köylüoğlu, S. R. K. Nielsen & A. Ş. Çakmak: *Hysteretic MDOF Model to Quantify Damage for TC Shear Frames subject to Earthquakes.* ISSN 1395-7953 R9601.

PAPER NO. 149: P. S. Skjærbæk, S. R. K. Nielsen & A. Ş. Çakmak: *Damage Location of Severely Damaged RC-Structures based on Measured Eigenperiods from a Single Response.* ISSN 0902-7513 R9518.

PAPER NO. 150: S. R. K. Nielsen & H. U. Köylüoğlu: *Path Integration applied to Structural Systems with Uncertain Properties.* ISSN 1395-7953 R9602.

PAPER NO. 151: H. U. Köylüoğlu & S. R. K. Nielsen: *System Dynamics and Modified Cumulant Neglect Closure Schemes.* ISSN 1395-7953 R9603.

PAPER NO. 153: R. C. Micaletti, A. Ş. Çakmak, S. R. K. Nielsen & H. U. Köylüoğlu: *A Solution Method for Linear and Geometrically Nonlinear MDOF Systems with Random Properties subject to Random Excitation.* ISSN 1395-7953 R9632.

PAPER NO. 154: J. D. Sørensen, M. H. Faber, I. B. Kroon: *Optimal Reliability-Based Planning of Experiments for POD Curves.* ISSN 1395-7953 R9542.

PAPER NO. 155: J. D. Sørensen, S. Engelund: *Stochastic Finite Elements in Reliability-Based Structural Optimization.* ISSN 1395-7953 R9543.

PAPER NO. 156: C. Pedersen, P. Thoft-Christensen: *Guidelines for Interactive Reliability-Based Structural Optimization using Quasi-Newton Algorithms.* ISSN 1395-7953 R9615.

PAPER NO. 157: P. Thoft-Christensen, F. M. Jensen, C. R. Middleton, A. Blackmore: *Assessment of the Reliability of Concrete Slab Bridges.* ISSN 1395-7953 R9616.

PAPER NO. 159: H. I. Hansen, P. Thoft-Christensen: *Wind Tunnel Testing of Active Control System for Bridges.* ISSN 1395-7953 R9662.

PAPER NO 160: C. Pedersen: *Interactive Reliability-Based Optimization of Structural Systems.* Ph.D.-Thesis. ISSN 1395-7953 R9638.

PAPER NO. 161: S. Engelund, J. D. Sørensen: *Stochastic Models for Chloride-initiated Corrosion in Reinforced Concrete.* ISSN 1395-7953 R9608.

PAPER NO. 165: P. H. Kirkegaard, F. M. Jensen, P. Thoft-Christensen: *Modelling of Surface Ships using Artificial Neural Networks.* ISSN 1593-7953 R9625.

PAPER NO. 167: S.R.K. Nielsen, R. Iwankiewicz: *Dynamic systems Driven by Non-Poissonian Impulses: Markov Vector Approach.* ISSN 1395-7953 R9705.